STUDIES OF VIRUS RECEPTOR INTERACTIONS AND VIRULENCE DETERMINANTS OF FELINE CALICIVIRUS

A Dissertation

Presented to the Faculty of the Graduate School

of Cornell University

In Partial Fulfillment of the Requirements for the Degree of

Doctor of Philosophy

by

Robert James Ossiboff

January 2009

STUDIES OF VIRUS RECEPTOR INTERACTIONS AND VIRULENCE DETERMINANTS OF FELINE CALICIVIRUS

Robert James Ossiboff, Ph. D.

Cornell University 2009

The virus-receptor interaction is critical for establishing infection in host cells. The interaction (i) allows the virion to attach specifically to the host cell membrane, (ii) is often required to permit the process of infection further downstream, and (iii) strongly influences viral tropism and pathogenesis.

Feline calicivirus (FCV) is a common feline pathogen. Infection is generally asymptomatic or causes mild upper respiratory signs and oral ulceration; morbidity is high while mortality is low. During the last decade however, there have been outbreaks of extremely virulent viruses that cause systemic disease and result in mortality rates as high as 50%. One objective of these studies was to characterize *in vitro* properties of FCV isolates of high and low virulence and to identify *in vitro* correlates to virulence.

FCV, a small nonenveloped virus containing a positive sense RNA genome, is known to bind two cellular receptors, feline junctional adhesion molecule A (fJAM-A) and α2,6 sialic acid. A second objective was to elucidate the details of the FCV-fJAM-A interaction by determining the regions of fJAM-A required for FCV binding and selecting FCV mutants resistant to neutralization by soluble fJAM-A.

Analysis of FCV *in vitro* properties demonstrated that highly virulent isolates were able to spread more efficiently in tissue culture than other isolates investigated. Highly virulent isolates were also more susceptible to neutralization by soluble fJAM-A than other isolates. Lastly, sequence analysis of the FCV structural protein

did not identify conserved sequence unique to highly virulent viruses.

Mutagenesis studies identified that while the binding of FCV to fJAM-A requires the extracellular membrane-distal loop, all domains of the protein were required for successful infection. Selection of FCV mutants resistant to receptor neutralization and measurements of protein hydrophobicity provided genetic and biological evidence indicating that FCV undergoes a significant conformational change upon interaction with fJAM-A.

This work shows that FCV interaction with fJAM-A results in changes to the capsid likely to be important for subsequent steps in infection, and suggests a determinant of virulence in FCV is accelerated entry post-binding.

BIOGRAPHICAL SKETCH

Robert J. Ossiboff, better known to friends as Oz, was born in Bridgeton, New Jersey in 1981. He grew up in southern New Jersey and attended elementary school at Upper Deerfield Township Schools and high school at Cumberland Regional, graduating in 1999. He attended Wake Forest University in Winston-Salem, North Carolina for one year before transferring to Loyola University Chicago where in 2003 he graduated *summa cum laude* with a bachelor's degree in biology. After knowing each other since elementary school, he married his wife Jess in December of 2002.

During his undergraduate education, Oz decided to pursue a career in veterinary medicine. He was accepted into the College of Veterinary Medicine at Cornell University and moved to Ithaca in the summer of 2003. Following the first year of his veterinary training, he participated in the Leadership Program for Veterinary Students. He was assigned to work with Dr. John S.L. Parker at the Baker Institute for Animal Health. His summer project investigating the growth kinetics of feline calicivirus served to both earn him the Leadership Program's Integrative Biology Award and strike his research interest. The following fall, he applied for entry into the dual DVM/Ph.D. degree program at Cornell, and was accepted in the spring of 2005. He took a leave from the veterinary curriculum starting in mid-spring 2005 and entered the graduate curriculum. In the fall of 2005, he returned to the lab of Dr. Parker to continue his work investigating feline calicivirus. He returned to the veterinary curriculum in mid-March 2008.

Upon completion of his Ph.D., he will remain at Cornell to finish the requirements of his DVM degree, expecting to graduate in 2010.

For Jess

ACKNOWLEDGMENTS

There are many people who deserve thanks for their help and support during my time spent here at Cornell. First, I would like to thank my advisor, Dr. John Parker, for the opportunity to work and learn under him. His guidance and support as both a mentor and an advisor was invaluable. I would also like to express my gratitude to Drs. Bob Weiss, Wayne Schwark, Joel Baines and Kenny Simpson for serving as members of my special committee. I also thank Alex Travis for his time as a proxy special committee member.

I especially thank the members of the Dual Degree Oversight Committee (past and present), particularly Drs. Colin Parrish, Alex Travis, and Hollis Erb for providing me with the opportunity and support that allowed me to pursue and complete my dissertation research. A special thanks to Janna Lamey for everything that she does for the dual degree program and its students. I am very grateful for her help regarding my request for an extra year of research, which made the completion of my dissertation in a timely manner possible.

I would like to thank all of my collaborators for the generous gift of reagents as well as for input and guidance, particularly Dr. Patricia Pesavento (University of California at Davis), Drs. Terry Dermody and Kristen Guglielmi (Vanderbilt University), Drs. B.V. Venkataram Prasad and Yi Zhou (Baylor College of Medicine), Dr. Slava Sosnovtsev (NIH), and Dr. Ian Goodfellow (Imperial College London).

I thank all of the people at the J.A. Baker Institute for Animal Health for creating such an enjoyable work environment; in particular, thanks to Jane Miller, Anita Hesser and Sue Williams for all of the administrative help. Thanks to all members (past and present) of the laboratories of Drs. Judy Appleton, Alexander Travis, and Colin Parrish who all likely provided help in some form or another at

some point. A special thanks to the members of the "grad office," Carole Harbison, Wendy Weichert, Danielle Buttke, Karla Stucker, and Laura Palermo, for all of the support and good times. I thank Christian Nelson for all his advice, whether it be scientific, personal, or just simply stupid. Without him I don't think I would have made it, and if I did, it certainly wouldn't have been as much fun.

All members of the Parker Lab (past and present) deserve many thanks for the technical assistance, advice (both scientific and personal), and encouragement they have offered me through the years. In particular, I appreciate the valuable contributions of Susanne Moessmer, Meagan Wisniewski, Caroline Coffey, Stephen Campbell, Lou Hom, and Alex Sheh. Thanks to all of the Leadership, veterinary, rotating graduate, and undergraduate students who taught me so much by letting me teach them.

I would like to thank my family for their support and encouragement. Finally, I would like to thank my wife Jess for all of her love, support, and perhaps most importantly, patience, through this process. I couldn't have done it without her.

TABLE OF CONTENTS

LIST OF FIGURES

LIST OF TABLES

CHAPTER 1

Introduction

1.1 Study Relevance

Feline calicivirus (FCV) is a common feline pathogen that causes a variety of clinical syndromes. While vaccination with attenuated-live FCV vaccines is widely practiced, vaccinated cats can still be asymptomatic carriers of the virus and are not protected from all circulating strains of FCV (Dawson et al., 1993, Gaskell et al., 1982, Knowles et al., 1990, Pedersen & Hawkins, 1995). Typically, FCV infection is either asymptomatic or causes mild upper respiratory signs, oral ulceration, and fever (Hoover & Kahn, 1975, Reubel et al., 1992). Morbidity is high, with prevalence rates of avirulent or mildly virulent FCV in multiple-cat environments as high as 36% (Bannasch & Foley, 2005, Binns et al., 2000). Fatal disease is unusual. In 1998 however, there was a reported outbreak of atypical FCV that caused severe systemic disease, with a fatal hemorrhagic-like fever being noted in some animals (Pedersen et al., 2000). Since that initial report, there have been multiple other documented outbreaks of extremely virulent FCV [termed virulent systemic (VS-) FCV due to the systemic nature of the symptoms caused by infection] that have resulted in mortality rates as high as 50% (Coyne et al., 2006, Hurley et al., 2004, Pesavento et al., 2004, Schorr-Evans et al., 2003). The extremely virulent nature of these viruses as well as the speed with which they can spread within veterinary hospitals and shelters (Pedersen et al., 2000, Schorr-Evans et al., 2003) makes their early identification imperative for limiting morbidity and mortality. Unfortunately, at present only pathologic examination of diseased tissues can confirm a FCV infection as being VS- in nature. Therefore, the identification of an *in vitro* characteristic of these virulent viruses would have great utility as a diagnostic. Understanding the molecular determinants of the shift in virulence of these viruses could also permit the creation of better vaccines or the development of antivirals or therapeutics to be used in the event of an outbreak.

The *Caliciviridae*, the virus family to which FCV belongs, contains several viruses of considerable medical and veterinary significance. Caliciviruses infect a wide variety of species including humans, rabbits, swine, bovines, sea lions, reptiles and cats (Green et al., 2000). The study of many viruses in this family is limited by the lack of culture systems. This is particularly true of the human noroviruses, which are responsible for > 90% of all cases of infectious gastroenteritis (Atreya, 2004, Mead et al., 1999). The absence of a cell culture system has greatly hindered norovirus investigation, for which there is urgent need for an effective vaccine (Estes et al., 2000). FCV can serve as a model for the related noroviruses; information gained regarding the interaction of FCV with cellular receptors is likely to be helpful in designing vaccines or therapeutics to prevent norovirus-receptor interactions.

1.2 Clinical signs of FCV infection

FCV infection in cats causes a variety of clinical presentations, ranging from asymptomatic to hemorrhagic-like systemic disease, and occurs in both acute and chronic forms (Reubel et al., 1992, Studdert, 1978). The most common clinical presentations of FCV infection are acute upper respiratory tract disease (URTD) and oral ulceration. Disease occurs after an incubation period of 2 to 10 days. Typical signs include fever (39.5 to 40.5° C), rhinitis, sneezing, excess salivation, serous or mucopurulent nasal and ocular discharge, and conjunctival hyperemia; disease may progress to include depression, anorexia, and /or lethargy. Ulcerative glossitis is frequently observed on the external nares, oral mucosa and tongue [as reviewed in (Hurley & Sykes, 2003, Studdert, 1978)]. Fatal disease is rare, although mortalities are occasionally observed in young kittens (< 12 weeks of age) and are generally associated with pneumonia (Kahn & Gillespie, 1971, Love & Baker, 1972).

Chronic FCV infection has also been implicated in the pathogenesis of feline gingivostomatitis. In some studies of the disease, it has been identified in up to 100% of cases (Knowles et al., 1991, Reubel et al., 1992), and in one case report, resolution of chronic gingivostomatitis resulted in the cessation of FCV shedding (Addie et al., 2003). However, while FCV isolated from a cat with chronic gingivostomatitis could cause acute disease experimentally, chronic disease could not be replicated with the isolated virus (Knowles et al., 1991, Poulet et al., 2000). Therefore, it is possible that FCV is not the cause of chronic gingivostomatitis, but instead an opportunistic infection.

FCV has also been documented to cause polyarthritis in cats, also referred to as "limping syndrome." This syndrome was reproduced experimentally in cats when infected with specific strains of FCV and caused synovitis when joints were directly inoculated with virus as well as when infected orally, albeit with less frequency, (Dawson et al., 1994, TerWee et al., 1997). Lameness has also been described in cats infected with strains associated with classical respiratory and oral signs (Poulet et al., 2000).

During the last decade there have been several outbreaks of extremely virulent FCV in both the US (Hurley et al., 2004, Pedersen et al., 2000, Schorr-Evans et al., 2003) and the UK (Coyne et al., 2006); these strains, termed VS-FCV, cause systemic disease and are associated with high mortality rates (50%). Clinical findings of these outbreaks include unresponsive fever, oral cavity and skin ulceration (lingual, mucocutaneous junctions, nose, pinnae, footpads, and distal extremities), edema of the head, pinnae, and paws, jaundice, and bleeding tendencies (Coyne et al., 2006, Hurley et al., 2004, Pesavento et al., 2004, Schorr-Evans et al., 2003). Outbreaks have ranged from a small number of affected animals to up to 50 (Hurley et al., 2004, Pesavento et al., 2008). In all reported outbreaks, vaccinated cats have been susceptible, suggesting

that currently available vaccines do not protect cats from VS disease. Captive exotic felids also appear to be susceptible to VS disease (Harrison et al., 2007).

Other documented disease syndromes associated with FCV infection are abortion (van Vuuren et al., 1999), neurologic signs (Sato et al., 2004), and lower urinary tract disease (Rice et al., 2002). FCV-like viruses have also been isolated from dogs with gastrointestinal disease (Evermann et al., 1985, Gabriel et al., 1996, Martella et al., 2002). Whether or not FCV was the causative agent for the observed clinical signs or if the virus was simply passing through the GI tract of the dogs is unclear.

1.3 Pathogenesis

FCV infection is believed to be transmitted oronasally, with cats being susceptible to infection via the nasal, oral or conjunctival routes; aerosol, droplet and fomite transmission are considered the most likely modes of infection (Radford et al., 2007, Studdert, 1978). The virus readily replicates in conjunctiva, oral mucosa and tongue epithelium (Studdert, 1978). However, virus can often be readily recovered from feces and intestines. As many of the *Caliciviridae* are gastrointestinal pathogens, it is possible fecal-oral routes of transmission and infection may be playing an important but currently overlooked role in FCV pathogenesis.

1.4 Taxonomy

FCV is a member of the family *Caliciviridae.* The family is divided into four genera: *Lagovirus, Norovirus, Sapovirus,* and *Vesivirus* (Green et al., 2000). Noroviruses and sapoviruses contain important human pathogens that cause acute gastroenteritis. The type lagovirus species is rabbit hemorrhagic disease virus (RHDV), and the genus includes other viruses that cause clinical disease of veterinary

importance in rabbits. FCV belongs to the genus vesivirus; other viruses of note within this genus that are of veterinary significance are San Miguel sea lion virus (SMSV) and vesicular exanthema of swine virus (VESV). The addition of two additional genera, *Becovirus* and *Recovirus*, has been recommended following genomic sequence analysis of pathogenic bovine enteric virus Newbury agent-1 and Tulane virus, a calicivirus isolated from stool samples from rhesus macaques (Farkas et al., 2008, Oliver et al., 2006).

1.5 Calicivirus genome structure and organization

Caliciviruses contain a single-stranded, positive sense RNA genome. The genome of FCV is ~ 7.7 kb in length, contains three open reading frames (ORFs), and is polyadenylated at its 3' terminus (see Figure 1.1) (Carter et al., 1992, Clarke & Lambden, 1997). The 5' ORF (ORF1) encodes a polyprotein (~ 1800 amino acids) that contains six non-structural proteins (Carter, 1989, Sosnovtseva et al., 1999). ORF2 and ORF3 encode the structural proteins; the beginning of ORF3 overlaps the end of ORF2 by 4 nucleotides. ORF2 encodes the major capsid protein (VP1; ~670 amino acids), and ORF3, located at the 3' end of the genome, encodes a minor structural protein (VP2; ~100 amino acids) (Carter, 1989, Sosnovtsev et al., 2005). During infection, there is abundant production of subgenomic RNAs (~2.4 kb) that are 3'-coterminal with the full length genome and contain ORFs 2 and 3 (Carter et al., 1992, Neill & Mengeling, 1988, Neill et al., 1991). RNA secondary structure (single stem loop) is predicted to exist in the 3' noncoding region of FCV (Seal et al., 1994).

1.6 Translation and processing

Translation of the calicivirus RNA genome and subgenome occurs in the absence of a 5'-cap or internal ribosome entry site. Instead, FCV genomic and

Figure 1.1. Translation and processing of the FCV genome and subgenome. A schematic representation of the translation of both the full-length and subgenomic mRNA of FCV and the resulting processing of proteins is shown. Individual proteins and designations currently used in the literature are indicated; the sites of cleavage by the viral proteinase (if applicable) are denoted by an arrow.

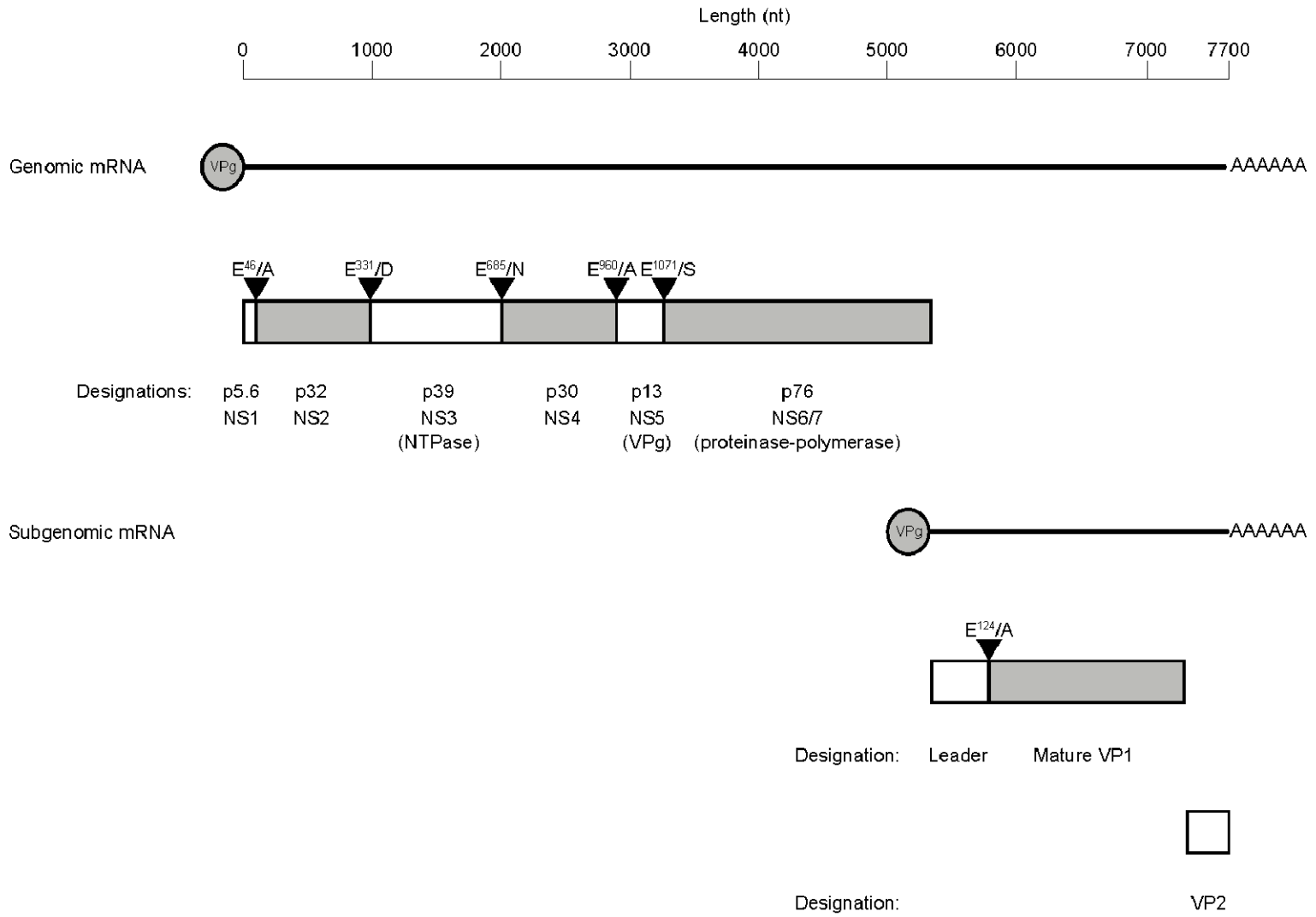
Length (nt)
0
1000
2000
3000
4000
5000
6000
7000
7700
Genomic mRNA
VPg
AAAAAA
E46/A
E331/D
E685/N
E960/A
E1071/S
Designations:
p5.6
NS1
p32
NS2
p39
NS3
(NTPase)
p30
NS4
p13
NS5
(VPg)
p76
NS6/7
(proteinase-polymerase)
Subgenomic mRNA
VPg
AAAAAA
E124/A
Designation:
Leader
Mature VP1
Designation:
VP2

subgenomic RNA are covalently linked to a virally-encoded 15.5 kD protein, VPg (Herbert et al., 1997, Sosnovtsev & Green, 2000). Interactions between calicivirus VPg and the eukaryotic initiation factors (eIFs) 4E and 3 have been demonstrated, and it is thought the VPG is acting as a cap substitute during the initiation of translation on virus mRNA (Chaudhry et al., 2006, Goodfellow et al., 2005). Removal of the VPG substantially decreases the efficiency of *in vitro* translation of FCV RNA (Burroughs & Brown, 1978, Dunham et al., 1998, Herbert et al., 1997), and mutation to a tyrosine residue within VPg thought to be important for covalent linkage to the FCV genome was lethal (Mitra et al., 2004).

Translation of ORF1 results in a polyprotein containing the FCV non-structural proteins. The polyprotein is autocatalytically processed by the virus-encoded proteinase-polymerase, which is located at the C-terminus of the polyprotein (Figure 1.1) (Sosnovtsev et al., 2002, Sosnovtseva et al., 1999). The liberated proteins p32 [NS2], p39 [NTPase; NS3] , p30 [NS4] , p13 [VPg; NS5], and p76 [proteinase-polymerase; NS6/7] participate in protein-protein interactions with each other as well as the structural proteins, presumably to play key roles in virus replication and encapsidation (Kaiser et al., 2006, Sosnovtsev et al., 2002). The function of an additional small protein, p5.6 [NS1], released from the N-terminus of the polyprotein, is unknown.

The structural proteins are translated from the second and third ORFs as found in both the full-length and subgenomic RNAs of FCV. ORF2 encodes the 73 kDa capsid precursor protein. The N-terminal end of the capsid precursor, the 11 kDa leader capsid, is cleaved from the mature 62 kDa capsid protein by the calicivirus proteinase-polymerase (Carter et al., 1992, Neill et al., 1991, Sosnovtsev et al., 1998). The minor structural capsid protein, VP2, is translated from ORF3. The reinitiation of ORF3 translation following termination of VP1 synthesis is achieved in a

termination/reinitiation process that requires upstream sequence located at the 3' end of ORF2 (Luttermann & Meyers, 2007). Although VP2 is not visible in the crystallographic structures of two caliciviruses, it is essential for productive replication in the synthesis and maturation of infectious FCV virions, and is possibly involved in RNA encapsidation (Sosnovtsev et al., 2005, Sosnovtsev & Green, 2000).

1.7 Calicivirus structure

The calicivirus virion is icosahedral with distinctive depressions that appear cup-like by negative-stain electron microscopy (Figure 1.2A); this characteristic appearance is the name-sake of the family (calici- is derived from the Latin word for cup-shaped, *calyx*). Cryo-electron microscopy (cryo-EM) reconstructions have been determined for noroviruses [virus-like particles (VLPs) of recombinant Norwalk virus (NV) and Parksville virus, and native murine norovirus], sapoviruses (recombinant Grimsby VLPs), lagoviruses [recombinant VLPs of RHDV], and vesiviruses [SMSV, primate calicivirus Pan-1, and most recently, FCV] (Bhella et al., 2008, Chen et al., 2004, Katpally et al., 2008, Prasad et al., 1994, Prasad et al., 2000, Thouvenin et al., 1997). Crystallographic structures have been determined for two members of the *Caliciviridae*, native SMSV (serotype 4) and VLPs of recombinant NV (Chen et al., 2006, Prasad et al., 1999).

Structural data show that caliciviruses exhibit T = 3 icosahedral symmetry. They are composed of 180 copies of the major capsid protein arranged into 90 arch-like dimers that form the icosahedral lattice. The characteristic cup-like depressions appear at the five- and three-fold positions, created by the protruding capsomeres (Figure 1.2B). The crystal structure of closely related SMSV4 (~50% identity to FCV mature capsid protein) and NV both consist of three quasiequivalent subunits (A, B, and C). A and B subunits form A/B dimers, and the two C subunits

Figure 1.2. Calicivirus structure. (A) Negative-stain transmission electron microscopy images of FCV particles. (B) Capsid structure of the closely related calicivirus, SMSV4. A, B, and C quasiequivalent positions and the 5- and 3-fold axes are indicated. (C) Structure of the SMSV4 capsid monomer demonstrating the structural domains of the protein: NTA (green), Shell (red), Protrusion (P1 subdomain, yellow; P2 subdomain, blue).

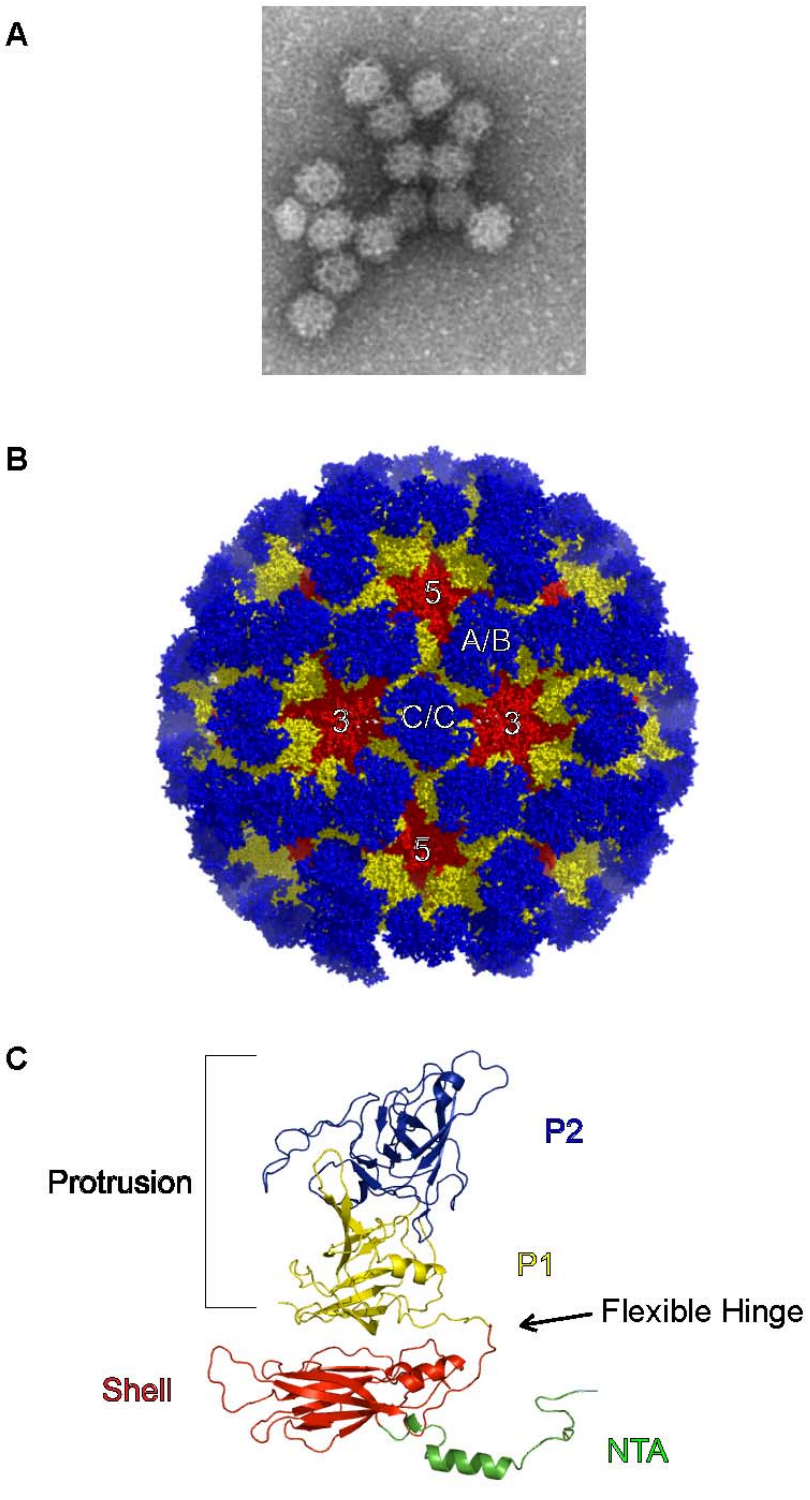
A
B
5
A/B
3
C/C
3
5
C
Protrusion
P2
P1
Flexible Hinge
Shell
NTA

interact to form C/C dimers. Individual subunits are composed of three structural domains: N-terminal arm (NTA), shell, and protruding domain (Figure 1.2C) (Chen et al., 2006, Prasad et al., 1999).

The shell domain forms an icosahedral scaffold that encapsidates the virus genome. The shell domain folds into an eight-stranded β-barrel, a common structural feature seen in the capsids of many other viruses (Harrison, 2001, Rossmann & Johnson, 1989). The eight strands form two four-stranded antiparallel sheets. In addition to shell-shell domain interactions, the β-barrel also interacts with the NTA domain. One strand of one β-sheet of the S domain interacts with the N-terminal loop of the NTA of the opposing subunit, forming extensive domain-swapping interactions. In SMSV, the β-barrel configuration and the shell/NTA domain interactions maintain the icosahedral symmetry of the capsid (Chen et al., 2006).

The protruding domain of caliciviruses can be divided into two distinct subdomains, the proximal P1 and the distal P2 subdomains (Figure 1.2C). The P2 subdomain is a large insertion in the P1 subdomain. As such, P2 divides P1 into two polypeptide segments located N- and C- terminal to P2. The fold of the calicivirus P domain, a twisted β-sheet formed by the four strands in the C-terminal portion of P1 and a lone α-helix, is not seen in any other proteins (Chen et al., 2006, Prasad et al., 1999). The P2 domain contains a compact barrel of six β-strands that are connected by loops of various lengths. Neutralizing epitopes of FCV mapped on the structure of SMSV consist of loops connecting the β-strands of the compact barrel (Chen et al., 2006, Radford et al., 1999, Tohya et al., 1997). Despite low sequence similarity between SMSV and NV, the six strands are arranged in a similar manner in each virus; the conservation of the fold in the P2 domain across two genera despite weak sequence homology suggests that this fold is conserved in all caliciviruses (Chen et al., 2006).

Interactions between residues in the protrusion domain are responsible for the formation of dimers. In SMSV4, only the distal P2 subdomain is involved in dimer formation, whereas in recombinant NV VLPs, both P1 and P2 contribute residues important for dimer formation (Chen et al., 2006, Prasad et al., 1999). The P domain alone of NV, when expressed in bacteria and purified, forms extensive dimers that demonstrate the same conformation seen in the crystal structure of recombinant NV VLPs (Choi et al., 2008).

In cryo-EM reconstructions of another norovirus, mouse norovirus, extensive interactions of both P1 and P2 result in the formation of a secondary shell created by the P1 subdomain. This conformation is made possible by the extension of the P domain away from the S domain by the flexible hinge region present in all caliciviruses (Figure 1.2) (Katpally et al., 2008). The structure of SMSV4 also shows an additional point of flexibility not observed in Norwalk virus, between the P1 and P2 subdomains (Chen et al., 2006). Conformational changes within the capsid are likely important for viral entry and delivery of genomic material (discussed in Section 1.10), and such areas of flexibility may play important roles in mediating such structural alterations.

1.8 Calicivirus cell surface receptors

Cellular receptors have been identified for human noroviruses, RHDV, and FCV. Both the human noroviruses and RHDV attach to complex carbohydrate histo-blood group antigens (HBGAs) on the surface of susceptible cells (Huang et al., 2005, Marionneau et al., 2002, Ruvoen-Clouet et al., 2000). For noroviruses, HBGAs appear to be required for efficient infection *in vivo* (Hutson et al., 2002). Furthermore, susceptibility to norovirus infection is dependent on the individual's HBGA expression (Lindesmith et al., 2003). Recent structural studies examining the binding

of HBGAs to recombinant P domain dimers show that the HBGAs bind in a surface-exposed shallow depression in the outermost face of the P-domain (Choi et al., 2008). However, human cells expressing the appropriate HBGAs are unable to efficiently endocytose or be infected by norovirus VLPs (White et al., 1996). Additionally, strains of human noroviruses have been identified that do not bind HBGAs (Huang et al., 2005, Lindesmith et al., 2005). In light of these facts, it is hypothesized that presently unidentified co-receptor(s) are necessary for infectious entry of noroviruses.

The kinetics and biochemical binding of FCV to a permissive cell line, Crandell-Reese feline kidney (CRFK) cells, was first investigated by Kreutz et al (1994). This study showed that the treatment of CRFK cells with proteases increased FCV binding while cells treated with neuraminidase and O-glycanase showed a decreased binding ability (Kreutz et al., 1994). Since that publication, two cellular receptors have been identified for FCV. Makino et al. (2006) used a cDNA library of a permissive feline cell line to identify that feline junctional adhesion molecule A (fJAM-A) as a cellular binding molecule of FCV. Expression of fJAM-A in non-permissive tissue culture cells led to binding and infection by a tissue culture adapted strain of FCV (F4); furthermore, an antibody generated against fJAM-A reduced the ability of FCV to bind to and infect permissive feline cells (Makino et al., 2006). Shortly thereafter, a carbohydrate receptor, α2,6-linked sialic acid, was identified (Stuart & Brown, 2007). Treatment of CRFK cells with selective neuraminidases showed that cleavage of α2,6- but not α2,3-linked sialic acid reduced the binding and infection by a tissue-culture adapted vaccine strain of FCV (F9). Treatment of cells with proteases and metabolic inhibitors suggested that the recognized carbohydrate moiety was present on a *N*-linked glycoprotein.

1.9 Junctional adhesion molecule A

Junctional adhesion molecule A (JAM-A) is a type I transmembrane glycoprotein (MW 36-41 kDa). It consists of a N-terminal signal peptide, an extracellular domain [composed of two immunoglobulin (Ig-) like domains - a membrane-distal D1 and a membrane-proximal D2], a transmembrane domain, and a short cytoplasmic domain that contains a type II PDZ domain-binding motif (Figure 1.3A) (Ebnet et al., 2000, Mandell & Parkos, 2005). The two Ig-like domains in the extracellular domain of the protein classify JAM-A as a member of the immunoglobulin superfamily (IgSF).

JAM-A belongs to a family of proteins important in maintaining intercellular tight junctions (Martin-Padura et al., 1998). In humans and mice, JAM-A localizes to the intercellular tight junctions of endothelial and epithelial cells (Liu et al., 2000, Mandell et al., 2004). Crystallographic structure of recombinant human and murine JAM-A shows that in solution, JAM-A forms homodimers that are stabilized by ionic and hydrophobic interactions between residues in the D1 domain dimerization motif (Fig. 1.3B) (Kostrewa et al., 2001, Prota et al., 2003). In addition, JAM-A has been shown to naturally form homodimers on the surface of cells (Bazzoni et al., 2000) . The formation of homodimers is critical in establishing a regulated tight junctional barrier between cells, and it is thought that homophilic interactions between JAM-A dimers on opposing cell surfaces are important for forming intercellular tight junctions (Liu et al., 2000, Mandell et al., 2004, Martin-Padura et al., 1998, Williams et al., 1999).

JAM-A is also expressed on the surface of platelets, leukocytes and erythrocytes (Gupta et al., 2000, Williams et al., 1999). It is believed to play a role in modulating leukocyte transmigration as well as platelet activation and aggregation (Babinska et al., 2002, Ozaki et al., 1999, Sobocka et al., 2004). Deficiencies in

Figure 1.3. JAM-A structure. (A) Schematic representation of feline JAM-A. (B & C) Crystal structure of hJAM-A ectodomain dimer as viewed from the side (B) and above (C). For one monomer, the membrane-distal D1 domain is shown in blue, the membrane-proximal D2 domain in red, and the linker region between the two domains in yellow. Panel C demonstrates the sites of contact between adjacent monomers in dimer formation.

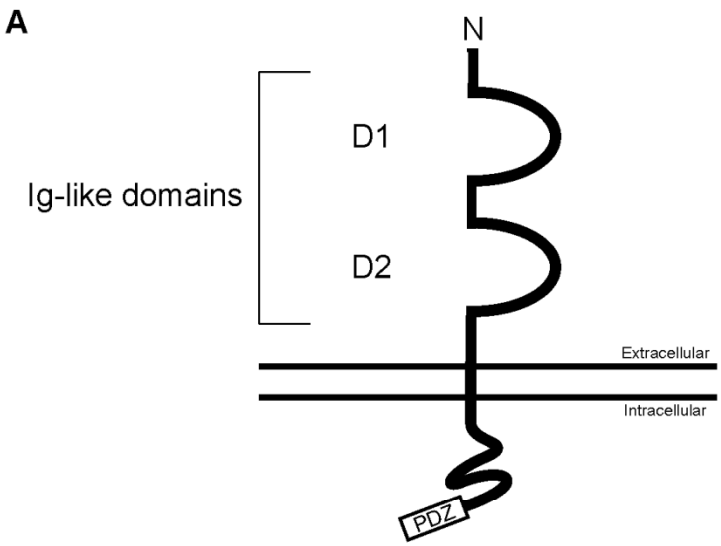
A
N
D1
Ig-like domains
D2
Extracellular
Intracellular
PDZ

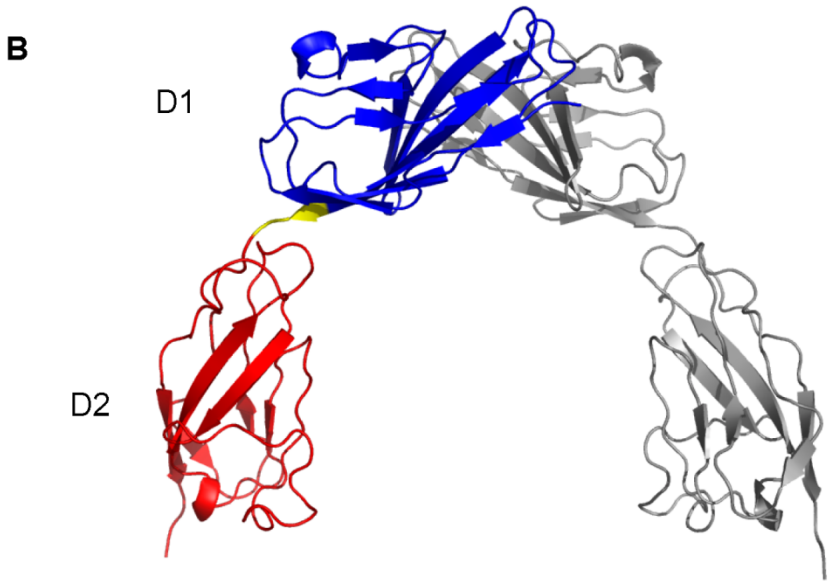
B
D1
D2

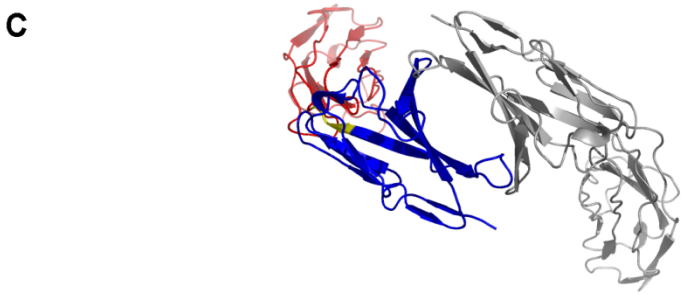
C

JAM-A expression or function result in leukocytes becoming trapped between endothelial cells as they respond to inflammation (Khandoga et al., 2005, Martin-Padura et al., 1998, Ostermann et al., 2005). Additionally, JAM-A has been shown to play a role in both angiogenesis (Naik et al., 2003a, Naik et al., 2003b) and cell migration of epithelial and endothelial cells (Naik & Naik, 2006, Severson et al., 2008). Severson et al (2008) showed in tissue culture cells that JAM-A dimerization regulated epithelial cell migration indirectly through signaling events that altered the expression levels of another adhesion protein, integrin β1. This suggests that JAM-JAM interactions are likely to play an important role in the regulation of expression levels of other cellular adhesion proteins.

1.10 IgSF cell surface proteins as viral receptors

Animal viruses utilize host cellular factors as receptors to allow for specific attachment to the host cell surface. IgSF proteins, of which JAM-A is a member, are important in the fundamental cellular processes of binding, adhesion, or recognition. As such, several different virus families utilize IgSF proteins as viral receptors. JAM-A has been shown to be a functional receptor for both FCV and mammalian orthoreoviruses (*Reoviridae*) (Barton et al., 2001, Makino et al., 2006). The σ1 attachment protein of reoviruses engages residues present within the dimerization motif of the human JAM-A D1 domain (Campbell et al., 2005, Forrest et al., 2003, Guglielmi et al., 2007). Coxsackie B viruses (*Picornaviridae*) and most adenovirus (*Adenoviridae*) subgroups utilize the coxsackievirus and adenovirus receptor (CAR) (Bergelson et al., 1997). Like JAM-A, CAR has two extracellular Ig-like domains, localizes to tight junctions in polarized epithelial cells or to sites of cell-cell contact, and forms homodimers mediated by a dimerization motif within its D1 domain dimerization motif (Cohen et al., 2001, Martin-Padura et al., 1998). Comparable to the

interaction of the reovirus σ1 protein with JAM-A, the adenovirus fiber knob protein also interacts with residues found mostly within the dimer interface of the CAR D1 domain (Bewley et al., 1999, Law & Davidson, 2005). Coxsackie B viruses interact with the distal end of the CAR D1 domain via surface residues in the canyon region of the capsid that surrounds the five-fold icosahedral axes (He et al., 2001). Poliovirus, another member of the *Picornaviridae*, uses a nectin-like protein PVR (the poliovirus receptor) (He et al., 2000). PVR contains three Ig-like loops in the extracellular domain; poliovirus engages the membrane distal D1 domain of PVR (He et al., 2000). Intercellular adhesion molecule-1 (ICAM-1) serves as the cellular receptor for three more members of the *Picornaviridae*, human rhinovirus (HRV14 and HRV16) and Coxsackie A virus (CAV21). These viruses also engage ICAM-A via the membrane distal D1 domains of the receptor (Kolatkar et al., 1999, Olson et al., 1993, Xiao et al., 2001). The spike glycoprotein of mouse hepatitis virus (*Coronaviridae*), binds to the murine carcinoembryonic antigen cell adhesion molecule (CEACAM) at the membrane distal D1 domain (Dveksler et al., 1993, Dveksler et al., 1991). Rabies virus (*Rhabdoviridae*) is able to enter cells expressing the neural cell adhesion molecule (CD56) (Thoulouze et al., 1998). Lastly, a PVR-like molecule, PVR-related protein 1, was capable of mediating the entry of several alphaherpesviruses, including herpes simplex virus 1 and 2, porcine pseudorabies virus, and bovine herpesvirus 1 (Geraghty et al., 1998). It is not known what regions of fJAM-A are required for FCV binding, but as illustrated above, the membrane distal D1 domain of the receptor is likely to be involved in the interaction.

1.11 Entry of nonenveloped viruses

To deliver their genomic material into the cytosol or nucleus in the host cell, viruses must breach the complex barrier of membranes surrounding the cell.

Enveloped viruses are surrounded by a lipid membrane; as such, delivery of the genome containing viral nucleocapsid is achieved following fusion of the viral and cellular membranes. However, nonenveloped viruses lacking a lipid bilayer must breach cellular membranes directly to gain access to the cytosol or nucleus. For most nonenveloped viruses, this is believed to occur following conformational changes within the capsid structure initiated by environmental or cellular factors such as receptors, low pH or proteases [as reviewed in (Tsai, 2007)].

For polioviruses, rhinoviruses, and most related enteroviruses, the cue promoting conformational change within the capsid is interaction with the cellular receptor at physiological temperatures (Crowell & Philipson, 1971, De Sena & Mandel, 1977, Lonberg-Holm & Korant, 1972). The induced conformational changes result in the formation of a 135S altered (A-) particle. Compared to the 160S native picornavirus virion, the A-particle displays (a) modified sedimentation behavior, (b) increased hydrophobicity, and (c) altered antigenicity (De Sena & Mandel, 1977, Fenwick & Cooper, 1962). Structurally, the N-terminus extension of one of capsid protein (VP1) and an additional myristoylated capsid protein (VP4), present on the interior of the native virion, are externalized or released, respectively, in the A-particle. The exposed VP1 N-terminal extension, which is predicted to form an amphipathic helix, enables the A particle to attach to liposomes (Fricks & Hogle, 1990); furthermore, A-particles form channels in planar bilayers (Tosteson & Chow, 1997). Together, these data suggest that in the presence of receptor, the channels become a pore, allowing the RNA genome to be extruded into the cytosol (Hogle, 2002). This hypothesis is supported by findings in live cells that poliovirus genome release is highly efficient and rapid, occurring within vesicles or membrane invaginations within 100-200 nm of the plasma membrane (Brandenburg et al., 2007).

For the first 30 minutes of experimental infections of poliovirus, A-particles are the predominant form of cell-associated virus, although a significant amount of A-particles elute from the cells. At later times post infection however, the appearance of a second altered form of the virus is noted. These particles sediment at 80S and are devoid of the RNA genome (De Sena & Mandel, 1977). The increase in prevalence of 80S particles correlates with the disappearance of 135S particles (Fricks & Hogle, 1990). The trigger for conversion to the 80S subunit is unknown, but it does not require receptor (Hogle, 2002).

For other nonenveloped viruses, such as papillomaviruses, reoviruses, and rotaviruses, conformational changes are triggered by cellular proteases. Papillomaviruses are taken into cells by endocytosis and are trafficked to the trans-Golgi. While in the trans-Golgi, the virus is exposed to the calcium-dependent serine endoprotease, furin. The papillomavirus minor virion protein L2 contains a consensus furin recognition site. Furin cleavage of the N terminus of the L2 protein is a necessary step for viral infection, and recent evidence suggests that cleavage of L2 exposes the membrane-disrupting C terminus which primes the virus for endosomal escape by membrane penetration (Kamper et al., 2006, Richards et al., 2006). Reovirus penetration of endolysosomal membranes also requires proteolytic priming within the endolysosomal system. Cysteinyl cathepsins B and L are responsible for the degradation of the reovirus outer capsid protein σ3 (Baer & Dermody, 1997, Ebert et al., 2002, Ebert et al., 2001). σ3 is normally in complex with an additional reovirus outer capsid protein, μ1; cleavage of σ3 allows for the conversion of μ1 into a protease-sensitive, hydrophobic conformer (Chandran et al., 2002, Liemann et al., 2002). This structural transition primes the particle for membrane penetration (Chandran et al., 2002). For rotaviruses, trypsin-mediated cleavage of the outer capsid protein VP4 within the intestinal lumen generates a protein fragment (VP5*) that is

able to disrupt membranes (Denisova et al., 1999, Estes et al., 1981). This cleavage event is what permits rotavirus to permeabilize cellular membranes (Arias et al., 1996).

Low endosomal pH is also an important cue for the conformational alterations of several nonenveloped viruses. Canine parvovirus (CPV) possesses a phospholipase (PLA_2) present at the N terminus of the VP1 structural protein (Suikkanen et al., 2003). Exposure to the acidic environment of the endolysosomal compartment triggered exposure of the N-terminus of VP1 and the activity of PLA_2; the exact role of the PLA_2 in parvovirus entry is unknown, but it is suggested that it has a critical function in the process (Mani et al., 2006, Suikkanen et al., 2003). Adenoviruses also undergo conformational alterations following exposure to low pH. Studies investigating the effect of pH on the ability of adenovirus to penetrate membranes showed that endosomal acidification enhanced membrane lysis by the virus (Seth et al., 1984); furthermore it was discovered that capsid disassembly occurs within endosomes and appeared to require acidification (Greber et al., 1993). The reduced pH of the endosome promotes membrane lysis by destabilizing the adenovirus capsid. This destabilization results in the dissociation of proteins and liberates a pH-independent membrane lytic factor (Wiethoff et al., 2005).

1.12 Entry of feline calicivirus

Little is known about the details regarding the entry process of FCV or any of the other members of the *Caliciviridae*. The sensitivity of FCV infection to the effects of chloroquine suggested that FCV entry into cells requires a low pH-dependent step (Kreutz & Seal, 1995). Expanding on the initial studies, Stuart & Brown (2006) found that FCV infects cells via clathrin-mediated endocytosis. Furthermore, they showed that early during entry, FCV permeabilizes membranes as evident by cell

susceptibility to the translational inhibitor, α-sarcin. Inhibition of cellular acidification prevented virus-induced intoxication by the translational inhibitor, suggesting that acidification is a required step for virus uncoating and cytoplasmic delivery of the genome (Stuart & Brown, 2006).

Recently, a cryo-EM reconstruction of FCV (vaccine isolate F9) complexed with fJAM-A was determined by Bhella et al (2008). As no crystallographic structure has been determined for either FCV or fJAM-A, the cryo-EM data was mapped to the crystal structures of SMSV4 and hJAM-A, respectively. The structure showed fJAM-A binding to FCV-F9 at 4°C induced significant alterations in the capsid structure, as evident by both a rotation of the P domain dimer about its local two-fold symmetry axis and a rotation of the S domain in the opposite direction of the P-domain rotation (Bhella et al., 2008). These data suggest that, as discussed for other nonenveloped viruses, conformational changes within the FCV particle are likely important in the process of entry and uncoating.

1.13 Virus capsids as metastable structures

Interactions of poliovirus with its cellular receptor result in the formation of the A-particle, exposing the N terminal extension of VP1 and releasing the myristoylated-VP4. While the receptor induced conformation to the A particle is irreversible, transient and reversible exposure of the N terminal extension of VP1 and VP4 occurs at physiologic temperatures (Li et al., 1994). This process has been termed "breathing" and it has also been demonstrated in another picornavirus (rhinovirus) as well in the nonenveloped insect virus, Flock house virus (*Nodaviridae*) (Bothner et al., 1998, Lewis et al., 1998). In rhinoviruses, "breathing" could be blocked through the use of WIN compounds, drugs that bind to a hydrophobic pocket in VP1 resulting in the stabilization of the capsid and inhibition of uncoating (Lewis et al., 1998). WIN-

resistant mutants generally blocked the binding of the molecules to the pocket by altering residues adjacent to the pocket. Although resistant to WIN compound neutralization, these viruses were so unstable they spontaneously lost VP4 at physiologic temperatures (Heinz et al., 1989, McKinlay, 1993).

Some plant viruses also exhibit capsid dynamics, but in the way of large-scale, reversible quaternary structure changes. This was first observed for Brome mosaic virus (BMV), an RNA virus with T=3 icosahedral symmetry, much like that found in the *Picornaviridae* and *Caliciviridae*. When BMV particles are treated with EDTA and exposed to neutral pH, the particles swell resulting in a 40 Å increase in diameter (Incardona & Kaesberg, 1964). Particle swelling is also observed in two other groups of plant viruses, the sobemovirus and tombusvirus groups [as reviewed by (Johnson, 2003)]. Structural studies later showed that virus particle expansion is due to charge repulsion at the quasi-3-fold symmetry axes following deprotonation of carboxyl clusters postulated to bind divalent metal ions (Durham & Hendry, 1977, Robinson & Harrison, 1982). The biological role of plant virus swelling is unknown, and it is unclear whether the phenomenon represents a single function for all plant viruses in which it is found (Johnson, 2003).

The structural flexibility of particles has also been studied through the use of biochemical inactivators such as azridines. The picornavirus foot-and-mouth disease virus (FMDV) demonstrates a higher buoyant density (1.43 g/ml) than other members of the *Picornaviridae* (poliovirus, coxsackie and ECHO viruses, and swine vesicular disease virus) which have a buoyant density in CsCl of 1.32 g/ml. FMDV is also unstable below pH 7, resulting in capsid disruption and RNA release, while the picornaviruses mentioned above are stable at pH 3 [as reviewed in (Witz & Brown, 2001)]. The more open structure of FMDV permits rapid inactivation by N-acetyl-ethyleneimine (AEI), an inactivant that reacts preferentially with viral nucleic acid

without affecting viral proteins, at both 25° and 37°C. In contrast, while poliovirus particles are inactivated rapidly by AEI at 37°C (when the particles are swollen due to breathing), they are inactivated much slower at 25°C (Burrage et al., 2000). Like FMDV, vesicular exanthema of swine virus (VESV), a member of the vesivirus genus of the *Caliciviridae* with a buoyant density of 1.38 g/ml, was rapidly inactivated following incubation with AEI at 37°C. Suspension of virus in 1M NaCl however reduced the diameter of the particles from 35 nm to 25 nm, and inactivation of VESV by AEI was reduced considerably (Witz & Brown, 2001).

Of all virus particles studied to date, such particle dynamics and fluctuations appear to be "built-in" (Johnson, 2003). For animal viruses, these dynamics suggest that the viruses are primed to undergo larger, concerted, and irreversible changes upon interaction with specific host factors (Hogle, 2002). The observation of virus breathing or A-particle conversion (in the absence of receptor in hypotonic buffers) at 37°C but not room temperature (Li et al., 1994, Wetz & Kucinski, 1991), suggests that the activation energy in this conversion pathway is high. This high activation energy may serve to kinetically trap the virus in a metastable state. Virus interactions with its receptor may then serve to lower the activation barrier for the conversion, triggering the conformational change. Such a barrier may be useful to the virus as it prevents virus aggregation that would likely occur due to the permanent exposure of the hydrophobic peptides (Johnson, 2003). Additionally, it would exclude entry into cells lacking the appropriate receptor(s).

1.14 Determinants of virulence

When virus infection results in clinical disease within the host, the resulting disease symptoms may exhibit dramatic variation in their severity. In some cases, these variations are a product of host-mediated pathogenesis, where more aggressive

responses to infection result in damage to host tissues. Such is the case for the pathogenesis of Dengue virus (*Flaviviridae*), which generally causes a benign syndrome termed dengue fever; however, infection can also cause dengue hemorrhagic fever, a severe syndrome characterized by hemostatic disorders, increased vascular permeability, and often internal bleeding and shock (Halstead, 1988). While virulent virus genotypes may play a minor role in causing dengue hemorrhagic fever (Holmes & Twiddy, 2003), current evidence suggests that the most likely cause of the severe syndrome is antibody dependent enhancement [as reviewed in (Stephenson, 2005)]. In this phenomenon, host dengue-specific antibodies bound to Fc receptors on the surface of monocytes and macrophages serve as co-receptor for the virus, enhancing the efficiency of virus binding and increasing the number of infected cells. Thereby, preexisting host antibodies to the virus serve to increase viral load, shorten incubation times, and ultimately increase disease severity.

Theiler's murine encephalomyelitis virus (TMEV) is a neurovirulent picornavirus of mice. Upon establishing a persistent infection, the virus induces axonal demyelination that leads to a spastic paralysis. The loss of myelin, however, is primarily immune-mediated [as reviewed in (Lipton et al., 2005)]. TMEV replication within the CNS triggers the expansion of virus-specific CD4+ T cells and the recruitment of monocytes. Recruited monocytes differentiate into macrophages. The activated macrophages and cytokines secreted by the activated T cells result in bystander damage to the myelin sheaths. The infection, and thereby myelin damage, is perpetuated by TMEV infection of macrophages recruited to the site.

However for other viruses, such as poliovirus (*Picornaviridae*), virulence is largely determined by the viral genotype. The vast majority of poliovirus infections are asymptomatic and characterized by a primary, transient viremia; in about 5% of the cases the virus spreads and replicates in other tissues causing a secondary viremia,

resulting in a sore throat, headache, and/or fever (Sabin, 1956). However, in less than 1% of poliovirus infections, paralytic disease occurs due to virus replication within motor neurons. Much of the work determining molecular determinants of poliovirus neurovirulence has been determined through the analysis of attenuated vaccine strains of neurovirulent isolates [as reviewed in (Blondel et al., 1998)]. While many mutations were found in the attenuated strains, there were several notable trends. All three vaccine strains contained changes to the 5' non coding region of the poliovirus genome that strongly associated with attenuation. The mutations were present within the internal ribosome entry site important in the initiation of translation. One hypothesis for attenuation is that alterations to the secondary structure of the IRES limit the binding of cellular initiation factors; an alternative explanation is that the mutations permit the binding of inhibitory factors present in neuronal cells (Blondel et al., 1998). Other mutations were present within the structural proteins VP1, VP3, and VP4 (Bouchard et al., 1995, Westrop et al., 1989). How the mutations in the structural proteins alter virulence is unknown, but it has been hypothesized they are implicated in viral uncoating or in viral assembly. While the investigation of attenuated mutants may provide insight for possible molecular determinants of virulence, it is difficult to determine if similar changes present in poliovirus populations play an important role in conferring neurovirulence. Nevertheless, it is clear that polioviruses are capable of producing a range of clinical disease that is not solely mediated by the host response.

In viruses that contain segmented genomes, such as reoviruses and bunyaviruses, genetic determinants of virulence can be tracked with the production of reassortant viruses. Reassortant viruses are produced following co-infection of permissive tissue culture cells with two different characterized viruses. By examining the disease phenotype produced by animals infected with the reassortant viruses and comparing it to the disease phenotype of the parent viruses, individual genome

segments can be linked with pathogenesis. Using reassortant reoviruses, many of the pathogenic phenotypes observed in infected mice infected have been mapped to specific viral gene segments (Hrdy et al., 1982, Sherry & Fields, 1989, Wilson et al., 1994). Reassortant bunyaviruses identified that both neurovirulence and neuroinvasiveness map to particular genome segments (Endres et al., 1991, Janssen et al., 1986).

In birds, the virulence of influenza is determined by the ability of the virus to spread systemically. Systemic pathogenesis has been linked primarily to properties of the hemagglutinin glycoprotein (HA) [as reviewed in (Steinhauer, 1999)]. The virus HA serves to both bind sialic acid-containing cell surface receptors and, following endocytosis, mediate fusion of the viral and cellular envelopes. It is translated as a precursor (HA_0) which is post-translationally cleaved into two subunits (HA_1 and HA_2). Cleavage of HA_0 is necessary for infectivity, as it activates the fusion potential of the HA. For most influenza viruses, the HA is cleaved by extracellular trypsin-like proteases. This limits the spread of the virus to host tissues where the appropriate proteases are encountered (Compans et al., 1970, Laver, 1971, Skehel, 1972). In contrast, the HAs of highly pathogenic viruses are cleaved intracellularly. This cleavage is performed by the ubiquitously expressed protease furin within the endoplasmic reticulum (Vey et al., 1992, Walker et al., 1994). The cleavage of HA by intracellular proteases is made possible by either the insertion of basic amino acids within the peptide connecting HA_1 and HA_2 or the lack of a carbohydrate moiety (Horimoto & Kawaoka, 1995, Horimoto & Kawaoka, 1997, Kawaoka et al., 1984, Kawaoka & Webster, 1989). In both cases it is believed that the changes allows for greater accessibility of the cleavage site for activating proteases than less pathogenic strains. Such intracellular cleavage permits the virus to spread systemically, which in avian hosts is associated with high virulence.

It is unknown whether the spectrum of disease syndromes observed in FCV infection is due to viral genotype, host response, or a combination of both. In a study by Foley et al (2006), affected tissues of cats experimentally inoculated with an FCV isolate causing systemic disease displayed elevated cytokines, suggesting that pathogenesis is at least partly immune-mediated. But, as the disease syndrome has been replicated using viruses isolated from virulent systemic outbreaks of FCV, there is likely a strong viral genetic component (Foley et al., 2006, Pedersen et al., 2000).

1.15 Thesis Overview

This thesis will investigate (a) the interactions between FCV and its cellular receptor fJAM-A at the molecular level, and (b) the molecular determinants of virulence in strains of FCV that cause different clinical disease syndromes.

In Chapter 2, a panel of FCV field isolates from animals various clinical histories will be studied and sequenced in an attempt to identify *in vitro* properties that correlate with virulence *in vivo*.

Chapter 3 will examine the regions and residues of fJAM-A required for FCV binding and infection through the creation of deletion and chimeric receptors and structure guided mutagenesis studies.

In Chapter 4, FCV isolates resistant to neutralization by soluble fJAM-A will be selected and mutations mapped onto the crystal structure of FCV-5 determined at a resolution of 3.6 Å. Furthermore, studies looking at the hydrophobicity of viruses preincubated with soluble receptor will be used to determine if FCV undergoes a conformational change after interacting with fJAM-A.

Finally, Chapter 5 will present a summary of the thesis research as well as a discussion of future research directions.

REFERENCES

Addie, D. D., Radford, A., Yam, P. S. & Taylor, D. J. (2003). Cessation of feline calicivirus shedding coincident with resolution of chronic gingivostomatitis in a cat. *J Small Anim Pract* **44**, 172-6.

Arias, C. F., Romero, P., Alvarez, V. & Lopez, S. (1996). Trypsin activation pathway of rotavirus infectivity. *J Virol* **70**, 5832-9.

Atreya, C. D. (2004). Major foodborne illness causing viruses and current status of vaccines against the diseases. *Foodborne Pathog Dis* **1**, 89-96.

Babinska, A., Kedees, M. H., Athar, H., Ahmed, T., Batuman, O., Ehrlich, Y. H., Hussain, M. M. & Kornecki, E. (2002). F11-receptor (F11R/JAM) mediates platelet adhesion to endothelial cells: role in inflammatory thrombosis. *Thromb Haemost* **88**, 843-50.

Baer, G. S. & Dermody, T. S. (1997). Mutations in reovirus outer-capsid protein sigma3 selected during persistent infections of L cells confer resistance to protease inhibitor E64. *J Virol* **71**, 4921-8.

Bannasch, M. J. & Foley, J. E. (2005). Epidemiologic evaluation of multiple respiratory pathogens in cats in animal shelters. *J Feline Med Surg* **7**, 109-19.

Barton, E. S., Forrest, J. C., Connolly, J. L., Chappell, J. D., Liu, Y., Schnell, F. J., Nusrat, A., Parkos, C. A. & Dermody, T. S. (2001). Junction adhesion molecule is a receptor for reovirus. *Cell* **104**, 441-51.

Bazzoni, G., Martinez-Estrada, O. M., Mueller, F., Nelboeck, P., Schmid, G., Bartfai, T., Dejana, E. & Brockhaus, M. (2000). Homophilic interaction of junctional adhesion molecule. *J Biol Chem* **275**, 30970-6.

Bergelson, J. M., Cunningham, J. A., Droguett, G., Kurt-Jones, E. A., Krithivas, A., Hong, J. S., Horwitz, M. S., Crowell, R. L. & Finberg, R. W. (1997). Isolation of a common receptor for Coxsackie B viruses and adenoviruses 2 and 5. *Science* **275**, 1320-3.

Bewley, M. C., Springer, K., Zhang, Y. B., Freimuth, P. & Flanagan, J. M. (1999). Structural analysis of the mechanism of adenovirus binding to its human cellular receptor, CAR. *Science* **286**, 1579-83.

Bhella, D., Gatherer, D., Chaudhry, Y., Pink, R. & Goodfellow, I. G. (2008). Structural insights into Calicivirus attachment and uncoating. *J Virol*.

Binns, S. H., Dawson, S., Speakman, A. J., Cuevas, L. E., Hart, C. A., Gaskell, C. J., Morgan, K. L. & Gaskell, R. M. (2000). A study of feline upper respiratory tract disease with reference to prevalence and risk factors for infection with feline calicivirus and feline herpesvirus. *J Feline Med Surg* **2**, 123-33.

Blondel, B., Duncan, G., Couderc, T., Delpeyroux, F., Pavio, N. & Colbere-Garapin, F. (1998). Molecular aspects of poliovirus biology with a special focus on the interactions with nerve cells. *J Neurovirol* **4**, 1-26.

Bothner, B., Dong, X. F., Bibbs, L., Johnson, J. E. & Siuzdak, G. (1998). Evidence of viral capsid dynamics using limited proteolysis and mass spectrometry. *J Biol Chem* **273**, 673-6.

Bouchard, M. J., Lam, D. H. & Racaniello, V. R. (1995). Determinants of attenuation and temperature sensitivity in the type 1 poliovirus Sabin vaccine. *J Virol* **69**, 4972-8.

Brandenburg, B., Lee, L. Y., Lakadamyali, M., Rust, M. J., Zhuang, X. & Hogle, J. M. (2007). Imaging Poliovirus Entry in Live Cells. *PLoS Biol* **5**, e183.

Burrage, T., Kramer, E. & Brown, F. (2000). Structural differences between foot-and-mouth disease and poliomyelitis viruses influence their inactivation by aziridines. *Vaccine* **18**, 2454-61.

Burroughs, J. N. & Brown, F. (1978). Presence of a covalently linked protein on calicivirus RNA. *J Gen Virol* **41**, 443-6.

Campbell, J. A., Schelling, P., Wetzel, J. D., Johnson, E. M., Forrest, J. C., Wilson, G. A., Aurrand-Lions, M., Imhof, B. A., Stehle, T. & Dermody, T. S. (2005). Junctional adhesion molecule a serves as a receptor for prototype and field-isolate strains of mammalian reovirus. *J Virol* **79**, 7967-78.

Carter, M. J. (1989). Feline calicivirus protein synthesis investigated by western blotting. *Arch Virol* **108**, 69-79.

Carter, M. J., Milton, I. D., Turner, P. C., Meanger, J., Bennett, M. & Gaskell, R. M. (1992). Identification and sequence determination of the capsid protein gene of feline calicivirus. *Arch Virol* **122**, 223-35.

Chandran, K., Farsetta, D. L. & Nibert, M. L. (2002). Strategy for nonenveloped virus entry: a hydrophobic conformer of the reovirus membrane penetration protein micro 1 mediates membrane disruption. *J Virol* **76**, 9920-33.

Chaudhry, Y., Nayak, A., Bordeleau, M. E., Tanaka, J., Pelletier, J., Belsham, G. J., Roberts, L. O. & Goodfellow, I. G. (2006). Caliciviruses differ in their functional requirements for eIF4F components. *J Biol Chem* **281**, 25315-25.

Chen, R., Neill, J. D., Estes, M. K. & Prasad, B. V. (2006). X-ray structure of a native calicivirus: structural insights into antigenic diversity and host specificity. *Proc Natl Acad Sci U S A* **103**, 8048-53.

Chen, R., Neill, J. D., Noel, J. S., Hutson, A. M., Glass, R. I., Estes, M. K. & Prasad, B. V. (2004). Inter- and intragenus structural variations in caliciviruses and their functional implications. *J Virol* **78**, 6469-79.

Choi, J. M., Hutson, A. M., Estes, M. K. & Prasad, B. V. (2008). Atomic resolution structural characterization of recognition of histo-blood group antigens by Norwalk virus. *Proc Natl Acad Sci U S A*.

Clarke, I. N. & Lambden, P. R. (1997). The molecular biology of caliciviruses. *J Gen Virol* **78 (Pt 2)**, 291-301.

Cohen, C. J., Shieh, J. T., Pickles, R. J., Okegawa, T., Hsieh, J. T. & Bergelson, J. M. (2001). The coxsackievirus and adenovirus receptor is a transmembrane component of the tight junction. *Proc Natl Acad Sci U S A* **98**, 15191-6.

Compans, R. W., Klenk, H. D., Caliguiri, L. A. & Choppin, P. W. (1970). Influenza virus proteins. I. Analysis of polypeptides of the virion and identification of spike glycoproteins. *Virology* **42**, 880-9.

Coyne, K. P., Jones, B. R., Kipar, A., Chantrey, J., Porter, C. J., Barber, P. J., Dawson, S., Gaskell, R. M. & Radford, A. D. (2006). Lethal outbreak of disease associated with feline calicivirus infection in cats. *Vet Rec* **158**, 544-50.

Crowell, R. L. & Philipson, L. (1971). Specific alterations of coxsackievirus B3 eluted from HeLa cells. *J Virol* **8**, 509-15.

Dawson, S., Bennett, D., Carter, S. D., Bennett, M., Meanger, J., Turner, P. C., Carter, M. J., Milton, I. & Gaskell, R. M. (1994). Acute arthritis of cats associated with feline calicivirus infection. *Res Vet Sci* **56**, 133-43.

Dawson, S., McArdle, F., Bennett, D., Carter, S. D., Bennett, M., Ryvar, R. & Gaskell, R. M. (1993). Investigation of vaccine reactions and breakdowns after feline calicivirus vaccination. *Vet Rec* **132**, 346-50.

De Sena, J. & Mandel, B. (1977). Studies on the in vitro uncoating of poliovirus. II. Characteristics of the membrane-modified particle. *Virology* **78**, 554-66.

Denisova, E., Dowling, W., LaMonica, R., Shaw, R., Scarlata, S., Ruggeri, F. & Mackow, E. R. (1999). Rotavirus capsid protein VP5* permeabilizes membranes. *J Virol* **73**, 3147-53.

Dunham, D. M., Jiang, X., Berke, T., Smith, A. W. & Matson, D. O. (1998). Genomic mapping of a calicivirus VPg. *Arch Virol* **143**, 2421-30.

Durham, A. C. & Hendry, D. A. (1977). Cation binding by tobacco mosaic virus. *Virology* **77**, 510-9.

Dveksler, G. S., Dieffenbach, C. W., Cardellichio, C. B., McCuaig, K., Pensiero, M. N., Jiang, G. S., Beauchemin, N. & Holmes, K. V. (1993). Several members of the mouse carcinoembryonic antigen-related glycoprotein family are functional receptors for the coronavirus mouse hepatitis virus-A59. *J Virol* **67**, 1-8.

Dveksler, G. S., Pensiero, M. N., Cardellichio, C. B., Williams, R. K., Jiang, G. S., Holmes, K. V. & Dieffenbach, C. W. (1991). Cloning of the mouse hepatitis virus (MHV) receptor: expression in human and hamster cell lines confers susceptibility to MHV. *J Virol* **65**, 6881-91.

Ebert, D. H., Deussing, J., Peters, C. & Dermody, T. S. (2002). Cathepsin L and cathepsin B mediate reovirus disassembly in murine fibroblast cells. *J Biol Chem* **277**, 24609-17.

Ebert, D. H., Wetzel, J. D., Brumbaugh, D. E., Chance, S. R., Stobie, L. E., Baer, G. S. & Dermody, T. S. (2001). Adaptation of reovirus to growth in the presence of protease inhibitor E64 segregates with a mutation in the carboxy terminus of viral outer-capsid protein sigma3. *J Virol* **75**, 3197-206.

Ebnet, K., Schulz, C. U., Meyer Zu Brickwedde, M. K., Pendl, G. G. & Vestweber, D. (2000). Junctional adhesion molecule interacts with the PDZ domain-containing proteins AF-6 and ZO-1. *J Biol Chem* **275**, 27979-88.

Endres, M. J., Griot, C., Gonzalez-Scarano, F. & Nathanson, N. (1991). Neuroattenuation of an avirulent bunyavirus variant maps to the L RNA segment. *J Virol* **65**, 5465-70.

Estes, M. K., Ball, J. M., Guerrero, R. A., Opekun, A. R., Gilger, M. A., Pacheco, S. S. & Graham, D. Y. (2000). Norwalk virus vaccines: challenges and progress. *J Infect Dis* **181 Suppl 2**, S367-73.

Estes, M. K., Graham, D. Y. & Mason, B. B. (1981). Proteolytic enhancement of rotavirus infectivity: molecular mechanisms. *J Virol* **39**, 879-88.

Evermann, J. F., McKeirnan, A. J., Smith, A. W., Skilling, D. E. & Ott, R. L. (1985). Isolation and identification of caliciviruses from dogs with enteric infections. *Am J Vet Res* **46**, 218-20.

Farkas, T., Sestak, K., Wei, C. & Jiang, X. (2008). Characterization of a rhesus monkey calicivirus representing a new genus of Caliciviridae. *J Virol* **82**, 5408-16.

Fenwick, M. L. & Cooper, P. D. (1962). Early interactions between poliovirus and ERK cells: some observations on the nature and significance of the rejected particles. *Virology* **18**, 212-23.

Foley, J., Hurley, K., Pesavento, P. A., Poland, A. & Pedersen, N. C. (2006). Virulent systemic feline calicivirus infection: local cytokine modulation and contribution of viral mutants. *J Feline Med Surg* **8**, 55-61.

Forrest, J. C., Campbell, J. A., Schelling, P., Stehle, T. & Dermody, T. S. (2003). Structure-function analysis of reovirus binding to junctional adhesion molecule 1. Implications for the mechanism of reovirus attachment. *J Biol Chem* **278**, 48434-44.

Fricks, C. E. & Hogle, J. M. (1990). Cell-induced conformational change in poliovirus: externalization of the amino terminus of VP1 is responsible for liposome binding. *J Virol* **64**, 1934-45.

Gabriel, S. S., Tohya, Y. & Mochizuki, M. (1996). Isolation of a calicivirus antigenically related to feline caliciviruses from feces of a dog with diarrhea. *J Vet Med Sci* **58**, 1041-3.

Gaskell, C. J., Gaskell, R. M., Dennis, P. E. & Wooldridge, M. J. (1982). Efficacy of an inactivated feline calicivirus (FCV) vaccine against challenge with United Kingdom field strains and its interaction with the FCV carrier state. *Res Vet Sci* **32**, 23-6.

Geraghty, R. J., Krummenacher, C., Cohen, G. H., Eisenberg, R. J. & Spear, P. G. (1998). Entry of alphaherpesviruses mediated by poliovirus receptor-related protein 1 and poliovirus receptor. *Science* **280**, 1618-20.

Goodfellow, I., Chaudhry, Y., Gioldasi, I., Gerondopoulos, A., Natoni, A., Labrie, L., Laliberte, J. F. & Roberts, L. (2005). Calicivirus translation initiation requires an interaction between VPg and eIF 4 E. *EMBO Rep* **6**, 968-72.

Greber, U. F., Willetts, M., Webster, P. & Helenius, A. (1993). Stepwise dismantling of adenovirus 2 during entry into cells. *Cell* **75**, 477-86.

Green, K. Y., Ando, T., Balayan, M. S., Berke, T., Clarke, I. N., Estes, M. K., Matson, D. O., Nakata, S., Neill, J. D., Studdert, M. J. & Thiel, H. J. (2000). Taxonomy of the caliciviruses. *J Infect Dis* **181 Suppl 2**, S322-30.

Guglielmi, K. M., Kirchner, E., Holm, G. H., Stehle, T. & Dermody, T. S. (2007). Reovirus binding determinants in junctional adhesion molecule-a. *J Biol Chem* **282**, 17930-40.

Gupta, S. K., Pillarisetti, K. & Ohlstein, E. H. (2000). Platelet agonist F11 receptor is a member of the immunoglobulin superfamily and identical with junctional adhesion molecule (JAM): regulation of expression in human endothelial cells and macrophages. *IUBMB Life* **50**, 51-6.

Halstead, S. B. (1988). Pathogenesis of dengue: challenges to molecular biology. *Science* **239**, 476-81.

Harrison, S. C. (2001). The familiar and the unexpected in structures of icosahedral viruses. *Curr Opin Struct Biol* **11**, 195-9.

Harrison, T. M., Sikarskie, J., Kruger, J., Wise, A., Mullaney, T. P., Kiupel, M. & Maes, R. K. (2007). Systemic calicivirus epidemic in captive exotic felids. *J Zoo Wildl Med* **38**, 292-9.

He, Y., Bowman, V. D., Mueller, S., Bator, C. M., Bella, J., Peng, X., Baker, T. S., Wimmer, E., Kuhn, R. J. & Rossmann, M. G. (2000). Interaction of the poliovirus receptor with poliovirus. *Proc Natl Acad Sci U S A* **97**, 79-84.

He, Y., Chipman, P. R., Howitt, J., Bator, C. M., Whitt, M. A., Baker, T. S., Kuhn, R. J., Anderson, C. W., Freimuth, P. & Rossmann, M. G. (2001). Interaction of coxsackievirus B3 with the full length coxsackievirus-adenovirus receptor. *Nat Struct Biol* **8**, 874-8.

Heinz, B. A., Rueckert, R. R., Shepard, D. A., Dutko, F. J., McKinlay, M. A., Fancher, M., Rossmann, M. G., Badger, J. & Smith, T. J. (1989). Genetic and molecular analyses of spontaneous mutants of human rhinovirus 14 that are resistant to an antiviral compound. *J Virol* **63**, 2476-85.

Herbert, T. P., Brierley, I. & Brown, T. D. (1997). Identification of a protein linked to the genomic and subgenomic mRNAs of feline calicivirus and its role in translation. *J Gen Virol* **78 (Pt 5)**, 1033-40.

Hogle, J. M. (2002). Poliovirus cell entry: common structural themes in viral cell entry pathways. *Annu Rev Microbiol* **56**, 677-702.

Holmes, E. C. & Twiddy, S. S. (2003). The origin, emergence and evolutionary genetics of dengue virus. *Infect Genet Evol* **3**, 19-28.

Hoover, E. A. & Kahn, D. E. (1975). Experimentally induced feline calicivirus infection: clinical signs and lesions. *J Am Vet Med Assoc* **166**, 463-8.

Horimoto, T. & Kawaoka, Y. (1995). Molecular changes in virulent mutants arising from avirulent avian influenza viruses during replication in 14-day-old embryonated eggs. *Virology* **206**, 755-9.

Horimoto, T. & Kawaoka, Y. (1997). Biologic effects of introducing additional basic amino acid residues into the hemagglutinin cleavage site of a virulent avian influenza virus. *Virus Res* **50**, 35-40.

Hrdy, D. B., Rubin, D. H. & Fields, B. N. (1982). Molecular basis of reovirus neurovirulence: role of the M2 gene in avirulence. *Proc Natl Acad Sci U S A* **79**, 1298-302.

Huang, P., Farkas, T., Zhong, W., Tan, M., Thornton, S., Morrow, A. L. & Jiang, X. (2005). Norovirus and histo-blood group antigens: demonstration of a wide spectrum of strain specificities and classification of two major binding groups among multiple binding patterns. *J Virol* **79**, 6714-22.

Hurley, K. E., Pesavento, P. A., Pedersen, N. C., Poland, A. M., Wilson, E. & Foley, J. E. (2004). An outbreak of virulent systemic feline calicivirus disease. *J Am Vet Med Assoc* **224**, 241-9.

Hurley, K. F. & Sykes, J. E. (2003). Update on feline calicivirus: new trends. *Vet Clin North Am Small Anim Pract* **33**, 759-72.

Hutson, A. M., Atmar, R. L., Graham, D. Y. & Estes, M. K. (2002). Norwalk virus infection and disease is associated with ABO histo-blood group type. *J Infect Dis* **185**, 1335-7.

Incardona, N. L. & Kaesberg, P. (1964). A Ph-Induced Structural Change in Bromegrass Mosaic Virus. *Biophys J* **4**, 11-21.

Janssen, R. S., Nathanson, N., Endres, M. J. & Gonzalez-Scarano, F. (1986). Virulence of La Crosse virus is under polygenic control. *J Virol* **59**, 1-7.

Johnson, J. E. (2003). Virus particle dynamics. *Adv Protein Chem* **64**, 197-218.

Kahn, D. E. & Gillespie, J. H. (1971). Feline viruses: pathogenesis of picornavirus infection in the cat. *Am J Vet Res* **32**, 521-31.

Kaiser, W. J., Chaudhry, Y., Sosnovtsev, S. V. & Goodfellow, I. G. (2006). Analysis of protein-protein interactions in the feline calicivirus replication complex. *J Gen Virol* **87**, 363-8.

Kamper, N., Day, P. M., Nowak, T., Selinka, H. C., Florin, L., Bolscher, J., Hilbig, L., Schiller, J. T. & Sapp, M. (2006). A membrane-destabilizing peptide in capsid protein L2 is required for egress of papillomavirus genomes from endosomes. *J Virol* **80**, 759-68.

Katpally, U., Wobus, C. E., Dryden, K., Virgin, H. W. t. & Smith, T. J. (2008). Structure of antibody-neutralized murine norovirus and unexpected differences from viruslike particles. *J Virol* **82**, 2079-88.

Kawaoka, Y., Naeve, C. W. & Webster, R. G. (1984). Is virulence of H5N2 influenza viruses in chickens associated with loss of carbohydrate from the hemagglutinin? *Virology* **139**, 303-16.

Kawaoka, Y. & Webster, R. G. (1989). Interplay between carbohydrate in the stalk and the length of the connecting peptide determines the cleavability of influenza virus hemagglutinin. *J Virol* **63**, 3296-300.

Khandoga, A., Kessler, J. S., Meissner, H., Hanschen, M., Corada, M., Motoike, T., Enders, G., Dejana, E. & Krombach, F. (2005). Junctional adhesion molecule-A deficiency increases hepatic ischemia-reperfusion injury despite reduction of neutrophil transendothelial migration. *Blood* **106**, 725-33.

Knowles, J. O., Dawson, S., Gaskell, R. M., Gaskell, C. J. & Harvey, C. E. (1990). Neutralisation patterns among recent British and North American feline calicivirus isolates from different clinical origins. *Vet Rec* **127**, 125-7.

Knowles, J. O., McArdle, F., Dawson, S., Carter, S. D., Gaskell, C. J. & Gaskell, R. M. (1991). Studies on the role of feline calicivirus in chronic stomatitis in cats. *Vet Microbiol* **27**, 205-19.

Kolatkar, P. R., Bella, J., Olson, N. H., Bator, C. M., Baker, T. S. & Rossmann, M. G. (1999). Structural studies of two rhinovirus serotypes complexed with fragments of their cellular receptor. *Embo J* **18**, 6249-59.

Kostrewa, D., Brockhaus, M., D'Arcy, A., Dale, G. E., Nelboeck, P., Schmid, G., Mueller, F., Bazzoni, G., Dejana, E., Bartfai, T., Winkler, F. K. & Hennig, M. (2001). X-ray structure of junctional adhesion molecule: structural basis for homophilic adhesion via a novel dimerization motif. *Embo J* **20**, 4391-8.

Kreutz, L. C. & Seal, B. S. (1995). The pathway of feline calicivirus entry. *Virus Res* **35**, 63-70.

Kreutz, L. C., Seal, B. S. & Mengeling, W. L. (1994). Early interaction of feline calicivirus with cells in culture. *Arch Virol* **136**, 19-34.

Laver, W. G. (1971). Separation of two polypeptide chains from the hemagglutinin subunit of influenza virus. *Virology* **45**, 275-88.

Law, L. K. & Davidson, B. L. (2005). What does it take to bind CAR? *Mol Ther* **12**, 599-609.

Lewis, J. K., Bothner, B., Smith, T. J. & Siuzdak, G. (1998). Antiviral agent blocks breathing of the common cold virus. *Proc Natl Acad Sci U S A* **95**, 6774-8.

Li, Q., Yafal, A. G., Lee, Y. M., Hogle, J. & Chow, M. (1994). Poliovirus neutralization by antibodies to internal epitopes of VP4 and VP1 results from reversible exposure of these sequences at physiological temperature. *J Virol* **68**, 3965-70.

Liemann, S., Chandran, K., Baker, T. S., Nibert, M. L. & Harrison, S. C. (2002). Structure of the reovirus membrane-penetration protein, Mu1, in a complex with is protector protein, Sigma3. *Cell* **108**, 283-95.

Lindesmith, L., Moe, C., Lependu, J., Frelinger, J. A., Treanor, J. & Baric, R. S. (2005). Cellular and humoral immunity following Snow Mountain virus challenge. *J Virol* **79**, 2900-9.

Lindesmith, L., Moe, C., Marionneau, S., Ruvoen, N., Jiang, X., Lindblad, L., Stewart, P., LePendu, J. & Baric, R. (2003). Human susceptibility and resistance to Norwalk virus infection. *Nat Med* **9**, 548-53.

Lipton, H. L., Kumar, A. S. & Trottier, M. (2005). Theiler's virus persistence in the central nervous system of mice is associated with continuous viral replication and a difference in outcome of infection of infiltrating macrophages versus oligodendrocytes. *Virus Res* **111**, 214-23.

Liu, Y., Nusrat, A., Schnell, F. J., Reaves, T. A., Walsh, S., Pochet, M. & Parkos, C. A. (2000). Human junction adhesion molecule regulates tight junction resealing in epithelia. *J Cell Sci* **113 (Pt 13)**, 2363-74.

Lonberg-Holm, K. & Korant, B. D. (1972). Early interaction of rhinoviruses with host cells. *J Virol* **9**, 29-40.

Love, D. N. & Baker, K. D. (1972). Sudden death in kittens associated with a feline picornavirus. *Aust Vet J* **48**, 643.

Luttermann, C. & Meyers, G. (2007). A bipartite sequence motif induces translation reinitiation in feline calicivirus RNA. *J Biol Chem* **282**, 7056-65.

Makino, A., Shimojima, M., Miyazawa, T., Kato, K., Tohya, Y. & Akashi, H. (2006). Junctional adhesion molecule 1 is a functional receptor for feline calicivirus. *J Virol* **80**, 4482-90.

Mandell, K. J., McCall, I. C. & Parkos, C. A. (2004). Involvement of the junctional adhesion molecule-1 (JAM1) homodimer interface in regulation of epithelial barrier function. *J Biol Chem* **279**, 16254-62.

Mandell, K. J. & Parkos, C. A. (2005). The JAM family of proteins. *Adv Drug Deliv Rev* **57**, 857-67.

Mani, B., Baltzer, C., Valle, N., Almendral, J. M., Kempf, C. & Ros, C. (2006). Low pH-dependent endosomal processing of the incoming parvovirus minute virus of mice virion leads to externalization of the VP1 N-terminal sequence (N-VP1), N-VP2 cleavage, and uncoating of the full-length genome. *J Virol* **80**, 1015-24.

Marionneau, S., Ruvoen, N., Le Moullac-Vaidye, B., Clement, M., Cailleau-Thomas, A., Ruiz-Palacois, G., Huang, P., Jiang, X. & Le Pendu, J. (2002). Norwalk virus binds to histo-blood group antigens present on gastroduodenal epithelial cells of secretor individuals. *Gastroenterology* **122**, 1967-77.

Martella, V., Pratelli, A., Gentile, M., Buonavoglia, D., Decaro, N., Fiorente, P. & Buonavoglia, C. (2002). Analysis of the capsid protein gene of a feline-like calicivirus isolated from a dog. *Vet Microbiol* **85**, 315-22.

Martin-Padura, I., Lostaglio, S., Schneemann, M., Williams, L., Romano, M., Fruscella, P., Panzeri, C., Stoppacciaro, A., Ruco, L., Villa, A., Simmons, D. & Dejana, E. (1998). Junctional adhesion molecule, a novel member of the immunoglobulin superfamily that distributes at intercellular junctions and modulates monocyte transmigration. *J Cell Biol* **142**, 117-27.

McKinlay, M. A. (1993). Discovery and development of antipicornaviral agents. *Scand J Infect Dis Suppl* **88**, 109-15.

Mead, P. S., Slutsker, L., Dietz, V., McCaig, L. F., Bresee, J. S., Shapiro, C., Griffin, P. M. & Tauxe, R. V. (1999). Food-related illness and death in the United States. *Emerg Infect Dis* **5**, 607-25.

Mitra, T., Sosnovtsev, S. V. & Green, K. Y. (2004). Mutagenesis of tyrosine 24 in the VPg protein is lethal for feline calicivirus. *J Virol* **78**, 4931-5.

Naik, M. U., Mousa, S. A., Parkos, C. A. & Naik, U. P. (2003a). Signaling through JAM-1 and alphavbeta3 is required for the angiogenic action of bFGF: dissociation of the JAM-1 and alphavbeta3 complex. *Blood* **102**, 2108-14.

Naik, M. U. & Naik, U. P. (2006). Junctional adhesion molecule-A-induced endothelial cell migration on vitronectin is integrin alpha v beta 3 specific. *J Cell Sci* **119**, 490-9.

Naik, M. U., Vuppalanchi, D. & Naik, U. P. (2003b). Essential role of junctional adhesion molecule-1 in basic fibroblast growth factor-induced endothelial cell migration. *Arterioscler Thromb Vasc Biol* **23**, 2165-71.

Neill, J. D. & Mengeling, W. L. (1988). Further characterization of the virus-specific RNAs in feline calicivirus infected cells. *Virus Res* **11**, 59-72.

Neill, J. D., Reardon, I. M. & Heinrikson, R. L. (1991). Nucleotide sequence and expression of the capsid protein gene of feline calicivirus. *J Virol* **65**, 5440-7.

Oliver, S. L., Asobayire, E., Dastjerdi, A. M. & Bridger, J. C. (2006). Genomic characterization of the unclassified bovine enteric virus Newbury agent-1 (Newbury1) endorses a new genus in the family Caliciviridae. *Virology* **350**, 240-50.

Olson, N. H., Kolatkar, P. R., Oliveira, M. A., Cheng, R. H., Greve, J. M., McClelland, A., Baker, T. S. & Rossmann, M. G. (1993). Structure of a human rhinovirus complexed with its receptor molecule. *Proc Natl Acad Sci U S A* **90**, 507-11.

Ostermann, G., Fraemohs, L., Baltus, T., Schober, A., Lietz, M., Zernecke, A., Liehn, E. A. & Weber, C. (2005). Involvement of JAM-A in mononuclear cell recruitment on inflamed or atherosclerotic endothelium: inhibition by soluble JAM-A. *Arterioscler Thromb Vasc Biol* **25**, 729-35.

Ozaki, H., Ishii, K., Horiuchi, H., Arai, H., Kawamoto, T., Okawa, K., Iwamatsu, A. & Kita, T. (1999). Cutting edge: combined treatment of TNF-alpha and IFN-gamma causes redistribution of junctional adhesion molecule in human endothelial cells. *J Immunol* **163**, 553-7.

Pedersen, N. C., Elliott, J. B., Glasgow, A., Poland, A. & Keel, K. (2000). An isolated epizootic of hemorrhagic-like fever in cats caused by a novel and highly virulent strain of feline calicivirus. *Vet Microbiol* **73**, 281-300.

Pedersen, N. C. & Hawkins, K. F. (1995). Mechanisms for persistence of acute and chronic feline calicivirus infections in the face of vaccination. *Vet Microbiol* **47**, 141-56.

Pesavento, P. A., Chang, K. O. & Parker, J. S. (2008). Molecular virology of feline calicivirus. *Vet Clin North Am Small Anim Pract* **38**, 775-86.

Pesavento, P. A., MacLachlan, N. J., Dillard-Telm, L., Grant, C. K. & Hurley, K. F. (2004). Pathologic, immunohistochemical, and electron microscopic findings in naturally occurring virulent systemic feline calicivirus infection in cats. *Vet Pathol* **41**, 257-63.

Poulet, H., Brunet, S., Soulier, M., Leroy, V., Goutebroze, S. & Chappuis, G. (2000). Comparison between acute oral/respiratory and chronic stomatitis/gingivitis isolates of feline calicivirus: pathogenicity, antigenic profile and cross-neutralisation studies. *Arch Virol* **145**, 243-61.

Prasad, B. V., Hardy, M. E., Dokland, T., Bella, J., Rossmann, M. G. & Estes, M. K. (1999). X-ray crystallographic structure of the Norwalk virus capsid. *Science* **286**, 287-90.

Prasad, B. V., Matson, D. O. & Smith, A. W. (1994). Three-dimensional structure of calicivirus. *J Mol Biol* **240**, 256-64.

Prasad, B. V. V., Hardy, M. E. & Estes, M. K. (2000). Structural studies of recombinant Norwalk capsids. *J Infect Dis* **181 Suppl 2**, S317-21.

Prota, A. E., Campbell, J. A., Schelling, P., Forrest, J. C., Watson, M. J., Peters, T. R., Aurrand-Lions, M., Imhof, B. A., Dermody, T. S. & Stehle, T. (2003). Crystal structure of human junctional adhesion molecule 1: implications for reovirus binding. *Proc Natl Acad Sci U S A* **100**, 5366-71.

Radford, A. D., Bennett, M., McArdle, F., Dawson, S., Turner, P. C., Williams, R. A., Glenn, M. A. & Gaskell, R. M. (1999). Quasispecies evolution of a hypervariable region of the feline calicivirus capsid gene in cell culture and persistently infected cats. *Vet Microbiol* **69**, 67-8.

Radford, A. D., Coyne, K. P., Dawson, S., Porter, C. J. & Gaskell, R. M. (2007). Feline calicivirus. *Vet Res* **38**, 319-35.

Reubel, G. H., Hoffmann, D. E. & Pedersen, N. C. (1992). Acute and chronic faucitis of domestic cats. A feline calicivirus-induced disease. *Vet Clin North Am Small Anim Pract* **22**, 1347-60.

Rice, C. C., Kruger, J. M., Venta, P. J., Vilnis, A., Maas, K. A., Dulin, J. A. & Maes, R. K. (2002). Genetic characterization of 2 novel feline caliciviruses isolated from cats with idiopathic lower urinary tract disease. *J Vet Intern Med* **16**, 293-302.

Richards, R. M., Lowy, D. R., Schiller, J. T. & Day, P. M. (2006). Cleavage of the papillomavirus minor capsid protein, L2, at a furin consensus site is necessary for infection. *Proc Natl Acad Sci U S A* **103**, 1522-7.

Robinson, I. K. & Harrison, S. C. (1982). Structure of the expanded state of tomato bushy stunt virus. *Nature* **297**, 563-568.

Rossmann, M. G. & Johnson, J. E. (1989). Icosahedral RNA virus structure. *Annu Rev Biochem* **58**, 533-73.

Ruvoen-Clouet, N., Ganiere, J. P., Andre-Fontaine, G., Blanchard, D. & Le Pendu, J. (2000). Binding of rabbit hemorrhagic disease virus to antigens of the ABH histo-blood group family. *J Virol* **74**, 11950-4.

Sabin, A. B. (1956). Pathogenesis of poliomyelitis; reappraisal in the light of new data. *Science* **123**, 1151-7.

Sato, Y., Ohe, K., Fukuyama, M., Furuhata, K., Kishikawa, S., Sakai, S., Kiuchi, A., Hara, M., Watanabe, T., Ishikawa, Y. & Taneno, A. (2004). Properties of a calicivirus isolated from cats dying in an agitated state. *Vet Rec* **155**, 800-5.

Schorr-Evans, E. M., Poland, A., Johnson, W. E. & Pedersen, N. C. (2003). An epizootic of highly virulent feline calicivirus disease in a hospital setting in New England. *J Feline Med Surg* **5**, 217-26.

Seal, B. S., Neill, J. D. & Ridpath, J. F. (1994). Predicted stem-loop structures and variation in nucleotide sequence of 3' noncoding regions among animal calicivirus genomes. *Virus Genes* **8**, 243-7.

Seth, P., Fitzgerald, D. J., Willingham, M. C. & Pastan, I. (1984). Role of a low-pH environment in adenovirus enhancement of the toxicity of a Pseudomonas exotoxin-epidermal growth factor conjugate. *J Virol* **51**, 650-5.

Severson, E. A., Jiang, L., Ivanov, A. I., Mandell, K. J., Nusrat, A. & Parkos, C. A. (2008). Cis-dimerization mediates function of junctional adhesion molecule a. *Mol Biol Cell* **19**, 1862-72.

Sherry, B. & Fields, B. N. (1989). The reovirus M1 gene, encoding a viral core protein, is associated with the myocarditic phenotype of a reovirus variant. *J Virol* **63**, 4850-6.

Skehel, J. J. (1972). Polypeptide synthesis in influenza virus-infected cells. *Virology* **49**, 23-36.

Sobocka, M. B., Sobocki, T., Babinska, A., Hartwig, J. H., Li, M., Ehrlich, Y. H. & Kornecki, E. (2004). Signaling pathways of the F11 receptor (F11R; a.k.a. JAM-1, JAM-A) in human platelets: F11R dimerization, phosphorylation and complex formation with the integrin GPIIIa. *J Recept Signal Transduct Res* **24**, 85-105.

Sosnovtsev, S. V., Belliot, G., Chang, K. O., Onwudiwe, O. & Green, K. Y. (2005). Feline calicivirus VP2 is essential for the production of infectious virions. *J Virol* **79**, 4012-24.

Sosnovtsev, S. V., Garfield, M. & Green, K. Y. (2002). Processing map and essential cleavage sites of the nonstructural polyprotein encoded by ORF1 of the feline calicivirus genome. *J Virol* **76**, 7060-72.

Sosnovtsev, S. V. & Green, K. Y. (2000). Identification and genomic mapping of the ORF3 and VPg proteins in feline calicivirus virions. *Virology* **277**, 193-203.

Sosnovtsev, S. V., Sosnovtseva, S. A. & Green, K. Y. (1998). Cleavage of the feline calicivirus capsid precursor is mediated by a virus-encoded proteinase. *J Virol* **72**, 3051-9.

Sosnovtseva, S. A., Sosnovtsev, S. V. & Green, K. Y. (1999). Mapping of the feline calicivirus proteinase responsible for autocatalytic processing of the nonstructural polyprotein and identification of a stable proteinase-polymerase precursor protein. *J Virol* **73**, 6626-33.

Steinhauer, D. A. (1999). Role of hemagglutinin cleavage for the pathogenicity of influenza virus. *Virology* **258**, 1-20.

Stephenson, J. R. (2005). Understanding dengue pathogenesis: implications for vaccine design. *Bull World Health Organ* **83**, 308-14.

Stuart, A. D. & Brown, T. D. (2006). Entry of feline calicivirus is dependent on clathrin-mediated endocytosis and acidification in endosomes. *J Virol* **80**, 7500-9.

Stuart, A. D. & Brown, T. D. (2007). Alpha2,6-linked sialic acid acts as a receptor for Feline calicivirus. *J Gen Virol* **88**, 177-86.

Studdert, M. J. (1978). Caliciviruses. Brief review. *Arch Virol* **58**, 157-91.

Suikkanen, S., Antila, M., Jaatinen, A., Vihinen-Ranta, M. & Vuento, M. (2003). Release of canine parvovirus from endocytic vesicles. *Virology* **316**, 267-80.

TerWee, J., Lauritzen, A. Y., Sabara, M., Dreier, K. J. & Kokjohn, K. (1997). Comparison of the primary signs induced by experimental exposure to either a pneumotrophic or a 'limping' strain of feline calicivirus. *Vet Microbiol* **56**, 33-45.

Thoulouze, M. I., Lafage, M., Schachner, M., Hartmann, U., Cremer, H. & Lafon, M. (1998). The neural cell adhesion molecule is a receptor for rabies virus. *J Virol* **72**, 7181-90.

Thouvenin, E., Laurent, S., Madelaine, M. F., Rasschaert, D., Vautherot, J. F. & Hewat, E. A. (1997). Bivalent binding of a neutralising antibody to a calicivirus involves the torsional flexibility of the antibody hinge. *J Mol Biol* **270**, 238-46.

Tohya, Y., Yokoyama, N., Maeda, K., Kawaguchi, Y. & Mikami, T. (1997). Mapping of antigenic sites involved in neutralization on the capsid protein of feline calicivirus. *J Gen Virol* **78 (Pt 2)**, 303-5.

Tosteson, M. T. & Chow, M. (1997). Characterization of the ion channels formed by poliovirus in planar lipid membranes. *J Virol* **71**, 507-11.

Tsai, B. (2007). Penetration of nonenveloped viruses into the cytoplasm. *Annu Rev Cell Dev Biol* **23**, 23-43.

van Vuuren, M., Geissler, K., Gerber, D., Nothling, J. O. & Truyen, U. (1999). Characterisation of a potentially abortigenic strain of feline calicivirus isolated from a domestic cat. *Vet Rec* **144**, 636-8.

Vey, M., Orlich, M., Adler, S., Klenk, H. D., Rott, R. & Garten, W. (1992). Hemagglutinin activation of pathogenic avian influenza viruses of serotype H7 requires the protease recognition motif R-X-K/R-R. *Virology* **188**, 408-13.

Walker, J. A., Molloy, S. S., Thomas, G., Sakaguchi, T., Yoshida, T., Chambers, T. M. & Kawaoka, Y. (1994). Sequence specificity of furin, a proprotein-processing endoprotease, for the hemagglutinin of a virulent avian influenza virus. *J Virol* **68**, 1213-8.

Westrop, G. D., Wareham, K. A., Evans, D. M., Dunn, G., Minor, P. D., Magrath, D. I., Taffs, F., Marsden, S., Skinner, M. A., Schild, G. C. & et al. (1989). Genetic basis of attenuation of the Sabin type 3 oral poliovirus vaccine. *J Virol* **63**, 1338-44.

Wetz, K. & Kucinski, T. (1991). Influence of different ionic and pH environments on structural alterations of poliovirus and their possible relation to virus uncoating. *J Gen Virol* **72 (Pt 10)**, 2541-4.

White, L. J., Ball, J. M., Hardy, M. E., Tanaka, T. N., Kitamoto, N. & Estes, M. K. (1996). Attachment and entry of recombinant Norwalk virus capsids to cultured human and animal cell lines. *J Virol* **70**, 6589-97.

Wiethoff, C. M., Wodrich, H., Gerace, L. & Nemerow, G. R. (2005). Adenovirus protein VI mediates membrane disruption following capsid disassembly. *J Virol* **79**, 1992-2000.

Williams, L. A., Martin-Padura, I., Dejana, E., Hogg, N. & Simmons, D. L. (1999). Identification and characterisation of human Junctional Adhesion Molecule (JAM). *Mol Immunol* **36**, 1175-88.

Wilson, G. A., Morrison, L. A. & Fields, B. N. (1994). Association of the reovirus S1 gene with serotype 3-induced biliary atresia in mice. *J Virol* **68**, 6458-65.

Witz, J. & Brown, F. (2001). Structural dynamics, an intrinsic property of viral capsids. *Arch Virol* **146**, 2263-74.

Xiao, C., Bator, C. M., Bowman, V. D., Rieder, E., He, Y., Hebert, B., Bella, J., Baker, T. S., Wimmer, E., Kuhn, R. J. & Rossmann, M. G. (2001). Interaction of coxsackievirus A21 with its cellular receptor, ICAM-1. *J Virol* **75**, 2444-51.

CHAPTER 2

Feline caliciviruses (FCV) isolated from cats with virulent systemic (VS) disease possess in vitro phenotypes distinct from other FCV isolates*

* **Ossiboff, R. J., Sheh, A., Shotton, J., Pesavento, P. A. & Parker, J. S. (2007).** Feline caliciviruses (FCVs) isolated from cats with virulent systemic disease possess in vitro phenotypes distinct from those of other FCV isolates. *J Gen Virol* **88,** 506-27.

[Author Alex Sheh was a technician in the lab who developed the plaque assay used in this study. Author Justine Shotton was a Leadership Program student who helped with the sequencing of the proteinase-polymerase coding region. Author Dr. Patricia Pesavento was a collaborator on this study and provided many of the highly virulent FCV isolates.]

2.1 Abstract

During the past decade, several outbreaks of severe systemic disease associated with *Feline calicivirus* (FCV) have occurred in the United States and the United Kingdom. This new disease has caused high mortality in the affected animals and has been termed virulent systemic (VS)-FCV disease. Currently, there are no genetic or *in vitro* diagnostic methods to distinguish viruses isolated from cases of VS-FCV disease from other isolates. Here we investigated five *in vitro* properties as well as the capsid and proteinase-polymerase sequences of a set of FCV isolates that included seven isolates from five distinct VS-FCV outbreaks ("VS isolates"). Although all of the FCV isolates we investigated had similar kinetics of growth under single-cycle conditions, VS isolates infected tissue culture cells more efficiently under multiple-cycle growth conditions. Moreover, we found that cells infected with VS isolates showed cytopathic effects earlier than cells infected with non-VS isolates, although no difference in relative ATP levels were noted at times when morphologic changes were first seen. Both VS- and other (non-VS) isolates of FCV demonstrated similar temperature stabilities. Phylogenetic analyses and alignments of the capsid and proteinase-polymerase regions of the genome did not reveal any conserved changes that correlated with virulence and the VS isolates did not segregate into a unique clade. Our results suggest that VS isolates have arisen independently several times since first being described and can more efficiently spread in tissue culture than other isolates when infected at low multiplicity.

2.2 Introduction

Feline calicivirus (FCV) is a common pathogen of cats. Infected cats can be clinically normal or show signs of oral ulceration and/or mild upper respiratory disease. Less commonly, limping, abortion, and severe pneumonia can occur;

however, fatal disease is unusual (Hurley et al., 2004, Pesavento et al., 2004, Coyne et al., 2006). The prevalence of avirulent or mildly virulent FCV in multiple cat environments is as high as 36% (Binns et al., 2000, Bannasch & Foley, 2005). During the last decade however, epizootics of a severe form of FCV disease with mortality rates as high as 50% have occurred (Hurley et al., 2004, Coyne et al., 2006). These epizootics, designated virulent systemic (VS-) FCV, have been reported in the United States, and recently in the United Kingdom (Pedersen et al., 2000, Schorr-Evans et al., 2003, Hurley et al., 2004, Coyne et al., 2006). The clinicopathologic features of VS-FCV disease differ substantially from 'classical' FCV disease; reported signs of VS-FCV disease include high persistent fever, anorexia, depression, facial and limb edema, sores or alopecia on the face, pinnae and feet, pulmonary edema, coagulation abnormalities, pancreatitis and hepatic necrosis (Pedersen et al., 2000, Hurley et al., 2004, Pesavento et al., 2004). In all of the reported outbreaks vaccinated cats have been affected, suggesting that current vaccines may not protect against VS disease (Coyne et al., 2006).

FCV belongs to the Vesivirus genus of the family Caliciviridae and contains a positive-sense RNA genome (~ 7.6 kb) packaged within a nonenveloped capsid. The icosahedral capsid is assembled from 90 homodimers of the major capsid protein VP1. Two genogroups of FCV have been defined by phylogenetic analysis. Of the isolates characterized, only isolates from Japan are members of genogroup II (Sato et al., 2002), while all other VS-FCV isolates studied to date appear to be members of genogroup I (Geissler et al., 1997, Glenn et al., 1999). All feline caliciviruses are considered to belong to a single antigenically diverse serotype, but individual isolates vary in their levels of cross neutralization (Kalunda et al., 1975). Initial reports indicate that VS-FCV isolates cannot be genetically distinguished from non-VS-FCV isolates (Hurley et al., 2004, Abd-Eldaim et al., 2005, Foley et al., 2006).

Here we characterized the in vitro growth properties, stabilities, cytopathic effects and sequences of seven VS-FCV isolates from five distinct VS-FCV outbreaks and compared them to the F9 vaccine strain and three non VS-FCV clinical isolates. Based on the results herein we conclude that the cohort of VS-FCV isolates we analyzed share the common properties of rapid growth kinetics and an increased propensity to spread in tissue culture in vitro. These properties appear to differ from both the F9 vaccine strain and the three non VS-FCV isolates and may in part explain the increased virulence of these viruses in vivo.

2.3 Methods

Cells and viruses. Crandell feline kidney (CRFK) cells were grown in Eagle's minimal essential medium (EMEM) (CellGro) supplemented with 5% fetal bovine serum (HyClone), 100 U ml^{-1} of penicillin, 100 μg ml^{-1} streptomycin, 0.25 μg ml^{-1} amphotericin B, 1 mM sodium pyruvate, and non-essential amino acids (CellGro). The clinical FCV isolates investigated in this study and the analyses performed are listed in Table 2.1. The FCV isolate VS-FCV-Ari was isolated from an infected cat during a VS-FCV outbreak in Sacramento, California in 1998. FCV isolates Kaos, George Walder, and Jengo were isolated from sick cats during a VS-FCV outbreak in Los Angeles, California in 2002. Isolates FCV-5, Deuce, and Georgie were isolated from VS-FCV infected cats from Massachusetts in 2001, North Carolina in 2004 and Florida in 2003, respectively. Isolates FCV-127, FCV-131, and FCV-796 were all obtained from Dr. Ed Dubovi at the New York State Animal Health Diagnostic Center at Cornell University. FCV-131 originated from a shelter in Harrisburg, PA that experienced an outbreak of non-VS FCV in 2003. FCV-127 came from a shelter in North Adams, Massachusetts where numerous cats suffered from a pneumonic form of FCV in 2004. FCV-796 was isolated from a cat in Tampa, Florida that presented with

Table 2.1. FCV isolates investigated

Isolate	Origin	Description	Analysis					
			Kinetics		Stability		ATP[¶]	SEQ[#]
			S*	M[†]	I[‡]	M[§]		
Ari	Sacramento, CA	VS-FCV, 1998	x					x
FCV-5	Bellingham, MA	VS-FCV, 2001	x	x	x	x	x	x
Kaos	Los Angeles, CA	VS-FCV, 2002	x	x	x		x	x
Jengo	Los Angeles, CA	VS-FCV, 2002	x					x
George Walder	Los Angeles, CA	VS-FCV, 2002	x					x
Georgie	Florida	VS-FCV, 2003						x
Deuce	North Carolina	VS-FCV, 2004	x	x	x	x	x	x
FCV-131	Harrisburg, PA	Non-VS-FCV, 2003					x	x
FCV-127	North Adams, MA	Non-VS-FCV, 2004	x	x	x	x	x	x
FCV-796	Tampa, FL	Non-VS-FCV, 2004	x	x	x	x	x	x
F9 (VR-782)	ATCC	Vaccine strain	x	x	x	x	x	x

* Single cycle growth curve
† Multiple cycle growth curve
‡ Thermal inactivation
§ Temperature maintenance
¶ ATP cell viability assay
# Proteinase-polymerase and capsid sequencing

excessive drooling and lingual ulceration in 2004. For the duration of the paper, strains FCV-127, -131, and -796 will be referred to as "non-VS." This designation is made based on the clinical history that accompanied the isolates. The F9 vaccine strain (VR-782) of FCV was obtained from the ATCC. Third passage viral stocks were prepared from twice plaque purified viruses amplified in CRFK cells.

Plaque assay. Viruses were titrated on CRFK cells. In brief, confluent CRFK monolayers were inoculated with serial virus dilutions in Dulbecco's modified Eagle's medium (DMEM) (CellGro) with 0.1% BSA (Calbiochem). Viral adsorption was carried out at room temperature for 60 min with gentle agitation every 10 minutes. Monolayers were then overlaid with 3 ml of EMEM containing 5% fetal bovine serum, 100 U ml^{-1} of penicillin, 100 μg ml^{-1} streptomycin, 0.25 μg ml^{-1} amphotericin B, 1 mM sodium pyruvate, non-essential amino acids, and 1% Bacto-agar (Difco Laboratories). After incubation at 37 ºC for 48 hours in humidified 5% CO_2, the overlay was removed, the cells fixed with 10% buffered formalin (Fisher), and stained with 1% (w/v) crystal violet solution. After washing, the plaques were counted and titer was expressed as plaque forming units per ml (p.f.u ml^{-1}).

Recovery of viral RNA, RT-PCR, sequencing and analysis. Total RNA was extracted from infected cell culture lysates using a commercial kit (RNEasy Mini, Qiagen). First strand cDNA from the capsid region of the genome was synthesized from viral RNA using a degenerate anti-sense primer (5'-YTGACCMAGTGCAGYCTTRTCCAATTC-3') (adapted from Poulet *et al.,* 2005), predicted to anneal to bp 7380-7405 of the FCV-Urbana sequence (GenBank accession: L40021), and Accuscript High-Fidelity reverse transcriptase (Stratagene), per manufacturer's directions. The open reading frame (ORF) was amplified by PCR using Pfu Ultra DNA polymerase (Stratagene) from the first strand cDNA template using the anti-sense primer above and a sense primer

(5'-TACACTGTGATGTGTTCGAAGTTTGAGC-3') (Martella *et al.*, 2002) that anneals to bp 5286-5313 of the FCV-Urbana genome. Thermal cycling conditions were 95 ºC for 2 minutes, followed by 40 cycles of 95 ºC for 30 seconds, 50 ºC for 1 minute, and 68 ºC, 3 minutes, with a final extension step of 68 ºC for 10 minutes. The resulting ~2.1 kb PCR products, encompassing the entirety of the capsid ORF, were purified and sequenced directly.

cDNA from the region encompassing the proteinase-polymerase region of ORF1 was amplified from viral RNA using the SuperScript One-Step RT-PCR system (Invitrogen) and sense (5'-ATTGGVAARGGYGGYGTNAARMAY-3') and anti-sense (5'-AGCACGTTAGCGCAGGTT-3') primers predicted to anneal to bp 3143-3166 and 5322-5339 of the FCV-Urbana genome, respectively. Thermal cycling conditions consisted of 50º C for 30 minutes, 94º C for 2 minutes, 5 cycles of 94º C for 15 seconds, 52º C for 1 minute, 72º C for 2.5 minutes, followed by 35 cycles of 94º C for 15 seconds, 52º C for 30 seconds, 72º C for 2.5 minutes, with a final extension step of 72º C for 10 minutes. The resulting ~2.2 kb PCR products were cloned into the pGEM T-Easy Vector (Promega) and sequenced by the Cornell University Life Sciences Core Laboratories Center.

Sequences were compared to other FCV capsid or proteinase-polymerase sequences contained in the NCBI Nucleotide database (http://www.ncbi.nlm.nih.gov/entrez/) (Table 2.2). Determination of ORFs and amino acid sequence was performed using Vector NTI Advance (Invitrogen Life Technologies). Sequence alignments were carried out using ClustalX (Thompson *et al.*, 1997). Similarity tables were constructed using Vector NTI Advance. Construction of phylogenetic trees inferred from nucleotide sequence was performed using 3 methods: the distance (neighbor-joining) method using the ClustalX software, the Bayesian method with the software MRBAYES (Huelsenbeck and Ronquist, 2001,

Table 2.2. FCV Isolates used in sequence analysis

Isolate	Genbank Accession(s)	Reference*
FCV-127	DQ910786[¶,#]	This paper
FCV-131	DQ910787[¶,#]	This paper
FCV-796	DQ910788[¶,#]	This paper
Deuce[†]	DQ910789[¶,#]	This paper
FCV-5[†]	DQ910790[¶,#]	This paper
Georgie[†]	DQ910791[¶,#]	This paper
George Walder[†]	DQ910792[¶,#]	This paper
Jengo[†]	DQ910793[¶,#]	This paper
Ari[†]	DQ910794[¶,#]	This paper
Kaos[†]	DQ910795[¶,#]	This paper
UTCVM-NH1	AY560113[¶,#]	Abd-Eldaim *et al.* (2005)
UTCVM-NH2	AY560114[¶,#]	Abd-Eldaim *et al.* (2005)
UTCVM-NH3	AY560115[¶,#]	Abd-Eldaim *et al.* (2005)
UTCVM-H1[†]	AY560116[¶,#]	Abd-Eldaim *et al.* (2005)
UTCVM-H2[†]	AY560117[¶,#]	Abd-Eldaim *et al.* (2005)
USDA	AY560118[¶,#]	Abd-Eldaim *et al.* (2005)
182cvs5A	AF031875[¶]	Baulch-Brown *et al.* (1999)
V83A	AF031876[¶]	Baulch-Brown *et al.* (1999)
V274	AF031877[¶]	Baulch-Brown *et al.* (1999)
V276	AF032106[¶]	Baulch-Brown *et al.* (1999)
V77	AF038126[¶]	Baulch-Brown *et al.* (1999)
F9[‡]	M86379[¶,#]	Carter *et al.* (1992)
2280	X99445[¶]	Geissler *et al.* (1997)
KS109	X99446[¶]	Geissler *et al.* (1997)
KS20	X99447[¶]	Geissler *et al.* (1997)
KS40	X99448[¶]	Geissler *et al.* (1997)
KS8	X99449[¶]	Geissler *et al.* (1997)
LS015	AF109464	Glenn *et al.* (1999)
F65	AF109465[¶,#]	Glenn *et al.* (1999)
JOK63	AF109466[¶]	Glenn *et al.* (1999)
LS012	AF109467[¶]	Glenn *et al.* (1999)
A4	AF109468[¶]	Glenn *et al.* (1999)
213/95	AF283778[¶]	Martella *et al.* (2002)
CVXPOLYCYS	M32296[#]	Neill *et al.* (1990)
CFI/68	M32819[¶]; U13992[#]	Neill *et al.* (1991); Unpublished
NADC	L09718[¶]	Seal *et al.* (1993)
KCD	L09719[¶]	Seal *et al.* (1993)
255	U07130[¶]	Seal & Neill (1995)
LLK	U07131[¶]	Seal & Neill (1995)

Table 2.2 (Continued)

Urbana	L40021[¶,#]	Sosnovtsev & Green (1995)
FCV2024[‡]	AF479590[¶,#]	Thumfart & Meyers (2002)
F4[‡]	D90357[¶];D31836[#]	Tohya *et al.* (1991); Oshikamo *et al.*(1994)
FCV-U1	AF357010[¶]	Unpublished
AF486286	AF486286[¶]	Unpublished
V66/97	AJ009721[¶]	Unpublished
FCV-U2	AY053460[¶]	Unpublished
Cranleigh	AY299541[¶]	Unpublished
FCV/DD/2006/GE	DQ424892[¶,#]	Unpublished
FRG[§]	NC_001543[#]	Meyers *et al.* (2000)
whn/China/03/2005[§]	DQ069282[¶]	Unpublished

* The reference cited is the first publication to provide sequence for the isolate. Isolates designated as unpublished do not have a publication associated with the accession.
† VS-FCV isolate
‡ Vaccine strain
§ Rabbit hemorrhagic disease virus (RHDV) isolate used as outgroup
¶ Capsid sequence
# Proteinase-polymerase sequence

Ronquist and Huelsenbeck, 2003), and the maximum-likelihood method using the software PAUP* Version 4.0 Beta (Sinauer Associates). Neighbour-joining and maximum-likelihood generated trees were bootstrapped with the corresponding, aforementioned software. Construction and bootstrapping of phylogenetic trees inferred from amino acid sequence was performed using ClustalW utilizing the BLOSUM series (80, 62, 40 and 30) weight matrices for proteins. Constructed trees were visualized using NJPLOT (Perriere & Gouy, 1996).

Temperature inactivation and stability experiments. Thermal inactivation of virus isolates was performed using a thermal cycler (MyCycler, BioRad). Virus samples were incubated at 37.0, 41.8, 46.2, 52.2, 56.9, and 62.0 °C in thin-wall PCR tubes (Fisher) for 30 min then plaque titrated. Viral stability was investigated by

maintaining virus in aliquots at room temperature, 4 ºC, and -80 ºC for up to 10 weeks. Aliquots in triplicate were plaque titrated at regular intervals.

Generation of single- and multiple-cycle growth curves. CRFK cell monolayers were infected with different FCV isolates at multiplicities of 5 and 0.01, for single- and multiple-cycle growth curves respectively. Virus was adsorbed to cells for 1 h at room temperature in DMEM plus 0.1% BSA; EMEM plus 5% fetal bovine serum supplemented as above was then added and the cells were incubated for various times at 37 °C in 5% CO_2. At various times post-infection samples were frozen and stored at -80 °C for later titration. Prior to plaque assay, all samples were frozen and thawed three times. Viral growth at each time point was calculated by subtracting the log10 p.f.u ml^{-1} at T = 0 from the log10 p.f.u ml^{-1} measured at the time point. Results are expressed as the change in plaque titer over time with the mean and standard deviation of three replicates shown.

Cell viability assay. The viability of infected CRFK cells was evaluated using a commercial assay of ATP levels (CellTiter-Glo Reagent, Promega) according to the manufacturer's recommendations. 96-well plates were read using a Veritas Microplate Luminometer (Turner Biosystems). Relative luminescence units of experimental wells were compared to control wells to determine percent change in ATP.

Statistical analyses. Comparisons of titer levels between sets of three replicates were analyzed by ANOVA using the Analyse-it (Analyse-it Software) statistical analysis add-in for Microsoft Excel. Graphs were prepared using Kaleidagraph (Synergy Software).

2.4 Results

Single cycle kinetics of growth of different FCV isolates in CRFK cells. We compared the growth kinetics of nine FCV isolates that differed in virulence (Table

Figure 2.1. Single and multiple cycle growth kinetics of selected FCV isolates. CRFK monolayers were infected with viruses at an m.o.i. of (A) 5 or (B) 0.01 and change in viral titer was determined by plaque assay. The mean $\log_{10}$ titer ($\log_{10}$ titer at each time point minus $\log_{10}$ titer at T=0) of three replicates is shown. Isolates from cats diagnosed with VS disease are shown with solid lines and hollow markers. The vaccine strain and non-VS isolates are displayed with dashed lines and solid markers. Significant time points as determined by analysis of variance are indicated (*).

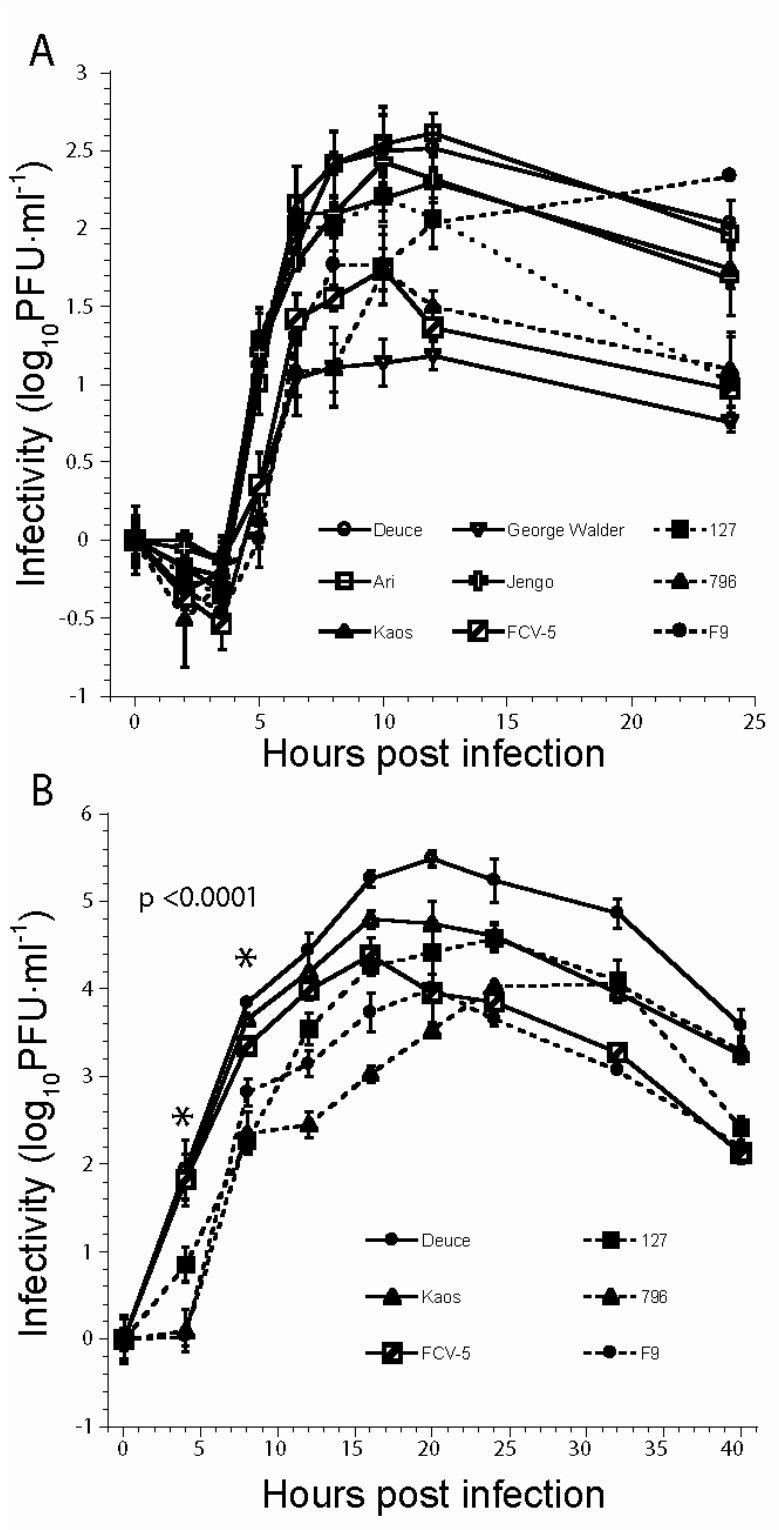
A
Infectivity (log_{10}PFU·ml^{-1})
Hours post infection
Deuce
George Walder
127
Ari
Jengo
796
Kaos
FCV-5
F9
B
p <0.0001
*
*
Infectivity (log_{10}PFU·ml^{-1})
Hours post infection
Deuce
127
Kaos
796
FCV-5
F9

2.1). We found that all of the FCV isolates tested grew rapidly during a single round of viral replication that was characterized by a lag phase of ~ 3.5 h followed by logarithmic growth that lasted 3 to 4.5 h (Figure 2.1A). Peak yields of virus were produced for all except vaccine strain, F9, at 8-12 h post-infection. We noted that viral yield of all the isolates except F9 decreased 0.5 to 1 $\log_{10}$ from peak titer at 8-12 h post-infection by 24 h post-infection. The single cycle growth kinetics of VS-FCV isolates were not statistically different from those of non-VS isolates; however, cells infected with the VS-FCV isolates Ari and Deuce yielded the most virus (2.5 $\log_{10}$). We conclude that FCV isolates have a short replicative cycle in CRFK cells (10 to 12 h) and that FCV isolates of differing virulence have similar single cycle growth kinetics, but may differ in the final yield of virus produced.

Multiple cycle kinetics of growth of FCV in CRFK cells. We noted that virulent FCV isolates tended to produce larger plaques and hypothesized that these isolates would spread faster than less virulent isolates in tissue culture. We therefore examined the growth kinetics of three VS-FCV isolates, two non-VS isolates, and the vaccine strain, F9, during multiple replicative cycles to evaluate their ability to spread in tissue culture. Consistent with their larger plaque size, we found that the growth kinetics of VS-FCV isolates were faster than those of non-VS isolates (Figure 2.1B). By 4 h post-infection (h p.i.) the titers of VS-FCV isolates were increasing logarithmically, and had yielded 2 $\log_{10}$ of infectious virus. In contrast, the vaccine strain F9 and isolate 796 had not yet entered logarithmic growth. FCV-127, a non-VS isolate that produced large plaques, was growing logarithmically at 4 h p.i., but had produced 10-fold less infectious virus than the three VS-FCV isolates. The differences in log titers at 4 and 8 h p.i. between the VS-FCV and non-VS isolates were statistically significant as determined by analysis of variance ($p < 0.0001$). The final yields of virus varied; however, the two highest yields (~5.5 and 4.8 $\log_{10}$) were

attained by VS-FCV isolates Deuce and Kaos, respectively. From these results we conclude that VS-FCV isolates appear to produce infectious virions earlier when cells are infected at low multiplicity and may attain higher yields than less virulent isolates in CRFK cells.

Cytopathic effect of different FCV isolates. During the multiple cycle growth kinetic experiments, we noted that cells infected with VS-FCV isolates displayed morphologic changes of rounding and detachment from the vessel surface earlier than other FCV isolates (Figure 2.2A). From 14 h p.i. onwards, we frequently observed clusters of VS-FCV infected cells that were rounded up and partially or fully detached from the plate surface. In contrast, few non-VS isolate-infected cells displayed such morphologic changes at 14 h p.i. and larger clusters of cells with such morphologic alterations were absent. Non-VS isolate FCV-127, which was isolated from a kitten with severe pneumonia, caused more severe morphologic changes than isolate FCV-796 suggesting that the severity of the cytopathic effects we saw in part correlated with virulence. These observations suggested that VS-FCV isolates caused increased cytopathogenicity. The mechanisms that underlie FCV cytopathogenicity are not fully understood, although FCV infection is known to induce apoptosis (Roberts *et al.,* 2003, Sosnovtsev *et al.,* 2003, Natoni *et al.,* 2006). To test the possibility that VS-FCV isolates caused increased cytopathic effect in infected cells, we measured the intracellular ATP levels of cells infected with VS-FCV, non-VS isolates and the F9 vaccine strain at different times after infection in cells infected at multiplicities of 0.01 and 5 (Figures 2.2B and 2.2C). Intracellular ATP levels have been used to quantify the cytotoxic effect of the cytokine tumor necrosis factor α (Crouch *et al.*, 1993) and as an indicator of the cytopathic effect of murine leukemia virus on CHO-K1 cells (Bruce *et al.*, 2005). Under multiple cycle growth conditions (m.o.i. = 0.01), at 14 h p.i. cells infected with VS-FCV isolates had ATP levels that were equal to or higher than

Figure 2.2. Intracellular ATP levels in FCV-infected cells.

(A) Confluent monolayers of CRFK cells were infected with the indicated FCV isolates at an m.o.i. of 0.01. At 14 h p.i. phase contrast images of cell morphology were collected using a 40× objective with a CCD camera. (B) Intracellular ATP levels in CRFK monolayers at different times following infection with viruses under multiple cycle conditions (m.o.i of 0.01) (C) or single cycle conditions (m.o.i. of 5). ATP levels were expressed as a percentage of the mean level of mock-infected cells. Each data point represents the mean ± standard deviation of three replicates. For clarity, the T=0 h data point in graph (B) has been omitted and an axis break is indicated between 0 and 12 h p.i. The omitted data point was not statistically different from the results determined at T=12 h. Isolates from cats diagnosed with VS disease are shown with solid lines and hollow markers. The vaccine strain and non-VS isolates are displayed with dashed lines and solid markers.

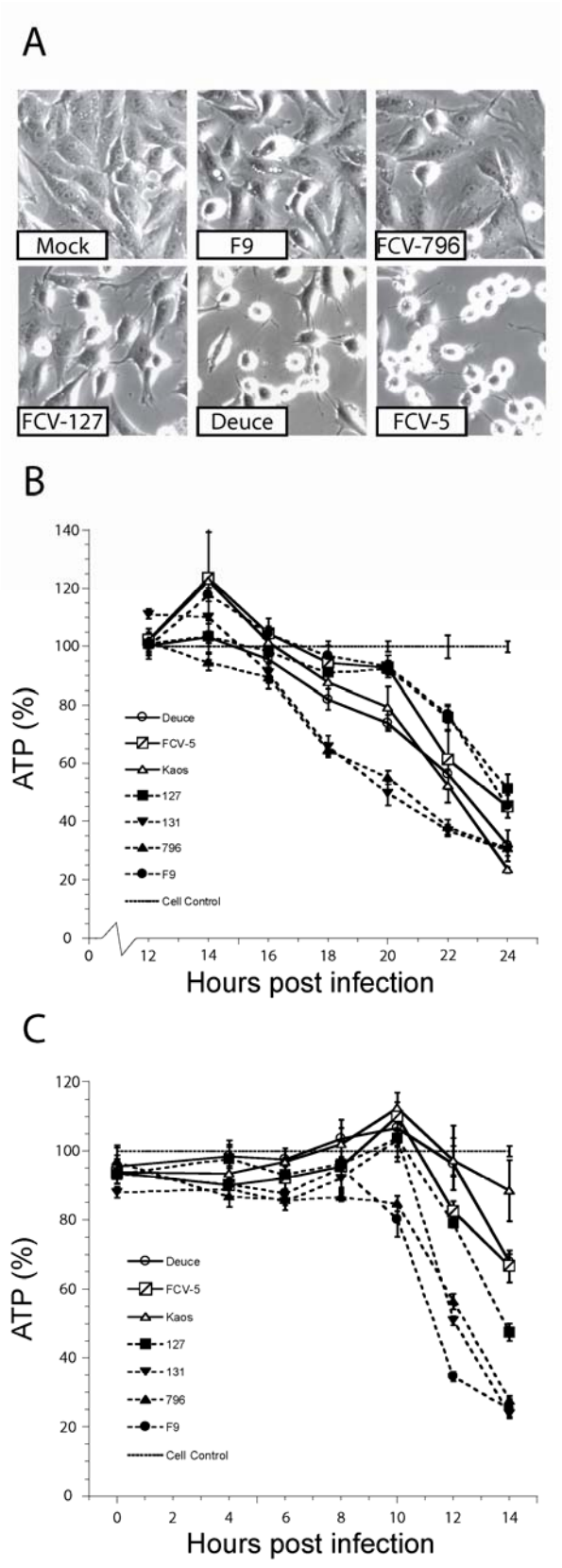
A
Mock
F9
FCV-796
FCV-127
Deuce
FCV-5
B
ATP (%)
Deuce
FCV-5
Kaos
127
131
796
F9
Cell Control
Hours post infection
C
ATP (%)
Deuce
FCV-5
Kaos
127
131
796
F9
Cell Control
Hours post infection

control levels, despite obvious changes in cell morphology (Figure 2.2A). ATP levels in cells infected with all FCV isolates diverged from control levels by 16 to 20 h p.i. (Figure 2.2B). Non-VS isolates 796 and 131 demonstrated the most rapid decrease in ATP with levels at 50% of control levels at 20 h p.i. For all of the isolates we investigated, the cellular ATP levels dropped to 25-50% of control levels by 24 h p.i. Under single cycle growth conditions (m.o.i. = 5), ATP levels in infected cells fell below control levels at 10 to 14 h p.i. (Figure 2.2C). Cells infected with the vaccine strain F9 displayed the earliest divergence from uninfected control ATP levels at 10 h p.i. By 14 h p.i., cells infected with non-VS isolates had ATP levels that were only 25-50% of the levels of the uninfected control, whereas, cells infected with VS-FCV isolates maintained ATP levels 70-90% of the control. We conclude that under multiple cycle conditions cells infected with VS-FCV isolates show cytopathic effects as early as 14 h p.i., although the ATP content of those cells is similar to uninfected cells. In addition, under single cycle conditions, cells infected with VS-FCV isolates maintain ATP levels longer than cells infected with the non-VS isolates and the vaccine strain F9.

Temperature inactivation of different FCV isolates. During VS-FCV outbreaks, rapid virus spread has been mediated partly by fomites (Pedersen *et al.*, 2000, Schorr-Evans *et al.*, 2003, Hurley *et al.,* 2004). These observations suggested to us that VS-FCV isolates might be more environmentally stable than non-VS isolates. To address this possibility, we examined the resistance of selected isolates to thermal inactivation (Table 2.1 and Figure 2.3). Aliquots of virus were incubated at 37.0, 41.8, 46.2, 52.2, 56.9, and 62.0 °C for 30 minutes in a thermal cycler and then assayed for infectivity by plaque assay. We found that all isolates substantially lost infectivity following a 30 minute incubation at 46.2 °C (Figure 2.3). The F9 vaccine strain was most sensitive to thermal inactivation, losing all infectivity following 30 min

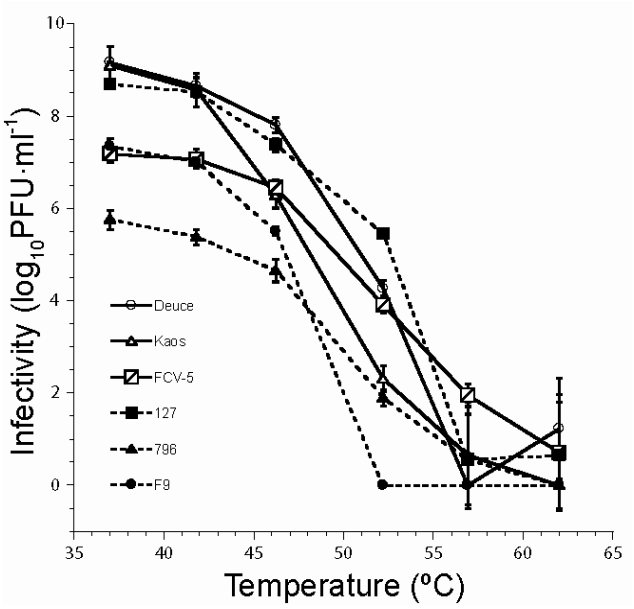

Figure 2.3. Thermal inactivation of FCV. Virus aliquots were incubated for 30 minutes at the indicated temperatures, and then the remaining infectivity was determined by plaque assay. Each data point represents the mean log_{10} p.f.u ml^{-1} ± standard deviation of three replicates. Isolates from cats diagnosed with VS disease are shown with solid lines and hollow markers. The vaccine strain and non-VS isolates are displayed with dashed lines and solid markers.

incubation at 52.2 °C. The other isolates were fully inactivated at 56.9 °C, except for isolate FCV-5 (fully inactivated at 62 °C). We conclude that all of the isolates we examined were more resistant to thermal inactivation than F9, but exhibited differing temperature stabilities with respect to each other.

Stability of different FCV isolates at room temperature, 4 °C and -80 °C. We further evaluated the stabilities of different FCV isolates, by assaying their infectivity following extended incubations at room temperature, 4 °C and -80 °C (Figure 2.4). Isolates stored at room temperature lost 2 to 5 $\log_{10}$ of infectivity after three days, with the two VS-FCV isolates Deuce and FCV-5 and the non-VS isolate 127 decreasing in infectivity by 2 to 3 $\log_{10}$ and the vaccine strain F9 and non-VS isolate 796 decreasing by 4 to 5 $\log_{10}$. By day 6, isolates FCV-5, 796 and F9 had completely lost infectivity. FCV-Deuce completely lost infectivity by day 10, while isolate 127 retained a low level of infectivity at the conclusion of the 12 day experiment (Figure 2.4). We noted that as viral titers dropped, the variability of the plaque assays increased with standard deviations ranging from 0.75 to 2 $\log_{10}$. We found no obvious correlation between the temperature stability of different FCV isolates and their virulence.

When a limited set of isolates, the vaccine strain F9 and two VS-FCV isolates (FCV-5 and Deuce) were maintained at 4 ºC, we observed that the vaccine strain F9 began to drop in titer by the 10^{th} day of the experiment (Figure 2.4). The VS-FCV isolates maintained full infectivity until day 21. By the third week, all isolates exhibited similar rates of infectivity loss and by 6 to 10 weeks had completely lost infectivity. Although the two VS-FCV strains demonstrated enhanced stability over the vaccine strain at 4 °C during the first two weeks of storage, further testing will be necessary to confirm that VS-FCV isolates are more stable at 4 °C than other FCV isolates. Similar to our findings above, as viral titers dropped, the variability of the

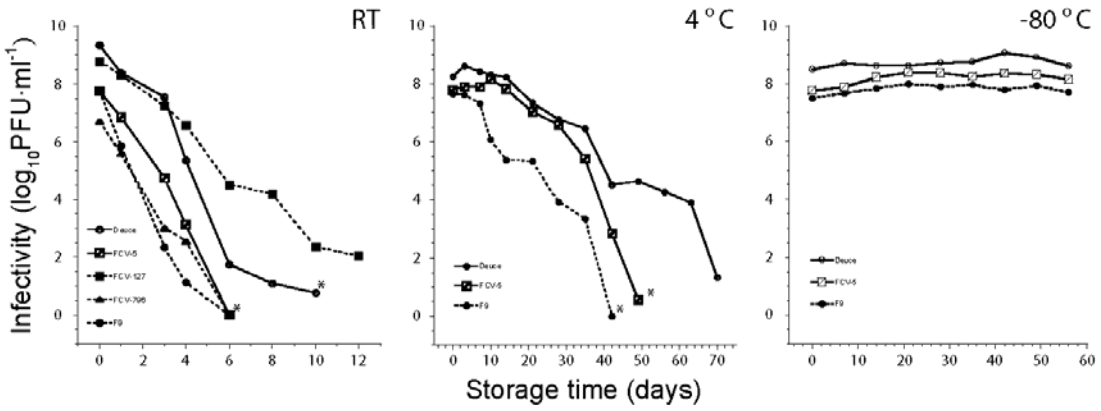

Figure 2.4. Stability of FCV over time when maintained at room temperature, 4 ºC and -80 ºC. Aliquots of virus were maintained at room temperature, 4 °C, and -80 °C for the indicated number of days then the remaining infectivity was determined by plaque assay. Each data point represents the mean $\log_{10}$ p.f.u ml^{-1} of three replicates. As viral titers dropped, the variability of the plaque assays increased. Standard deviations ranged from 0.75 to 2 $\log_{10}$ beginning on the fourth day of the room temperature experiment, and from 1.5 to 3 $\log_{10}$ beginning on day 35 of the 4 °C experiment. Therefore, the standard deviation bars have been omitted for clarity. Titers were also observed to oscillate around the zero titer mark for isolates FCV-5, Deuce, F9, and 796 by values up to 1.5 $\log_{10}$ (RT assay) and 3 $\log_{10}$ (4 °C assay). These data points have also been omitted for clarity. The first data point indicating loss of infectivity is indicated (*). Isolates from cats diagnosed with VS disease are shown with solid lines and hollow markers. The vaccine strain and non-VS isolates are displayed with dashed lines and solid markers.

plaque assays increased. None of the isolates tested lost infectivity when stored at 80 °C for 8 weeks (Figure 2.4).

Sequence comparison of VS-FCV isolates and other FCV isolates.

Abd-Eldaim *et al.* (2005) and Foley *et al*. (2006) have suggested that certain residues within the hypervariable region of the capsid protein sequence are unique to VS-FCV isolates. We therefore sequenced the capsid VP1-encoding second ORF of the FCV genome for all the isolates and performed nucleotide and primary amino acid sequence alignments and phylogenetic analyses to investigate the relatedness of these sequences and 37 other FCV complete capsid sequences (Table 2.2). Capsid amino acid sequence alignments (ClustalW) revealed that no residues were unique to the VS-FCV isolates we investigated. We used *Rabbit hemorrhagic disease virus* (RHDV), a Calicivirus in the genus *Lagovirus,* as an outgroup to root the phylogenies. Using nucleotide (neighbor-joining method) and amino acid (BLOSUM) based phylogenies, we found that the VS-FCV isolates did not form a unique clade (Figures 2.5A and B). As expected, isolates collected from the same outbreak of VS-FCV in Los Angeles, CA in 2002 (George Walder, Jengo, and Kaos) clustered together in nucleotide and amino acid analyses, with determined bootstrap values of 100%. The VS-FCV isolates Ari, Georgie, Deuce and FCV-5 as well as two other previously described VS-FCV isolates (Abd-Eldaim *et al.*, 2005) were not closely related. Trees generated utilizing the Bayesian method and maximum likelihood method of phylogenetic inference also showed a clustering of the three VS-FCV isolates from the Los Angeles outbreak while the remainder of the VS-FCV isolates were scattered throughout the tree.

We also sequenced the portion of the first ORF that encodes the proteinase-polymerase (pro-pol). Sequences from isolates investigated in this paper were compared with 14 previously published pro-pol sequences (Table 2.2). Similar to

Figure 2.5. Phylogenetic analysis of FCV capsid nucleotide and protein sequences. Phylogenetic analysis was performed on the (A) nucleotide sequences and (B) protein sequences of ORF2 for all the FCV isolates used in this study and 37 other FCV sequences obtained from Genbank. Trees were generated using the nearest-neighbor distance method. *Rabbit hemorrhagic disease virus* (RHDV) was used as an outgroup for each analysis; outgroup branch lengths have been shortened for simplicity. VS-FCV isolates sequenced in this paper (*), VS-FCV isolates previously sequenced (†), and FCV field isolates sequenced in this paper (‡) are indicated. Vaccine strains are underlined, and the strain name provided in parentheses. Bootstrap values greater than 90% are indicated.

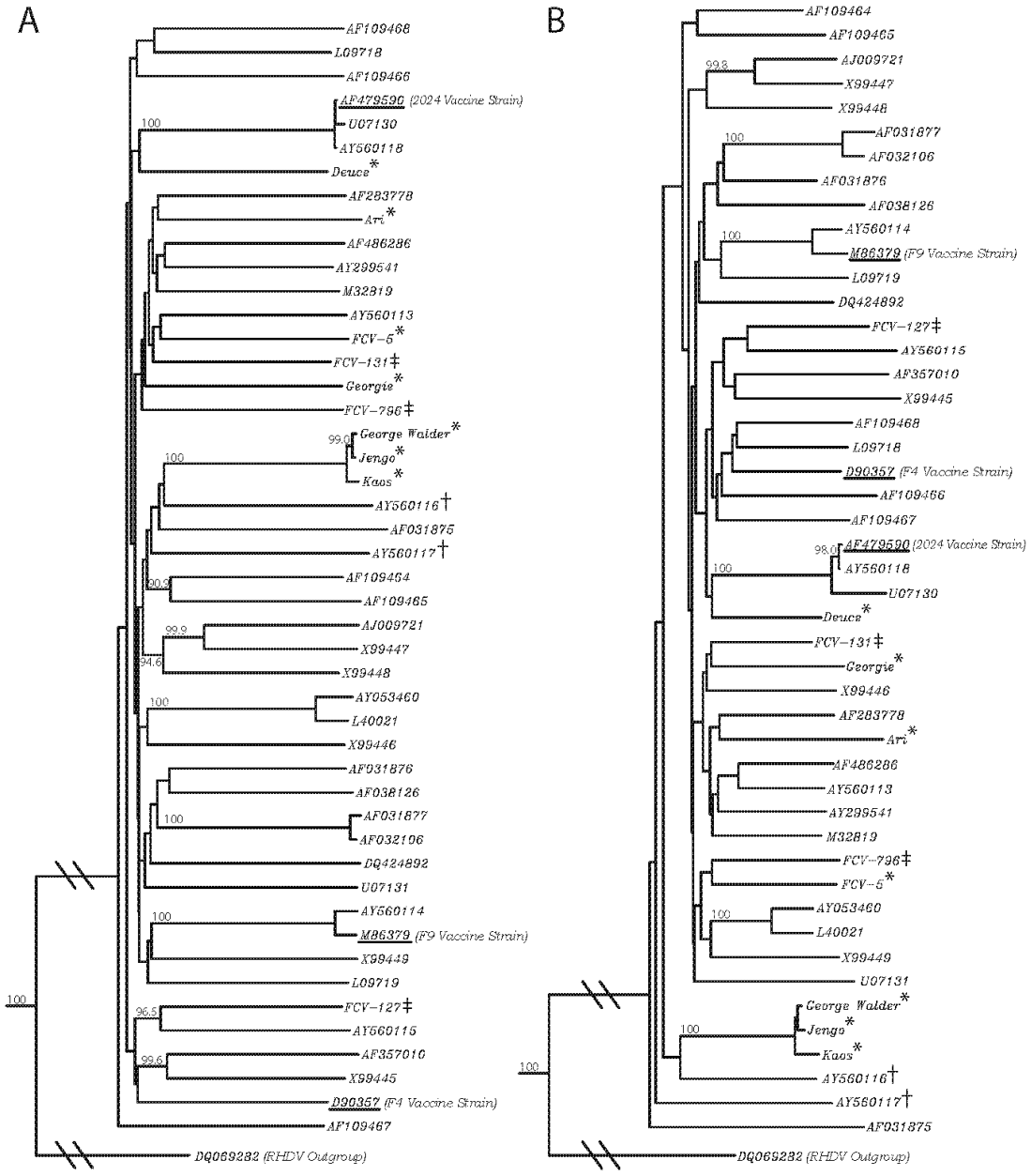
A
AF109468
L09718
AF109466
AF479590 (2024 Vaccine Strain)
U07130
AY560118
Deuce*
AF283778
Ari*
AF486286
AY299541
M32819
AY560113
FCV-5*
FCV-131‡
Georgie*
FCV-796‡
George Walder*
Jengo*
Kaos*
AY560116†
AF031875
AY560117†
AF109464
AF109465
AJ009721
X99447
X99448
AY053460
L40021
X99446
AF031876
AF038126
AF031877
AF032106
DQ424892
U07131
AY560114
M86379 (F9 Vaccine Strain)
X99449
L09719
FCV-127‡
AY560115
AF357010
X99445
D90357 (F4 Vaccine Strain)
AF109467
DQ069282 (RHDV Outgroup)
B
AF109464
AF109465
AJ009721
X99447
X99448
AF031877
AF032106
AF031876
AF038126
AY560114
M86379 (F9 Vaccine Strain)
L09719
DQ424892
FCV-127‡
AY560115
AF357010
X99445
AF109468
L09718
D90357 (F4 Vaccine Strain)
AF109466
AF109467
AF479590 (2024 Vaccine Strain)
AY560118
U07130
Deuce*
FCV-131‡
Georgie*
X99446
AF283778
Ari*
AF486286
AY560113
AY299541
M32819
FCV-796‡
FCV-5*
AY053460
L40021
X99449
U07131
George Walder*
Jengo*
Kaos*
AY560116†
AY560117†
AF031875
DQ069282 (RHDV Outgroup)

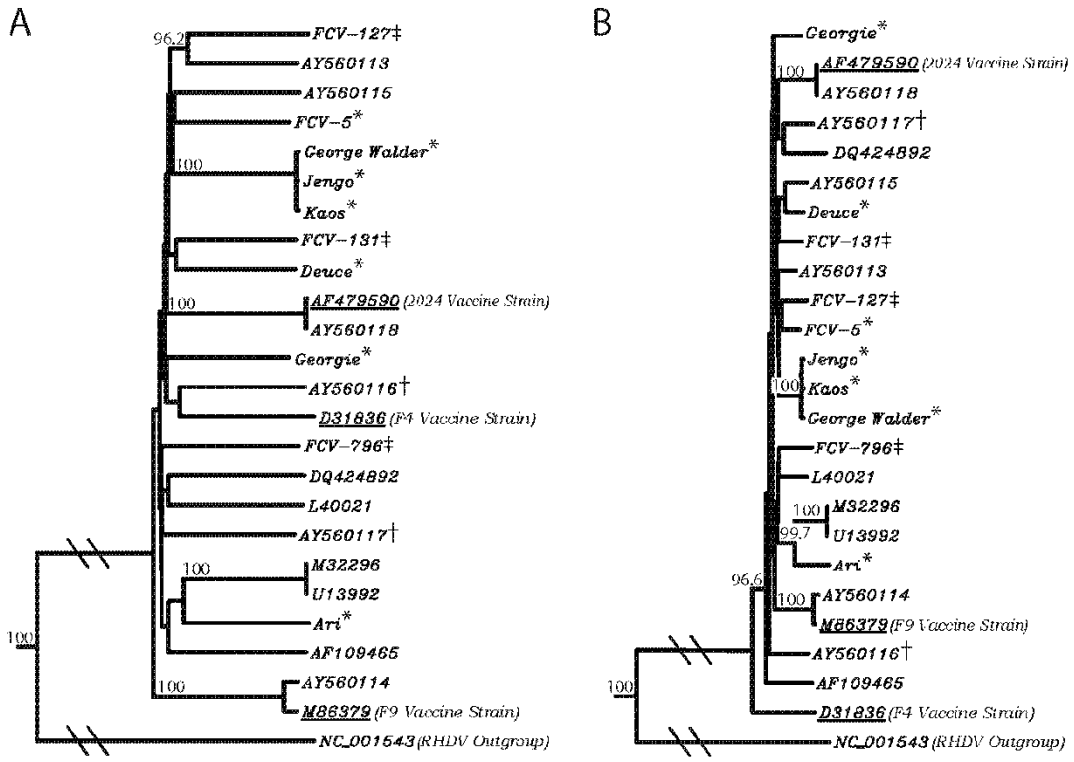

Figure 2.6. Phylogenetic analysis of FCV proteinase-polymerase nucleotide and protein sequences. Phylogenetic analysis was performed on the (A) nucleotide sequence and (B) protein sequence of the proteinase-polymerase for all FCV isolates used in this study and 14 other FCV sequences obtained from GenBank. Trees were generated using the nearest-neighbor distance method. *Rabbit hemorrhagic disease virus* (RHDV) was used as an outgroup for each analysis; outgroup branch lengths have been shortened for simplicity. VS-FCV isolates sequenced in this paper (*), VS-FCV isolates previously sequenced (†), and FCV field isolates sequenced in this paper (‡) are indicated. Vaccine strains are underlined, and the strain name provided in parentheses. Bootstrap values greater than 90% are indicated.

results from the capsid region, pro-pol sequence alignments (ClustalW) revealed no residues unique to the VS-FCV isolates investigated. The overall nucleotide identity was 80.6 ± 3.1% and the amino acid identity was 92.9 ± 2.1%. This was not different than the nucleotide (82.6 ± 5.4%) or primary amino acid (94.4 ± 2.2%) sequence similarity between the VS- isolates investigated. Phylogenetic trees were rooted as above, using the sequence of the RHDV pro-pol. Both nucleotide (neighbor-joining method) and amino acid (BLOSUM) based phylogenies were similar to those of the capsid sequences and VS-FCV isolates did not segregate from other FCV isolates (Figures 2.6A and B). The three isolates from the 2002 Los Angeles outbreak grouped together (bootstrap values of 100%). The sequences of the other VS-FCV isolates Deuce, Georgie, FCV-5, Ari, and the two Tennessee isolates were not closely related. Similar results were obtained when phylogenies were inferred using Bayesian and maximum-likelihood methods. We conclude that VS-FCV isolates do not represent a unique clade of FCV, but instead appear to have arisen independently multiple times in different geographic locations.

2.5 Discussion

The reported outbreaks of VS-FCV have been characterized by severe clinical disease, rapid spread and high mortality rates (Pedersen et al., 2000, Schorr-Evans et al., 2003, Hurley et al., 2004, Pesavento et al., 2004, Coyne et al., 2006). As vaccinated cats appear to be as susceptible to this form of FCV as unvaccinated cats, disease control is currently problematic. A major difficulty is that viruses associated with VS disease cannot be distinguished from other FCV isolates in vitro. One study reported that sequences from a small set of VS-FCV isolates were no more similar to each other than to other non-VS field isolates of FCV (Abd-Eldaim et al., 2005). Despite this, the disease has been reproduced in experimental animals indicating that

the genetic differences are likely hidden by the high variability of the FCV genome (Pedersen et al., 2000). The initial goal of our study was to identify in vitro phenotypes of VS-FCV isolates that would distinguish them from other less virulent FCV isolates and which could be used as a correlate to identify the underlying genotype(s) associated with FCV virulence.

Previous reports have described the single cycle growth kinetics of "classical" isolates of FCV (Studdert et al., 1970, Kreutz & Seal, 1995). This is the first report of single cycle growth kinetics of VS-FCV isolates, as well the first report of multiple cycle growth kinetics for any FCV isolate. All of the FCV isolates we investigated displayed similar single cycle growth kinetics, and our findings are generally similar to those previously published (Studdert et al., 1970, Kreutz & Seal, 1995). Although VS- and non-VS isolates displayed similar kinetics, the VS-FCV isolates tended to replicate to higher titer suggesting higher per cell yields. In contrast, during multiple cycle growth we observed that the three VS-FCV isolates produced infectious virions earlier and/or to substantially higher titer than the vaccine/non-VS isolate group. Given that the VS- and non-VS isolates had similar kinetics of growth during a single cycle of replication, these findings indicate that VS-FCV isolates infect CRFK cells more efficiently than non-VS strains. Such efficiency suggests that differences in virus attachment, entry, establishment of replication sites or release from cells may determine the increased growth of VS-FCV isolates and perhaps play a role in the increased pathogenicity of VS-FCV isolates.

In addition to more efficient infection, we also observed that cells infected with VS-FCV isolates at a low multiplicities displayed cytopathic effects earlier than those infected with non-VS field isolates or the vaccine strain. Surprisingly, VS-FCV infected cells had similar or higher ATP levels than the uninfected controls at time points when cytopathic effects were first readily seen. Under single cycle conditions,

VS-FCV-infected cells maintained ATP levels for longer than the non-VS isolates. By maintaining cellular ATP levels, VS-FCV isolates may delay the onset of the final stages of apoptosis, thus allowing the production and/or release of more virus particles. Recently it was reported that intracellular pools of ATP and other nucleotides are able to directly block cytochrome C-initiated apoptosome formation and caspase activation (Chandra et al., 2006). Alternatively, maintaining intracellular ATP levels may serve to promote energy-dependent apoptotic cell death and prevent cellular necrosis (Chiarugi, 2005). This may prove advantageous to viral replication in vivo by limiting the inflammatory reaction initiated by necrotic cells.

Fomite transmission has been implicated as an important factor in the rapid spread observed during the documented VS-FCV outbreaks (Pedersen, et al., 2000, Hurley, et al., 2004). We therefore hypothesized that VS-FCV isolates might possess increased environmental stability over non-VS isolates. However, while individual isolates displayed minor differences in their sensitivity to temperature inactivation, there was no correlation with virulence. We noted, however, that the vaccine strain F9 was completely inactivated at a lower temperature than the other isolates we tested, suggesting that some capsid stability was lost during the selection for attenuation of the F9 strain. The F9 strain has been extensively used to evaluate the sensitivity of caliciviruses to environmental inactivation by various methods (Duizer et al., 2004, Tree et al., 2005, Malik et al., 2006). Our results suggest that these findings should be tempered by the knowledge that field strains may be more resistant to inactivation than vaccine strains.

Minor differences in stability between isolates after extended incubation at room temperature or 4 °C did not correlate with virulence. In contrast to a previous report that indicated that virions were more stable when maintained at 4 °C (Komolafe, 1979), we found that all of the isolates we tested lost infectivity when

stored for longer than 2-3 weeks at 4 °C, but retained full infectivity when stored at -80 °C. The reasons for these differences are unclear, but may be due to stabilizing effects of serum proteins within the lysate (Komolafe, 1979). Additionally, we also found that infectivity was maintained after as many as 56 freeze/thaw cycles. Therefore, FCV appears to tolerate multiple freeze/thaw cycles without loss of infectivity, indicating that storage of viral lysates at -80 °C is optimal.

Previous analyses of the capsid and pro-pol sequences of VS-FCV isolates found them to be no more similar to each other than to other non-VS isolates (Hurley et al., 2004, Abd-Eldaim et al., 2005, Foley et al., 2006). Our sequence analyses support these conclusions and suggest that the different VS-FCV isolates have arisen independently in distinct geographic locations. These studies also suggested that there were amino acid sequences within the hypervariable region (residues 426-452) of the capsid that were unique to VS-FCV isolates. However, when we analyzed all the available VS-FCV sequences together, we found there were no sequences or amino acid changes unique to all VS- isolates in the capsid or pro-pol regions.

We recognize that many of our conclusions are based on two assumptions. The first is that the VS-FCV samples we are characterizing still possess the virulent nature of the original isolate. Passage in tissue culture has been limited to prevent selection of variants. Furthermore, three of the isolates we characterized have been used to reproduce the VS-FCV disease in cats (Ari, Pedersen et al., 2000; FCV-5, Rong et al., 2006; Kaos, unpublished). While the other isolates have not been tested in vivo, the experience thus far is that VS-FCV isolates can be passed at least three times in tissue culture without loss of virulence, and perhaps up to 20 times (Rong, et al., 2006). The second is that all strains considered non-VS isolates do not cause VS disease. However, it is possible that many cases of VS-FCV go undetected. The investigated isolate FCV-127 originated from a shelter where numerous cats died due

to pneumonia. In all experiments, isolate 127 behaved more like a VS-FCV isolate than the other non-VS field isolates. Thus, we speculate that the differences in viral growth patterns we noted between VS and non-VS viruses may in fact be shared by other 'virulent' FCV isolates. Currently, the only means to verify a particular isolate causes VS disease is by reproducing the disease syndrome in an experimentally infected cat.

In summary, we have investigated several viral characteristics in an attempt to define an in vitro phenotype unique to virulent systemic strains. Our findings indicate that there are differences between VS and non-VS isolates that may serve as markers for virulence. We are currently further evaluating the genetic bases of these differences.

2.6 Acknowledgments

We thank Dr. Neils Pedersen and Dr. Kate F. Hurley for the generous gift of reagents. Aziza Solomon, Lynne Anguish, and Christian Nelson provided excellent technical assistance. We thank Dr. Ed Dubovi of the New York State Animal Health Diagnostic Center at Cornell University for providing VS and other FCV isolates. We thank Karin Hoelzer for advice on phylogenetic analysis. We thank Dr. Hollis Erb for advice on statistical analyses. This work was supported by grants from the Cornell Feline Health Center, and the Winn foundation Miller trust. R. J. O. is the recipient of a scholarship from Cornell University.

REFERENCES

Abd-Eldaim, M., Potgieter, L. & Kennedy, M. (2005). Genetic analysis of feline caliciviruses associated with a hemorrhagic-like disease. *J Vet Diagn Invest* **17**, 420-9.

Bannasch, M. J. & Foley, J. E. (2005). Epidemiologic evaluation of multiple respiratory pathogens in cats in animal shelters. *J Feline Med Surg* **7**, 109-19.

Baulch-Brown, C., Love, D. & Meanger, J. (1999). Sequence variation within the capsid protein of Australian isolates of feline calicivirus. *Vet Microbiol* **68**, 107-17.

Binns, S. H., Dawson, S., Speakman, A. J., Cuevas, L. E., Hart, C. A., Gaskell, C. J., Morgan, K. L. & Gaskell, R. M. (2000). A study of feline upper respiratory tract disease with reference to prevalence and risk factors for infection with feline calicivirus and feline herpesvirus. *J Feline Med Surg* **2**, 123-33.

Bruce, J. W., Bradley, K. A., Ahlquist, P. & Young, J. A. (2005). Isolation of cell lines that show novel, murine leukemia virus-specific blocks to early steps of retroviral replication. *J Virol* **79**, 12969-78.

Carter, M. J., Milton, I. D., Turner, P. C., Meanger, J., Bennett, M. & Gaskell, R. M. (1992). Identification and sequence determination of the capsid protein gene of feline calicivirus. *Arch Virol* **122**, 223-35.

Chandra, D., Bratton, S. B., Person, M. D., Tian, Y., Martin, A. G., Ayres, M., Fearnhead, H. O., Gandhi, V. & Tang, D. G. (2006). Intracellular nucleotides act as critical prosurvival factors by binding to cytochrome C and inhibiting apoptosome. *Cell* **125**, 1333-46.

Chiarugi, A. (2005). "Simple but not simpler": toward a unified picture of energy requirements in cell death. *Faseb J* **19**, 1783-8.

Coyne, K. P., Jones, B. R., Kipar, A., Chantrey, J., Porter, C. J., Barber, P. J., Dawson, S., Gaskell, R. M. & Radford, A. D. (2006). Lethal outbreak of disease associated with feline calicivirus infection in cats. *Vet Rec* **158**, 544-50.

Crouch, S. P., Kozlowski, R., Slater, K. J. & Fletcher, J. (1993). The use of ATP bioluminescence as a measure of cell proliferation and cytotoxicity. *J Immunol Methods* **160**, 81-8.

Duizer, E., Bijkerk, P., Rockx, B. De Groot, A., Twisk, F. & Koopmans, M. (2004). Inactivation of caliciviruses. *Appl Environ Microbiol* **70**, 4538-43.

Foley, J., Hurley, K., Pesavento, P. A., Poland, A. & Pedersen, N. C. (2006). Virulent systemic feline calicivirus infection: local cytokine modulation and contribution of viral mutants. *J Feline Med Surg* **8**, 55-61.

Geissler, K., Schneider, K., Platzer, G., Truyen, B., Kaaden, O. R. & Truyen, U. (1997). Genetic and antigenic heterogeneity among feline calicivirus isolates from distinct disease manifestations. *Virus Res* **48**, 193-206.

Glenn, M., Radford, A. D., Turner, P. C., Carter, M., Lowery, D., DeSilver, D. A., Meanger, J., Baulch-Brown, C., Bennett, M. & Gaskell, R. M. (1999). Nucleotide sequence of UK and Australian isolates of feline calicivirus (FCV) and phylogenetic analysis of FCVs. *Vet Microbiol* **67**, 175-93.

Huelsenbeck, J. P. & Ronquist, F. (2001). MRBAYES: Bayesian inference of phylogenetic trees. *Bioinformatics* **17**, 754-5.

Hurley, K. E., Pesavento, P. A., Pedersen, N. C., Poland, A. M., Wilson, E. & Foley, J. E. (2004). An outbreak of virulent systemic feline calicivirus disease. *J Am Vet Med Assoc* **224**, 241-9.

Kalunda, M., Lee, K. M., Holmes, D. F. & Gillespie, J. H. (1975). Serologic classification of feline caliciviruses by plaque-reduction neutralization and immunodiffusion. *Am J Vet Res* **36**, 353-6.

Komolafe, O. O. (1979). Effect of storage on the integrity of purified feline calicivirus particles. *Microbios* **26**, 137-46.

Kreutz, L. C. & Seal, B. S. (1995). The pathway of feline calicivirus entry. *Virus Res* **35**, 63-70.

Martella, V., Pratelli, A., Gentile, M., Buonavoglia, D., Decaro, N., Fiorente, P. & Buonavoglia, C. (2002). Analysis of the capsid protein gene of a feline-like calicivirus isolated from a dog. *Vet Microbiol* **85**, 315-22.

Meyers, G., Wirblich, C., Thiel, H. J. & Thumfart, J. O. (2000). Rabbit hemorrhagic disease virus: genome organization and polyprotein processing of a calicivirus studied after transient expression of cDNA constructs. *Virology* **276**, 349-63.

Natoni, A., Kass, G. E., Carter, M. J. & Roberts, L. O. (2006). The mitochondrial pathway of apoptosis is triggered during feline calicivirus infection. *J Gen Virol* **87**, 357-61.

Neill, J. D. (1990). Nucleotide sequence of a region of the feline calicivirus genome which encodes picornavirus-like RNA-dependent RNA polymerase, cysteine protease and 2C polypeptides. *Virus Res* **17**, 145-60.

Neill, J. D., Reardon, I. M. & Heinrikson, R. L. (1991). Nucleotide sequence and expression of the capsid protein gene of feline calicivirus. *J Virol* **65**, 5440-7.

Oshikamo, R., Tohya, Y., Kawaguchi, Y., Tomonaga, K., Maeda, K., Takeda, N., Utagawa, E., Kai, C. & Mikami, T. (1994). The molecular cloning and sequence of an open reading frame encoding for non-structural proteins of feline calicivirus F4 strain isolated in Japan. *J Vet Med Sci* **56**, 1093-9.

Pedersen, N. C., Elliott, J. B., Glasgow, A., Poland, A. & Keel, K. (2000). An isolated epizootic of hemorrhagic-like fever in cats caused by a novel and highly virulent strain of feline calicivirus. *Vet Microbiol* **73**, 281-300.

Perriere, G. & Gouy, M. (1996). WWW-query: an on-line retrieval system for biological sequence banks. *Biochimie* **78**, 364-9.

Pesavento, P. A., MacLachlan, N. J., Dillard-Telm, L., Grant, C. K. & Hurley, K. F. (2004). Pathologic, immunohistochemical, and electron microscopic findings in naturally occurring virulent systemic feline calicivirus infection in cats. *Vet Pathol* **41**, 257-63.

Poulet, H., Brunet, S., Leroy, V. & Chappuis, G. (2005). Immunisation with a combination of two complementary feline calicivirus strains induces a broad cross-protection against heterologous challenges. *Vet Microbiol* **106**, 17-31.

Roberts, L. O., Al-Molawi, N., Carter, M. J. & Kass, G. E. (2003). Apoptosis in cultured cells infected with feline calicivirus. *Ann N Y Acad Sci* **1010**, 587-90.

Rong, S., Slade, D., Floyd-Hawkins, K., and Wheeler, D. (2006). Characterization of a highly virulent feline calicivirus and attenuation of this virus. *Virus Re.* **122,** 95-108.

Ronquist, F. & Huelsenbeck, J. P. (2003). MrBayes 3: Bayesian phylogenetic inference under mixed models. *Bioinformatics* **19**, 1572-4.

Sato, Y., Ohe, K., Murakami, M., Fukuyama, M., Furuhata, K., Kishikawa, S., Suzuki, Y., Kiuchi, A., Hara, M., Ishikawa, Y. & Taneno, A. (2002). Phylogenetic analysis of field isolates of feline calcivirus (FCV) in Japan by sequencing part of its capsid gene. *Vet Res Commun* **26**, 205-19.

Schorr-Evans, E. M., Poland, A., Johnson, W. E. & Pedersen, N. C. (2003). An epizootic of highly virulent feline calicivirus disease in a hospital setting in New England. *J Feline Med Surg* **5**, 217-26.

Seal, B. S., Ridpath, J. F. & Mengeling, W. L. (1993). Analysis of feline calicivirus capsid protein genes: identification of variable antigenic determinant regions of the protein. *J Gen Virol* **74 (Pt 11)**, 2519-24.

Seal, B. S. & Neill, J. D. (1995). Capsid protein gene sequence of feline calicivirus isolates 255 and LLK: further evidence for capsid protein configuration among feline caliciviruses. *Virus Genes* **9**, 183-7.

Sosnovtsev, S. & Green, K. Y. (1995). RNA transcripts derived from a cloned full-length copy of the feline calicivirus genome do not require VpG for infectivity. *Virology* **210**, 383-90.

Sosnovtsev, S. V., Prikhod'ko, E. A., Belliot, G., Cohen, J. I. & Green, K. Y. (2003). Feline calicivirus replication induces apoptosis in cultured cells. *Virus Res* **94**, 1-10.

Studdert, M. J., Martin, M. C. & Peterson, J. E. (1970). Viral diseases of the respiratory tract of cats: isolation and properties of viruses tentatively classified as picornaviruses. *Am J Vet Res* **31**, 1723-32.

Thompson, J. D., Gibson, T. J., Plewniak, F., Jeanmougin, F. & Higgins, D. G. (1997). The CLUSTAL_X windows interface: flexible strategies for multiple sequence alignment aided by quality analysis tools. *Nucleic Acids Res* **25**, 4876-82.

Thumfart, J. O. & Meyers, G. (2002). Feline calicivirus: recovery of wild-type and recombinant viruses after transfection of cRNA or cDNA constructs. *J Virol* **76**, 6398-407.

Tohya, Y., Masuoka, K., Takahashi, E. & Mikami, T. (1991). Neutralizing epitopes of feline calicivirus. *Arch Virol* **117**, 173-81.

Tree, J. A., Adams, M. R. & Lees, D. N. (2005). Disinfection of feline calicivirus (a surrogate for norovirus) in wastewaters. *J Appl Microbiol* **98**, 155-62.

CHAPTER 3

Identification of regions and residues in feline junctional adhesion molecule A (fJAM-A) required for feline calicivirus (FCV) binding and infection*

***Ossiboff, R. J. & Parker, J. S. (2007).** Identification of regions and residues in feline junctional adhesion molecule required for feline calicivirus binding and infection. *J Virol* **81**, 13608-21.

3.1 Abstract

The feline junctional adhesion molecule A (fJAM-A) is a functional receptor for feline calicivirus (FCV). fJAM-A is a member of the immunoglobulin superfamily (IgSF) and consists of two Ig-like extracellular domains (D1 and D2), a membrane-spanning domain, and a short cytoplasmic tail. To identify regions of fJAM-A that interact with FCV, we purified recombinant fJAM-A ecto-, D1, and D2 domains. We found that preincubation of FCV with the ectodomain or D1 was sufficient to inhibit FCV infection in plaque reduction assays. In ELISA assays, FCV binding to fJAM-A ectodomain was concentration-dependent and saturable; however, FCV bound D1 alone weakly and was unable to bind D2. To characterize FCV binding to surface expressed fJAM-A, we transfected truncated and chimeric forms of fJAM-A into a non-permissive cell line and assayed binding by flow cytometry. Only D1 was necessary for FCV binding to cells and all other domains could be replaced. Using a structure-guided mutational approach, we identified three mutants of fJAM-A within D1 (D42N, K43N and S97A) that exhibited a significantly decreased capacity to bind FCV. In contrast to our finding that D1 mediated FCV binding, we found that all domains of fJAM-A were necessary to confer susceptibility to FCV infection. Furthermore, surface expression of fJAM-A was not sufficient to permit FCV infection by all of the isolates we investigated. This indicates that (i) other cellular factors are required to permit productive FCV infection, and (ii) that individual FCV isolates differ in what factors they require.

3.2 Introduction

Members of the *Caliciviridae* are small, nonenveloped viruses that carry a positive-stranded RNA genome of ~7-8 kb. Despite including important human and animal pathogens, the *Caliciviridae* family is relatively understudied. Feline

caliciviruses (FCVs), members of the *Vesivirus* genus, are highly contagious pathogens that cause a variety of mild to severe disease syndromes in cats. Recently, feline Junctional Adhesion Molecule-A (fJAM-A) was identified as a functional receptor for FCV, the first proteinaceous receptor identified for any member of the *Caliciviridae* (Makino et al., 2006).

Virus entry often requires multiple interactions between virus particles and cell surface receptors. These interactions are critical determinants of productive virus entry and are often important factors in viral pathogenesis. Increasingly, it is being found that viral entry is not a passive process, but often involves activation of distinct cellular signaling pathways that program correct endocytic uptake of the viral particle and/or prime the cell for viral replication (Marsh & Helenius, 2006). Both a carbohydrate (α-2,6 sialic acid) and the cell surface glycoprotein fJAM-A have been shown to be involved in FCV binding to cells (Makino et al., 2006, Stuart & Brown, 2007). The roles these molecules play in FCV entry have not been determined.

JAM-A is a type I transmembrane glycoprotein (MW 36-41 kDa) and a member of the immunoglobulin superfamily (IgSF). It consists of a N-terminal signal peptide, an extracellular domain (composed of two Ig-like domains - a membrane-distal D1 and a membrane-proximal D2), a transmembrane domain, and a short cytoplasmic domain (Ebnet et al., 2000, Mandell & Parkos, 2005). JAM-A localizes to intercellular tight junctions of endothelial and epithelial cells in humans and mice, and is expressed on the surface of platelets, leukocytes and erythrocytes (Liu et al., 2000, Mandell et al., 2004, Martin-Padura et al., 1998, Ozaki et al., 1999). In solution, JAM-A forms homodimers that are stabilized by ionic and hydrophobic interactions between residues in the D1 domain dimerization motif. Homodimer formation is critical in establishing a regulated tight junctional barrier between cells, and it is thought that homophilic interactions between JAM-A dimers on opposing cell surfaces

are important for forming intercellular tight junctions (Liu et al., 2000, Mandell et al., 2004, Martin-Padura et al., 1998, Ozaki et al., 1999, Williams et al., 1999). JAM-A is also believed to play an important role in modulating leukocyte diapedesis and platelet aggregation (Babinska et al., 2002a, Babinska et al., 2002b, Khandoga et al., 2005, Malergue et al., 1998, Martin-Padura et al., 1998).

Several different virus families use IgSF cell surface proteins as receptors. The σ1 attachment protein of mammalian orthoreoviruses (*Reoviridae*) engages residues present within the dimerization motif of the human JAM-A D1 domain (Barton et al., 2001, Campbell et al., 2005, Forrest et al., 2003, Guglielmi et al., 2007). Coxsackie B viruses (*Picornaviridae*) and most adenovirus (*Adenoviridae*) subgroups utilize the coxsackievirus and adenovirus receptor (CAR) (Bergelson et al., 1997). Like JAM-A, CAR has two extracellular Ig-like domains, localizes to tight junctions in polarized epithelial cells or to sites of cell-cell contact, and forms homodimers mediated by a dimerization motif within its D1 domain dimerization motif (Cohen et al., 2001, Martin-Padura et al., 1998). Comparable to the interaction of the reovirus σ1 protein with JAM-A, the adenovirus fiber knob protein also interacts with residues found mostly within the dimer interface of the CAR D1 domain (Bewley et al., 1999, Law & Davidson, 2005). Coxsackie B viruses interact with the distal end of the CAR D1 domain via surface residues in the canyon region of the capsid that surrounds the five-fold icosahedral axes (He et al., 2001). Other *Picornaviridae*, including human rhinoviruses (HRV14, HRV16), Coxsackie A virus (CAV21), and poliovirus (PV1, PV2, PV3), also use IgSF receptors (ICAM-I, ICAM-I, and PVR, respectively) (Rossmann et al., 2002).

Makino *et al.* showed that expression of fJAM-A cDNA in non-permissive hamster and human cell lines conferred susceptibility to FCV infection, and that infection could be blocked with fJAM-A antiserum (Makino et al., 2006). However, a

direct interaction between the virus and receptor was not investigated. In the present study, we used both sequence comparisons and structures of the human and murine JAM-A molecules to guide mutational analyses of the domains and residues of fJAM-A required for FCV binding and infection. We show that FCV binds to the membrane-distal D1 domain of fJAM-A close to the linker region between the D1 and D2 domains. Replacing two specific fJAM-A residues (Asp 42, Lys 43) with the corresponding human sequence substantially diminished virus binding and infection. Although the D1 domain was necessary for FCV binding, it was insufficient for infection. We found that both the D1 and D2 domains of fJAM-A were required for saturable binding of FCV; the cytoplasmic and transmembrane domains were required in addition to the extracellular domain for infection of non-permissive CHO cells. Lastly, we found that expression of fJAM-A in non-permissive cell lines was not sufficient for productive infection by all of the FCV isolates we investigated.

3.3 Methods

Cells and viruses. Crandell-Reese feline kidney (CRFK; ATCC #CCL-94) and HeLa (ATCC #CCL-2) cells were grown in Eagle's minimal essential medium (EMEM; CellGro) supplemented with 5% fetal bovine serum (HyClone), 100 U ml^{-1} of penicillin, 100 μg ml^{-1} streptomycin, 0.25 μg ml^{-1} amphotericin B, 1 mM sodium pyruvate, and non-essential amino acids (CellGro). Adherent Chinese hamster ovary (CHO-K1; ATCC #CCL-61) cells were grown in Ham's F12 (Hyclone) supplemented with 10% fetal bovine serum, 100 U ml^{-1} of penicillin, 100 μg ml^{-1} streptomycin, 0.25 μg ml^{-1} amphotericin B, 1 mM sodium pyruvate, and non-essential amino acids. Suspension Chinese hamster ovary (CHO-S) cells (Invitrogen) were grown in CHO-Serum Free Medium (-SFM; Gibco). Flp-In T-REx 293 (Invitrogen) cells were maintained in Dulbecco's modified essential medium (DMEM; Hyclone)

supplemented with 10% fetal bovine serum, 100 U ml^{-1} of penicillin and 100 μg ml^{-1} streptomycin. Chinese hamster lung (CHL; ATCC #CRL-1935) and Vero (ATCC #CCL-81) cells were grown in EMEM supplemented with 10% fetal bovine serum, 100 U ml^{-1} of penicillin, 100 μg ml^{-1} streptomycin, 0.25 μg ml^{-1} amphotericin B, 1 mM sodium pyruvate, and non-essential amino acids.

The F9 vaccine strain (VR-782) of FCV was obtained from the ATCC. The viral isolates FCV-5, Deuce, Kaos, 127 and 131 were previously characterized (Ossiboff et al., 2007). Third passage viral stocks were prepared from twice plaque-purified viruses amplified in CRFK cells.

RT-PCR, 3'- and 5'- RACE, and sequencing of fJAM-A. A cDNA of fJAM-A was prepared from total RNA isolated from CRFK cells using RT-PCR and 5' and 3' random amplification of complementary DNA ends. This cDNA was sequenced for correctness (Cornell University Life Sciences Core Laboratories Center) and cloned into the pCI-neo vector (Promega) to create the pCI-fJAM-A plasmid. Details of the primers used for amplification and the cloning strategy are available upon request.

Generation and purification of recombinant fJAM-A-GST fusion proteins. The fJAM-A extracellular domain (amino acid residues 26-232) and single Ig-like domains D1 (residues 26-127) and D2 (residues 132-232) were amplified by PCR from the pCI-fJAM-A plasmid using primers that incorporated *BamHI* and *SalI* restriction sites (Table 3.1). Amplified fragments were cloned into a modified pET-41A vector (Novagen) that has a 3C protease cleavage site introduced following the N-terminal GST and 6× His tags. *E.coli* (BL21) were grown at 25ºC and protein expression of the recombinant plasmids was induced by addition of 0.4 mM isopropyl-β-D-thiogalactopyranoside (IPTG). Bacteria were harvested by centrifugation, resuspended in phosphate-buffered saline (PBS) (137 mM NaCl, 3 mM KCl, 8 mM Na_2HPO_4 [pH 7.5]) containing 0.2% Triton X-100, 1 mM dithiothreitol, and 1 mM

Table 3.1. Primers used to create GST-fusion proteins

Ectodomain	Sense	5'-TAGGATCCGGCAGGGGCGCAGTG-3'
	Antisense	5'-AGGTCGACCTCCGCGGCTTCCAT-3'
D1	Sense	5'-TAGGATCCGGCAGGGGCGCAGTG-3'
	Antisense	5'-AGGTCGACCACAGTGAGCTGGAC-3'
D2	Sense	5'-TAGGATCCTCCAAGCCCACGGTC-3'
	Antisense	5'-AGGTCGACCTCCGCGGCTTCCAT-3'

phenylmethylsulfonylflouride, and lysed by sonication. Recombinant proteins were purified by affinity chromatography using GSTrap Fast Flow columns and Glutathione Sepharose 4 Fast Flow beads (GE Healthcare). GST was expressed and purified from the empty, modified pET41A vector as described above. When GST-free proteins were desired, GST and His tags were cleaved from the recombinant protein using HRV 3C protease (Novagen), and removed from the fJAM-A-containing fraction by passing the samples back over GSTrap columns. The cleaved proteins contained 4 additional non-native, N-terminal amino acids (Gly-Pro-Arg-Gly) and 17 additional non-native, C-terminal amino acids, including a His tag (Val-Asp-Lys-Leu-Ala-Ala-Ala-Leu-Glu-His-His-His-His-His-His-His-His).

Generation of rabbit fJAM-A specific antiserum. Endotoxin was removed from the purified fJAM-A ectodomain using an AffinityPak Detoxigel endotoxin removing gel (Pierce). Antibody was produced in a rabbit inoculated three times at three week intervals with the purified ectodomain (Cornell Center for Research Animal Resources). Pre-immune samples were tested by both ELISA and immunofluorescence to verify lack of reactivity. Antiserum was aliquoted and stored at -20ºC.

Electrophoresis and immunoblot analysis of recombinant fJAM-A. Soluble, recombinant fJAM-A full length ectodomain and single Ig-like loop (D1 and D2) GST-fusion and 3C-cleaved proteins were separated on 4-15% gradient SDS-

PAGE gels (Bio-Rad). Gels were stained with Coomassie blue or transferred to nitrocellulose membranes. Membranes were blocked in PBS with 5% non-fat milk powder, and then incubated with the fJAM-A rabbit antiserum diluted in blocking buffer. After washing with PBS/0.1% Tween-20, membranes were incubated with HRP-conjugated goat anti-rabbit IgG (Jackson Labs). After washing, SuperSignal enhanced chemiluminescence substrate (Pierce) was used to detect immunoreactive bands. Membranes were stripped (Restore Western Blot Stripping Buffer; Pierce), reblocked with blocking buffer, and then incubated with a horseradish-peroxidase-conjugated anti-GST antibody (GE Healthcare) diluted in blocking buffer. Detection of immunoreactive bands was performed as described above.

Detection of surface fJAM-A in transiently transfected CHO cells. CHO-K1 cells (3×10^5 per well) in six-well plates containing 18 mm glass cover slips were transiently transfected with pCI-fJAM-A or empty vector using FuGENE 6 (Roche) according to the manufacturer's directions. At 24 h post-transfection (p.t.), cover slips were washed with PBS, incubated with the fJAM-A rabbit antiserum (diluted in PBS plus 1% BSA) for 1 h on ice, washed, fixed in 2% paraformaldehyde (PFA) in PBS for 15 min, washed, and then incubated with Alexa 594-conjugated goat anti-rabbit IgG (Invitrogen) and DAPI (4'-6'-diamidino-2-phenylindol; Invitrogen) for 1 h. The cover slips were mounted on slides using Prolong (Invitrogen). A Nikon TE2000 inverted microscope equipped with a 60 × 1.4 NA oil objective linked to a Coolsnap HQ CCD camera (Roper) and Openlab software (Improvision) were used to collect fluorescence and phase contrast images. Images were then prepared for publication using Photoshop and Illustrator software (Adobe Systems).

Specificity of fJAM-A antiserum. CRFK and HeLa cells were seeded in six-well plates containing cover slips as above and incubated overnight. Cells on cover slips were washed and then incubated with either fJAM-A rabbit antiserum or a mouse

mAb against hJAM-A (BV-16; Santa Cruz Biotechnology). The cells were washed and fixed before being incubated with either Alexa-594 conjugated goat anti-rabbit or goat anti-mouse IgG and DAPI. Cover slips were mounted on slides with Prolong. Images were obtained as described above.

fJAM-A antiserum plaque reduction. Ten-fold dilutions of fJAM-A rabbit antiserum in PBS plus 1% BSA were incubated with CRFK cells for 1 h on ice. Control wells were incubated with PBS plus 1% BSA, or a 1:10 dilution of rabbit pre-immune serum in PBS plus 1% BSA. Virus was adsorbed (~20 PFU, as titered on CRFK cells/well) to cell monolayers for 1 h at room temperature. Monolayers were then overlaid with EMEM containing 5% fetal bovine serum and 1% bacto-agar. After incubation at 37ºC for 48 h in humidified 5% CO_2, the overlay was removed, the cells fixed with 10% buffered formalin, and stained with 1% (w/v) crystal violet solution. The plaques were counted and percent reduction from controls calculated.

fJAM-A ectodomain, D1 and D2 plaque reduction. Two-fold dilutions of purified fJAM-A ectodomain, D1, D2, or GST were incubated with FCV-5 (~20 PFU/well) in DMEM plus 0.1% BSA for 1 h on ice; control samples were incubated with medium only. The virus/receptor mixture was adsorbed to CRFK monolayers for 1 h at room temperature. Monolayers were then overlaid with 3 ml of EMEM containing 5% fetal bovine serum and 1% Bacto-agar. After incubation at 37ºC for 48 h in humidified 5% CO_2, the overlay was removed and plaques were stained as above. Plaques were counted and percent reduction from controls calculated.

ELISA binding of FCV to fJAM-A ectodomain, D1 and D2. Purified fJAM-A ectodomain, D1 or D2 (5 μM solutions) in carbonate/bicarbonate buffer (Sigma) was bound to 96- well ELISA plates at 4ºC overnight. Wells were blocked with PBS containing 0.05% Tween 20 (PBS-T) plus 0.5% BSA for 1 h at room temperature and washed three times with PBS-T. Two-fold dilutions of FCV-5 (initial dilution 1:10)

were prepared, and 50 μL of each dilution was bound to plates for 1 h at room temperature. After washing, bound virus was detected with rabbit anti-FCV-5 followed by HRP-conjugated goat anti-rabbit IgG. Antibodies diluted in blocking buffer were incubated with plates for 1 h at room temperature. After washing, substrate, 2,2'-Azino-bis(3-Ethylbenzthiazoline-6-Sulfonic Acid) (ABTS; Sigma) in a citric acid/sodium phosphate buffer, was added to each well and incubated for 15 min. Absorbance was measured at 595 nm on a Microplate Biokinetics Reader (BioTek Instruments).

Creation of fJAM-A deletion, chimeric and point mutants. Deletion and chimeric mutants were prepared using a general strategy of amplifying individual domains, introducing unique restriction sites on either end, and then joining the domains together in the expression vector pCI-Neo to create the desired constructs. fJAM-A deletion mutants are named according to the Ig-like domain deleted. Deletion mutants were: ΔD1/D2 (fJAM-A amino acid residues 1-27, 128-298; fJAM-A residue 129 changed from a valine to a glycine); D1/ΔD2 (fJAM-A 1-127, 233-298). Chimeric construct were named to indicate the source of the Ig-like domains from N- to C-termini (fJAM-A, fJ; hJAM-A, hJ; or hCAR, hC). The chimeric mutants created were: hJ/fJ (hJAM-A 1-128, fJAM-A 128-298); hC/fJ (hCAR 1-144, fJAM-A 128-298); fJ/hJ (fJAM-A 1-131, hJAM-A 133-234, fJAM-A 234-298); fJ/hC (fJAM-A 1-127, hCAR 138-227, fJAM-A 234-298). The GPI-fJAM-A chimeric construct was created by coupling the fJAM-A ectodomain to the glycosylphosphatidylinositol (GPI) anchor of human decay accelerating factor (hDAF) (fJAM-A 1-231, hDAF 345-364; an additional alanine was added between the segments). The full length open reading frames of hCAR and hJAM-A were also cloned into pCI-Neo. The PCR primers used to generate the deletion and chimeric mutants are listed in Table 3.2. fJAM-A D1 point mutants were generated using the Quick Change Site Directed mutagenesis

Table 3.2 Primers used to create JAM-A chimeric and deletion mutants

Construct	Template	Orientation	Primer (5'-3') (Restriction sites underlined)
fJAM-A	fJAM-A	Sense	TAGCTAGCATCGCCAATGGGGACCGA
		Antisense	TAACGCGTGGGACCAGGGTCACACCAG
ΔD1/D2	fJAM-A	Sense	ACACGTACGGGGAGGTCAGCGTCCAGCTC ACTGTGTTGAATGTGGGGGGCATT
		Antisense	TAACGCGTGGGACCAGGGTCACACCAG
D1/ΔD2	fJAM-A	Sense	TAGCTAGCATCGCCATGGGGACCGA
		Antisense	TAACCTAGGCGGCCCAACGCCAGGGA
	fJAM-A	Sense	ATCCTAGGTCCTCCATCCAAGCCCACG
		Antisense	TAACGCGTGGGACCAGGGTCACACCAG
hJAM-A	hJAM-A	Sense	TAGCTAGCATCGCCATGGGGACAAAG
		Antisense	ATCTCGAGGGCCTCACACCAGGAATGA
hCAR	hCAR	Sense	ATGCTAGCGCCACCATGGCGCTCCT
		Antisense	CTCTCGAGCTATACTATAGACCCATCC
fJ/hJ	hJAM-A	Sense	ATCGTACGGGGAGGTCAGCGTCCAGCTCA CTGTGCTTGTGCCTCCATCCAAG
		Antisense	ATGCGGCCGCCACAATGCCCCCCACATTC CGCTCCACAGCTTCCAT
	fJAM-A	Sense	AAGCGGCCGCACTTGTCACACTCATTCTC
		Antisense	TAACGCGTGGGACCAGGGTCACACCAG
fJ/hC	hCAR	Sense	ATCGTACGGGGAGGTCAGCGTCCAGCTCA CTGTGCTTGTTAAGCCTTCAGGT
		Antisense	ATGCGGCCGCCACAATGCCCCCCACATTT AGACGCAACAGGCACT
	fJAM-A	Sense	AAGCGGCCGCACTTGTCACACTCATTCTC CT
		Antisense	TAACGCGTGGGACCAGGGTCACACCAG
hJ/fJ	hJAM-A	Sense	TAGCTAGCATCGCCATGGGGACAAAG
		Antisense	TAGGTACCACGATGAGCTTGACCTT
	fJAM-A	Sense	ATGGTACCTCCATCCAAGCCCA
		Antisense	TAACGCGTGGGACCAGGGTCACACCAG
hC/fJ	hCAR	Sense	ATGCTAGCGCCACCATGGCGCTCCT
		Antisense	TAGGTACCGCACCTGAAGGCTTAACAAG
	fJAM-A	Sense	ATGGTACCTCCATCCAAGCCCA
		Antisense	TAACGCGTGGGACCAGGGTCACACCAG
GPI-fJAM-A	fJAM-A	Sense	TAGCTAGCATCGCCATGGGGACCGA
		Antisense	TAATGCGGCCGCTTCCATGCGCACAGCCT CT
	hDAF	Sense	TAATGCGGCCGCTCCAAATAAAGGAAGT GGAACC
		Antisense	ATTACGCGTTAAGTCAGCAAGCCCATG

Table 3.3 Primers used to create fJAM-A point mutants

Mutation	Orientation	Primer (5'-3') (Restriction sites underlined)
Y31H	Sense	CAGGGGCGCAGTGCATACTTCTGAGCCCG
	Antisense	CGGGCTCAGAAGTATGCACTGCGCCCCTG
D36E	Sense	GTGTATACTTCTGAGCCCGAGGTCAGGGTACCTGAGGAC
	Antisense	GTCCTCAGGTACCCTGACCTCGGGCTCAGAAGTATACAC
E41Q	Sense	CCCGATGTCAGGGTACCTCAGGACAAACCCGCCAAGTTG
	Antisense	CAACTTGGCGGGTTTGTCCTGAGGTACCCTGACATCGGG
D42N	Sense	CCCGATGTCAGGGTACCTGAGAACAAACCCGCCAAGTTG
	Antisense	CAACTTGGCGGGTTTGTTCTCAGGTACCCTGACATCGGG
D42K	Sense	GCCCGATGTCAGGGTACCTGAGAAGAAACCCGCCAAGTTG
	Antisense	CAACTTGGCGGGTTTCTTCTCAGGTACCCTGACATCGGGC
D42A	Sense	CCCGATGTCAGGGTACCTGAGGCCAAACCCGCCAAGTTG
	Antisense	CAACTTGGCGGGTTTGGCCTCAGGTACCCTGACATCGGG
K43N	Sense	CCCGATGTCAGGGTACCTGAGGACAACCCCGCCAAGTTG
	Antisense	CAACTTGGCGGGGTTGTCCTCAGGTACCCTGACATCGGG
N56S	Sense	CGGGCTTCTCCAGCCCGCGCGTGGAG
	Antisense	CTCCACGCGCGGGCTGGAGAAGCCCG
K75N	Sense	CACCAGCCTCGTTTGTTATAATAACAAGATCACGGCCT
	Antisense	AGGCCGTGATCTTGTTATTATAACAAACGAGGCTGGTG
A83E	Sense	GATCACGGCCTCATATGAAGACCGAGTCACCTTCTCG
	Antisense	CGAGAAGGTGACTCGGTCTTCATATGAGGCCGTGATC
S89L	Sense	GCAGACCGAGTCACCTTCAAGCACAGTGGCATCACTTTC
	Antisense	GAAAGTGATGCCACTGTGCTTGAAGGTGACTCGGTCTGC
H90P	Sense	CGAGTCACCTTCTCGCCCAGTGGCATCACTTTC
	Antisense	GAAAGTGATGCCACTGGGCGAGAAGGTGACTCG

Table 3.3 (Continued)

H96K	Sense	CGCACAGTGGCATCACTTTCAAGTCGGTGACGCGTAAAGACACG
	Antisense	CGTGTCTTTACGCGTCACCGACTTGAAAGTGATGCCACTGTGCG
H96E	Sense	GGCATCACTTTCGAGTCGGTGACGCGTAAAGACACGGGGACG
	Antisense	CGTCCCCGTGTCTTTACGCGTCACCGACTCGAAAGTGATGCC
S97A	Sense	GGCATCACTTTCCATGCGGTGACGCGTAAAGACACGGG
	Antisense	CCCGTGTCTTTACGCGTCACCGCATGGAAAGTGATGCC
K101E	Sense	CCATTCGGTGACGCGTGAAGACACGGGGACGTACAC
	Antisense	GTGTACGTCCCCGTGTCTTCACGCGTCACCGAATGG
D113E	Sense	CGTACACTTGCATGGTGTCTGACGAGGGCGGCAACACATACGGG
	Antisense	CCCGTATGTGTTGCCGCCCTCGTCAGACACCATGCAAGTGTACG

strategy (Stratagene). The PCR primers used to generate the point mutants are listed in Table 3.3. Common molecular cloning techniques, including overlap PCR, Quikchange site directed mutagenesis, and PCR mutagenesis, were utilized to create the constructs discussed above. All constructs were sequenced for correctness.

Virus-binding assay by flow cytometry. CHO-S cells (10^6 cells/sample) were transiently transfected with plasmid DNA constructs using FuGENE 6. Cells were incubated at37ºC in an 8% CO_2 humidified atmosphere on a shaker set to 125 revolutions per minute for 24 h. Cells were washed once in PBS and incubated with FCV (MOI = 5) in PBS plus 1% BSA on ice for 30 min. After washing twice, the cells were incubated with an antibody for the appropriate receptor (fJAM-A rabbit antiserum; anti-hJAM-A mouse mAb; anti-hCAR mouse mAb [Ambion]) and an antibody against the virus (anti-FCV mouse mAb [Custom Monoclonals

International]; rabbit anti-FCV antiserum) in PBS plus 1% BSA for 30 min on ice. Cells were washed and then fixed in FACS fix buffer (PBS plus 1% PFA and 0.05% NaN_3). After washing, cells were incubated with the appropriate secondary antibody, either Alexa 647-conjugated goat anti-rabbit or goat anti-mouse IgG for the receptor, and either Alexa 488-conjugated goat anti-mouse or goat anti-rabbit IgG for the virus in PBS plus 1% BSA for 30 min on ice. Cells were washed, suspended in FACS fix, and analyzed with a FACSCalibur (Becton Dickinson). Transfected cells were gated on positive surface receptor expression and ~10,000 gated cells were analyzed for each sample.

Virus-infection assay by flow cytometry. CHO-S cells (10^6/sample) were transfected with receptor constructs using FuGENE 6. After overnight incubation, the cells were washed in cold PBS and virus was adsorbed (MOI = 0.5; in PBS plus 1% BSA) on ice for 30 min. Immediately following virus adsorption, the cells were washed to remove unbound virus. Samples to assay virus binding were then incubated on ice with fJAM-A rabbit antiserum in PBS plus 1% BSA, washed, and fixed. Samples to be tested for infection were resuspended in 2 ml CHO-SFM and incubated at 37°C for 24 h with shaking. After 24 h, infected samples were washed in cold PBS, incubated with the fJAM-A antiserum as above, then washed, and fixed. All samples were then incubated with an anti-FCV mouse mAb in PBS plus 0.1% Triton X-100 and 10% normal goat serum, followed by Alexa 647-conjugated goat anti-rabbit and Alexa 488-conjugated goat anti-mouse IgG in PBS plus 0.1% Triton X-100 and 10% normal goat serum. After washing, the cells were suspended in FACS buffer and analyzed with a FACSCalibur cytometer. Transfected cells were gated on positive surface receptor expression and ~10,000 gated cells in each sample were analyzed for expression of FCV capsid antigen.

Creation of a stably fJAM-A transduced CHO-K1 cell line. CHO-K1 cells were transfected with pCI-fJAM-A using FuGENE 6. 24 h p.t., G418 (1.2 mg/ml; Cellgro) was added to the growth medium. Cells were maintained and passaged in the selective medium, and clones selected using cloning cylinders (Fisher). Clonal populations were maintained in 400 μg/ml G418.

Virus-infection plaque assay. CHO-K1, Flp-In T-REx 293, Vero, HeLa, or CHL cells were seeded in six-well plates at a concentration of 3×10^5 cells per well in 2 ml of appropriate growth medium. The next day, cells were transfected using FuGENE 6 and 1 μg DNA of either pCI-fJAM-A or empty vector pCI-Neo (mock); cells were incubated for 24 h to allow for protein expression. CRFK, non-transfected CHO-K1, and stably transfected CHO-K1 cells expressing fJAM-A were seeded in six-well plates at a concentration of 4×10^5 cells per well in appropriate growth medium 16 h before infection. Before virus inoculation, cells were washed in PBS, and then incubated with selected FCV isolates (MOI = 0.5) diluted in PBS plus 1% BSA for 1 h at room temperature. After virus adsorption, the cells were washed with PBS, and prewarmed growth medium was added. Samples for each virus were frozen immediately at -80ºC to calculate input titers; the remaining samples were incubated at 37ºC for 24 or 48 h, then frozen at -80ºC, and subjected to three freeze/thaw cycles. Plaque assays were performed as previously described (Ossiboff et al., 2007). The change in plaque titer was calculated by subtracting the $\log_{10}$ titer of input virus from the $\log_{10}$ titer at 24 or 48 h. The mean and standard deviation of three replicates of a representative experiment are shown.

Statistical analyses. Analyse-it (Analyse-it Software) statistical analysis add-in for Microsoft Excel was used to perform ANOVA where necessary. Graphs were prepared using Kaleidagraph (Synergy Software). Protein images were prepared using PyMOL (DeLano Scientific) (Delano, 2002).

3.4 Results

Expression and purification of the fJAM-A ectodomain and D1, and D2 subdomains. To determine if FCV directly binds to the ectodomain of fJAM-A and identify which of the two Ig-like domains FCV interacts with, we prepared the ectodomain (amino acids 26-232) and the individual Ig-like D1 (amino acids 26-127) and D2 (amino acids 132-232) domains of fJAM-A for expression in bacteria. The fJAM-A domains were expressed as GST-fusion proteins in a modified pET41a plasmid that has a hepatitis C virus 3C protease site inserted in frame at the fusion site (Figure 3.1A). After purification by affinity chromatography, the expressed GST fusion proteins were of the expected size by SDS-polyacrylamide gel electrophoresis analysis (GST-fJAM-A, 53 kDa; GST-D1, 41 kDa; and GST-D2, 41 kDa) (Figure 3.1B). In addition, when the fusion proteins were cleaved with 3C protease and the GST portion removed (see *3.3 Methods*), the ectodomain, D1 and D2 proteins were of the expected sizes (ecto- [25 kDa], D1 [13.5 kDa] and D2 domain [13.5 kDa]) (Figure 3.1B).

Detection of fJAM-A. To detect expression of fJAM-A cDNA, we prepared a rabbit antiserum against the purified fJAM-A cleaved ectodomain. This antiserum detected both GST-fused and cleaved fJAM-A proteins in immunoblots, while an anti-GST antibody recognized only the GST fusion proteins (Figure 3.1C). To test the specificity of the fJAM-A antiserum, we expressed the full-length fJAM-A cDNA in CHO-K1 cells, which do not form coherent tight junctions or express endogenous JAM-A (Martin-Padura et al., 1998, Ostermann et al., 2002). We detected surface expression of fJAM-A in CHO-K1 cells transfected with pCI-fJAM-A, but not cells transfected with empty vector (Figure 3.1D). As reported for expression of murine and human JAM-A, we found that fJAM-A was distributed throughout the plasma membrane (Mandell et al., 2004, Martin-Padura et al., 1998). To further test the

Figure 3.1. Characterization of recombinant fJAM-A ectodomain and fJAM-A specific rabbit antisera. (A) GST-Ecto, GST-D1, and GST-D2 were expressed in *E. coli* (BL21). Soluble recombinant proteins were purified by affinity chromatography. The fJAM-A regions of the recombinant proteins were released by 3C protease cleavage and (B) the predicted sizes of the fusion and cleaved proteins verified by SDS-polyacrylamide gel electrophoresis. A rabbit polyclonal antiserum against soluble fJAM-A ectodomain was prepared and (C) its capacity to specifically recognize the purified fusion and cleavage proteins confirmed by immunoblotting; a higher concentration of antibody was used to detect the cleaved D2 (indicated by an asterisk). Membranes were also probed with anti-GST. (D) Surface expression of fJAM-A in CHO cells by fluorescence microscopy. CHO-K1 cells were transfected with pCI-fJAM-A to express full-length fJAM-A or the empty vector, pCI-Neo. The cells were fixed at 24 h p.t. and immunostained with fJAM-A rabbit antiserum followed by Alexa 594-conjugated goat anti-rabbit IgG. Nuclei were stained with DAPI. (E) The fJAM-A rabbit antiserum recognizes JAM-A on feline CRFK, but not human HeLa cells. CRFK or HeLa cells were immunostained with either anti-fJAM-A or anti-hJAM-A (mAb BV16) followed by Alexa 594-conjugated goat anti-rabbit or Alexa 594-conjugated goat anti-mouse IgG; nuclei were stained with DAPI.

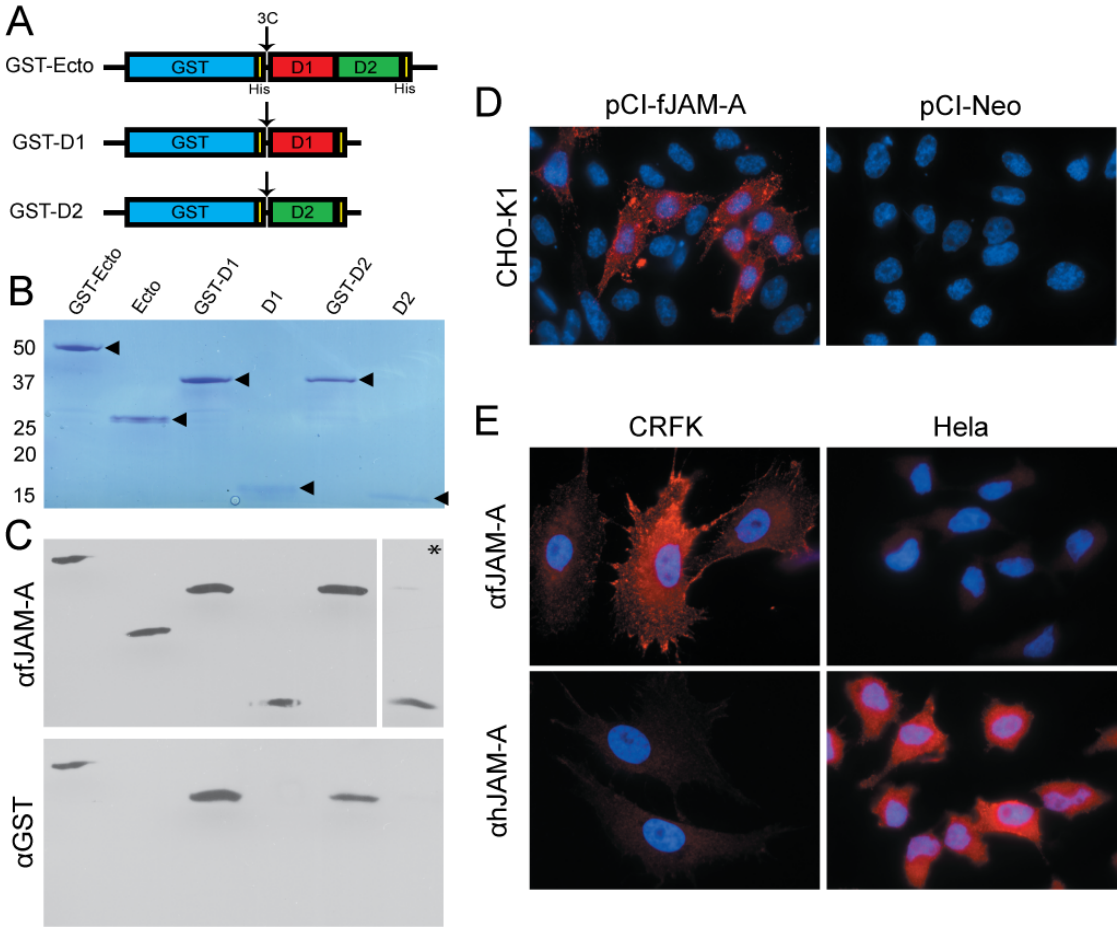
A
3C
GST-Ecto
GST
D1
D2
His
His
GST-D1
GST
D1
GST-D2
GST
D2
B
GST-Ecto
Ecto
GST-D1
D1
GST-D2
D2
50
37
25
20
15
C
αfJAM-A
αGST
*
D
pCI-fJAM-A
pCI-Neo
CHO-K1
E
CRFK
Hela
αfJAM-A
αhJAM-A

specificity of the antiserum, CRFK and HeLa cells were stained with either the fJAM-A antiserum or a mouse mAb against hJAM-A (Figure 3.1E). The anti-fJAM-A bound to CRFK but not HeLa cells, while anti-hJAM-A bound HeLa but not CRFK cells. We also tested CHL and Flp-In T-REx 293 cells and, as expected, found that the fJAM-A antiserum did not recognize any cell surface antigen.

A rabbit antiserum against fJAM-A inhibits FCV plaque formation in CRKF cells. Makino *et al*. showed that fJAM-A mouse antiserum partially inhibited FCV binding and blocked infection in permissive CRFK cells (Makino et al., 2006). We therefore tested the fJAM-A rabbit antiserum for its capacity to neutralize FCV infection of CRFK cells. We found that preincubation of cells with a 1:100 dilution of fJAM-A antiserum almost completely inhibited plaque formation (Figure 3.2). In contrast, preincubation of monolayers with a 1:10 dilution of pre-immune serum had no substantial effect on the number of plaques formed (Figure 3.2). A 1:100 dilution of the fJAM-A antiserum also inhibited infection by other FCV isolates (F9, Kaos, Deuce, 127, and 131). Based on these findings, we conclude that the fJAM-A rabbit antiserum can inhibit FCV infection of CRFK cells.

Purified soluble fJAM-A ecto- and D1 domains neutralize FCV infection. Neutralization of virus following incubation with soluble receptor has been demonstrated for a number of viruses (Goodfellow et al., 2005, Kaplan et al., 1990, Martin et al., 1993). Therefore, we used plaque reduction assays to assess the capacity of the fJAM-A ectodomain to neutralize FCV-5 infection. We found that preincubation of FCV-5 with fJAM-A ectodomain reduced viral infectivity by ~ 50% at 234 nM fJAM-A ectodomain, and abolished infectivity at concentrations > 938 nM (Figure 3.3A). The fJAM-A ectodomain consists of two Ig-like domains: the membrane-distal D1 and membrane-proximal D2. We found that preincubation of FCV-5 with purified D1 domain inhibited viral infectivity at similar concentrations to

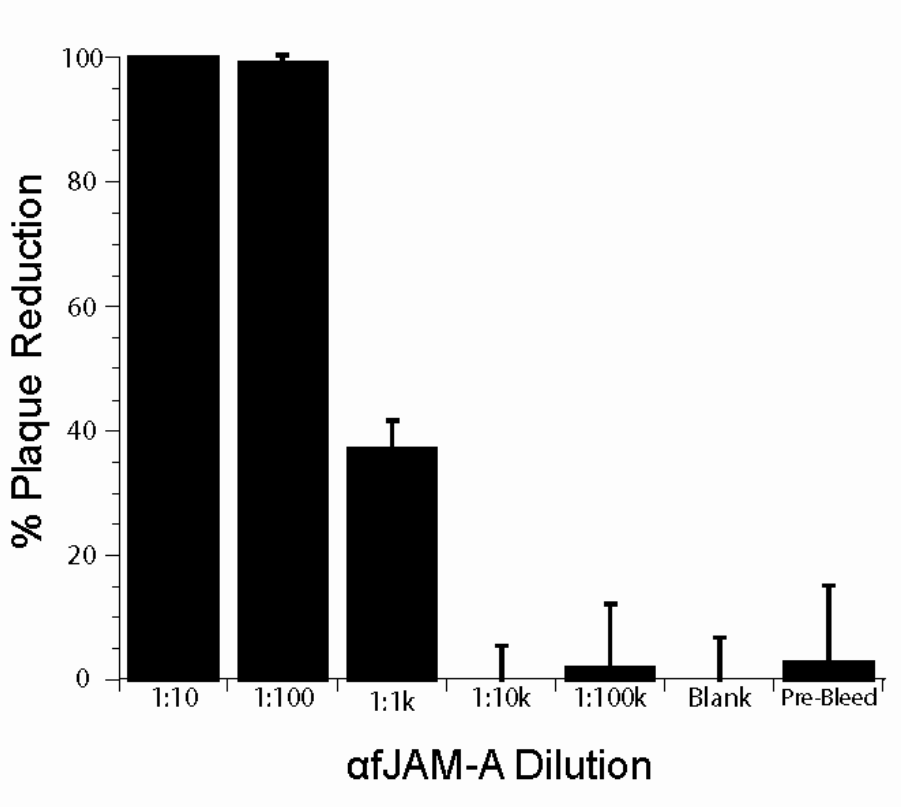

Figure 3.2. Inhibition of FCV infection of CRFK cells by fJAM-A antiserum. Serial dilutions of anti-fJAM-A or a 1:10 dilution of rabbit pre-immune serum were pre-incubated with monolayers of CRFK cells for 1 h on ice. The cells were then inoculated with ~20 PFU of FCV-5 and incubated for an additional 1 h at room temperature. The cells were then overlaid with EMEM 5% FBS and 1% Bacto-agar and cultured at 37°C for 48 h. The number of plaques in each well was counted and the results expressed as the percentage plaque reduction from infected monolayers that were untreated. Results shown are the mean plaque reduction ± standard deviation of 6 replicate wells of a single representative experiment.

Figure 3.3. Binding of fJAM-A ectodomain and the D1 and D2 Ig-like domains to FCV and their effect on infectivity. (A) FCV-5 was incubated with purified fJAM-A ectodomain, D1, D2, or GST for 1 h on ice and then adsorbed to a monolayer of CRFK cells for 1 h at room temperature. The cells were then overlaid with EMEM, 5% FBS and 1% bacto-agar and incubated at 37°C for 48 h. The numbers of plaques in each well were counted and the data expressed as the percentage of plaque reduction relative to monolayers infected with untreated virus. Data shown is the mean of 6 replicates ± standard deviation from one representative experiment. ANOVA was performed on three concentrations (3.75, 0.234, and 0.029 μM) to determine statistical differences; significant concentrations are indicated by an asterisk. (B) ELISA plates were coated with 5 μM solutions of soluble fJAM-A ectodomain, D1 or D2. Serial dilutions of FCV-5 were incubated with the immobilized proteins for 1 h and then the plates were washed extensively. Bound FCV-5 was detected with rabbit anti-FCV serum followed by HRP-conjugated goat anti-rabbit IgG. Colorimetric HRP substrate was added and the amount of bound FCV-5 was quantified by absorbance at 595 nm. The mean and standard deviations are shown, n=3. As above, ANOVA was performed on three concentrations; significant concentrations are indicated by an asterisk.

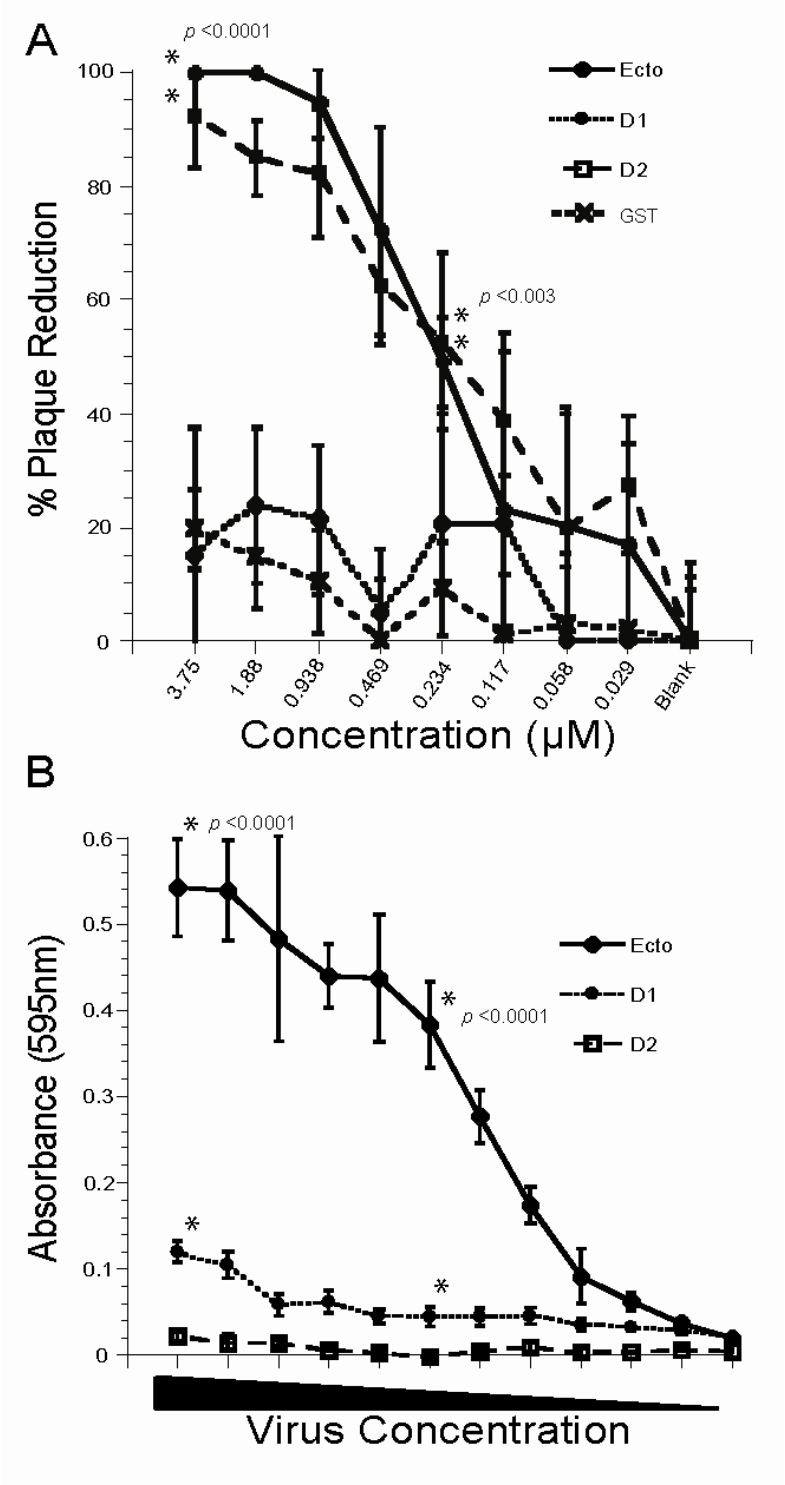
A
p <0.0001
p <0.003
Ecto
D1
D2
GST
% Plaque Reduction
100
80
60
40
20
0
3.75
1.88
0.938
0.469
0.234
0.117
0.058
0.029
Blank
Concentration (µM)
B
p <0.0001
p <0.0001
Ecto
D1
D2
Absorbance (595nm)
0.6
0.5
0.4
0.3
0.2
0.1
0
Virus Concentration

fJAM-A ectodomain (Figure 3.3A). In contrast, preincubation of FCV-5 with purified D2 domain or GST had no effect on infectivity at any of the concentrations we tested (Figure 3.3 A). Plaque reduction by the ecto- and D1 domains was statistically greater than the D2 domain at 2 of the 3 concentrations (3.75 and 0.234 μM) we analyzed by ANOVA ($p < 0.0001$ and $p < 0.003$, respectively). Preincubation of FCV-5 with the GST-fusion proteins inhibited viral infectivity to the same extent as the cleaved forms of the proteins (data not shown). In addition, we found that addition of purified fJAM-A to cells after virus was adsorbed for 1 h on ice had no effect on virus infectivity (data not shown). We conclude from these results that the full-length fJAM-A ectodomain and the membrane-distal D1 domain can inhibit FCV-5 infection of CRFK cells when preincubated with virus, most likely by preventing virus binding to the fJAM-A receptors present on the surface of the cells.

Purified FCV-5 particles directly bind to purified fJAM-A ectodomain and the D1 domain by ELISA. Our findings thus far strongly suggested that FCV directly interacted with fJAM-A ectodomain. To test this hypothesis, we used an ELISA to detect direct binding of viral particles to the fJAM-A ecto-, D1, and D2 domains bound to 96-well plates. We found saturable concentration-dependent binding of FCV-5 to plate-bound fJAM-A ectodomain (Figure 3.3B). Higher concentrations of FCV bound the plate-bound fJAM-A at similar levels to the highest concentration of FCV shown in Figure 3.3B (data not shown). We also found that FCV-5 bound to the D1 domain at low levels (Figure 3.3B); however, this binding was non-saturable and did not significantly change with increasing concentrations of virus. In contrast, FCV did not bind the D2 domain at any of the concentrations we tested (Figure 3.3B). ANOVA analysis of three concentrations showed significantly more viral binding to the ecto- and D1 domains than the D2 domain at all but the lowest concentration of virus ($p<0.0001$). We also assayed binding of fJAM-A ecto-, D1, or

D2 domains to viral particles when virus was bound to the plate. Under these conditions, although we detected saturable concentration-dependent binding of soluble fJAM-A to virus bound to the solid-phase, we were unable to detect any substantial binding of either the D1 or D2 domains to plate-bound virus using the fJAM-A rabbit antiserum to detect the bound proteins (data not shown). We hypothesized that our difficulty in detecting binding of the D1 domain to virus bound to the plate was because the fJAM-A antiserum competed with the virus for binding of D1. As the purified fJAM-A ectodomain, D1 and D2 proteins all possessed a C-terminal His tag (Figure 3.1A), we also used a rabbit anti-His polyclonal antibody to detect binding of fJAM-A ectodomain, D1, or D2 to plate-bound virus. Using the anti-His antibody, our findings were similar to the results shown in Fig. 3B; we were able to detect concentration-dependent saturable binding of fJAM-A ectodomain and low levels of D1 binding, but no detectable binding of D2 to the plate bound virus (data not shown). We conclude that FCV-5 can bind directly to the fJAM-A D1 and full-length ectodomain, but that saturable concentration-dependent binding requires the D2 domain. In addition our results suggest that the fJAM-A antiserum inhibits the interaction between purified D1 and virus particles perhaps by competing for binding to regions of the fJAM-A ectodomain that are involved in FCV binding.

FCV binding to fJAM-A deletion and chimeric mutants. To analyze the regions of fJAM-A responsible for virus binding, we prepared deletion and chimeric mutants of fJAM-A for expression in CHO-S cells (Figure 3.4A). The D1 and D2 domains were deleted or replaced with those of the related IgSF molecules, human JAM-A or human CAR. Binding of virus to CHO-S cells expressing the different surface receptor molecules was detected by flow cytometry (Figure 3.4B). We found that virus bound to nearly 80% of cells that expressed cell surface full-length fJAM-A. However, FCV-5 did not bind above control levels to cells that expressed the single

Figure 3.4. FCV binding to CHO cells expressing fJAM-A deletion and chimeric mutants. (A) A panel of fJAM-A deletion and chimeric mutants was created to investigate FCV binding. Chimeric receptors were generated by exchanging single Ig-like loops from IgSF proteins fJAM-A (red), hJAM-A (yellow) and hCAR (blue). Deletion constructs lacking single Ig-like domains, as well as a construct in which the transmembrane and cytoplasmic domains were replaced with a GPI-anchor, were generated. (B) CHO-S cells were transfected with each construct. At 24 h p.t., FCV was adsorbed to the cells on ice for 30 minutes. After washing with cold PBS, the bound virus and cell surface fJAM-A were detected with mouse anti-FCV mAb and rabbit anti-fJAM-A antibodies followed by Alexa 488-conjugated goat anti-mouse IgG and Alexa 647-conjugated goat anti-rabbit IgG. Virus binding and receptor expression were analyzed by flow cytometry. (C) Virus binding was measured by determining the percentage of receptor positive cells that were positive for virus. The mean ($n \geq 3$) (1×10^4 cells) ± standard deviation is shown.

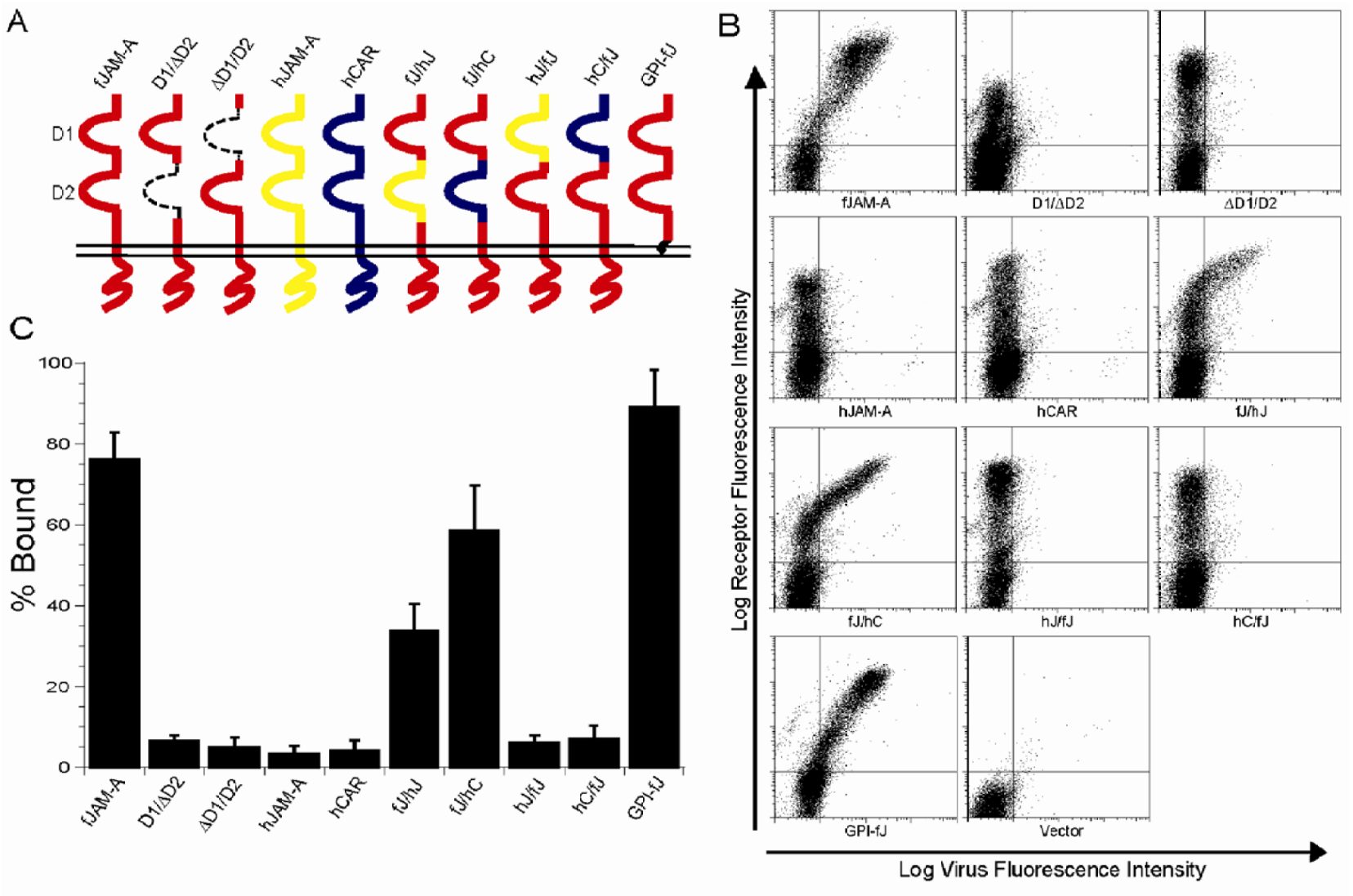
A
fJAM-A
D1/ΔD2
ΔD1/D2
hJAM-A
hCAR
fJ/hJ
fJ/hC
hJ/fJ
hC/fJ
GPI-fJ
D1
D2
B
fJAM-A
D1/ΔD2
ΔD1/D2
hJAM-A
hCAR
fJ/hJ
fJ/hC
hJ/fJ
hC/fJ
GPI-fJ
Vector
Log Receptor Fluorescence Intensity
Log Virus Fluorescence Intensity
C
% Bound
100
80
60
40
20
0
fJAM-A
D1/ΔD2
ΔD1/D2
hJAM-A
hCAR
fJ/hJ
fJ/hC
hJ/fJ
hC/fJ
GPI-fJ

D1 or D2 Ig-like loops (Figure 3.4C). In addition, virus did not bind to native hJAM-A or hCAR. In contrast, FCV-5 bound to cells expressing chimeric receptors that contained the fJAM-A D1 fused with the hJAM-A or hCAR D2 domains, albeit at lower levels than wild type receptor (~25% and 60%, respectively; Figure 3.4C). We observed only background levels of virus binding to cells that expressed chimeric receptors that consisted of the D1 from hJAM-A or hCAR in the fJAM-A background. FCV bound to CHO-S cells expressing a GPI-anchored form of fJAM-A at similar levels as cells expressing wild type receptor. The background level of virus binding to cells transfected with empty vector was 3% (Figure 3.4B). We also investigated the binding of FCV isolates Deuce and F9 to the full panel of chimeric receptors by immunofluorescence and found levels of binding similar to that of FCV-5. The binding of FCV isolates Deuce, F9, 127, 131 and Kaos to both the full-length fJAM-A receptor and the GPI-anchored form was detected by flow cytometry. We noted similar binding levels for all isolates. We conclude that the fJAM-A D1 domain was necessary for FCV binding and that the cytosolic and transmembrane domains were not required. However, it appears that the context in which the D1 domain is presented on the cell surface is important, as FCV was unable to bind the fJAM-A D1 when it was expressed alone, possibly because the viral particle cannot access the domain when it lies close to the cell membrane.

FCV binding to fJAM-A D1 point mutants. To identify individual regions of fJAM-A D1 required for FCV binding, we compared the amino acid sequence of the human and feline D1 domain and identified non-identical residues (Figure 3.5A). Dissimilar surface exposed residues are indicated on a model of the hJAM-A structure (PDB ID # 1NBQ; Figure 3.5B). We prepared eleven point mutants by replacing selected feline residues with the corresponding residue of hJAM-A. In addition, we prepared a mutant (E60R/K62E) that reversed the charges on 2 of the 4 residues

Figure 3.5. FCV binding to fJAM-A D1 point mutants. (A) The amino acid sequences of the D1 domain of fJAM-A (res 26-125) and hJAM-A (27-126) were aligned and nonidentical residues identified (highlighted by red boxes). (B) Identified residues were mapped on the hJAM-A crystal structure (PDB ID# 1NBQ; red and blue residues), and 11 surface exposed residues were selected to mutate to the hJAM-A sequence (blue residues; images were created in PyMOL, Delano Scientific). A dimerization mutant (E60R/K62E) that reverses the charges on 2 of the 4 charged residues in the dimerization motif was also created. (C) CHO-S cells were transfected with each of the constructs. At 24 h p.t., cells were incubated with FCV-5 on ice for 30 minutes, followed by immunostaining to detect surface expression of receptor and FCV binding, and then analyzed by flow cytometry. (D) After gating for receptor positive cells, virus binding was measured and expressed as a percentage. The mean of at least 3 replicates (1×10^4 cells each) ± standard deviation is shown. To further investigate the decreased binding observed with the point mutant D42N, additional mutants were made to reverse or eliminate the charge on residue 42, as well as to alter other charged residues in the vicinity of residue 42. (E) Virus binding to cells expressing the constructs was measured by flow cytometry and (F) virus binding was determined as above. The mean ($n \geq 3$; 1×10^4 cells each) ± standard deviation is shown. Constructs indicated by an asterisk were bound by significantly lower levels of virus as determined by ANOVA ($p<0.0001$).

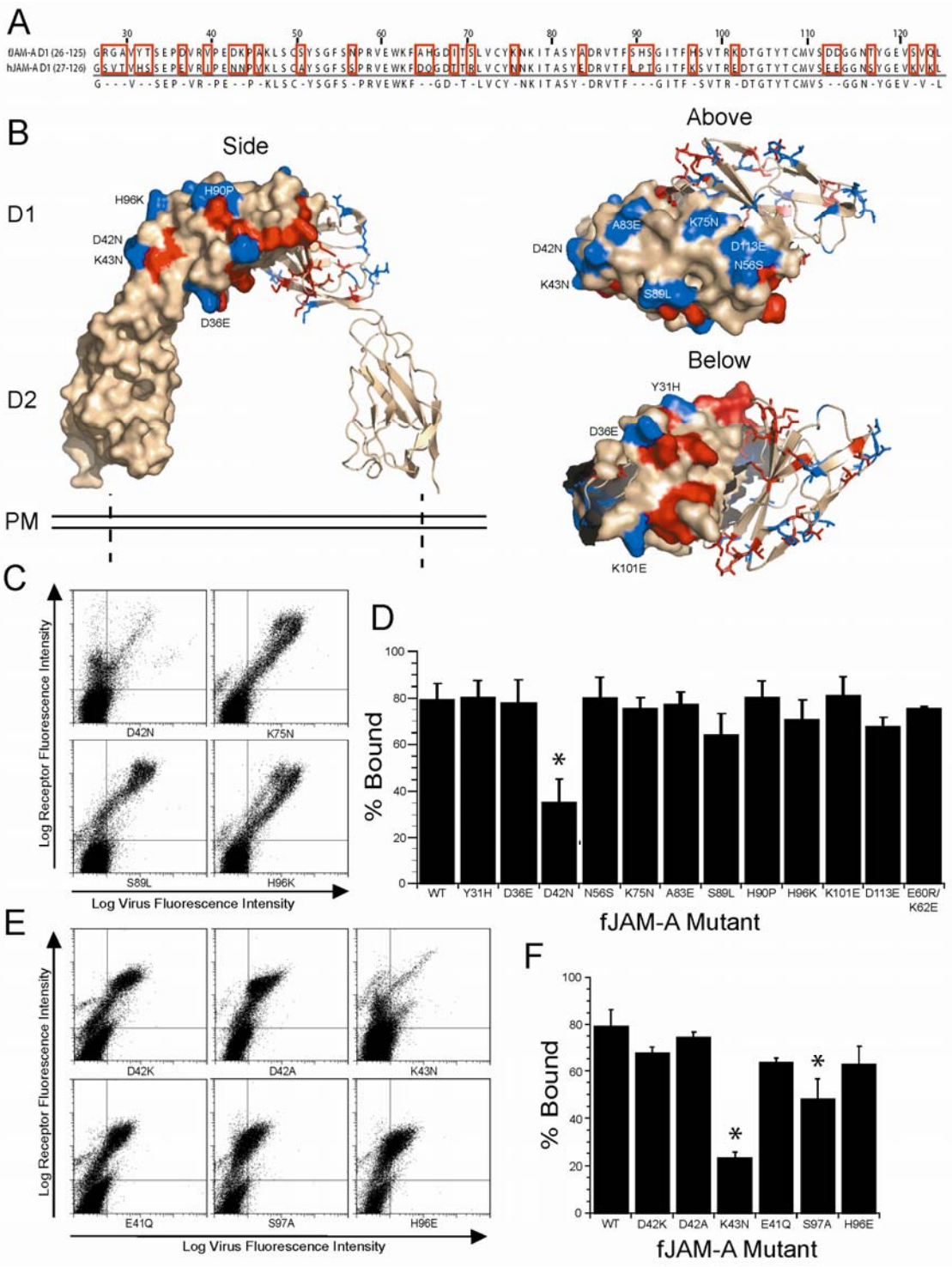
A
fJAM-AD1 (26-125)
hJAM-AD1 (27-126)
B
Side
Above
Below
D1
D2
PM
H96K
H90P
D42N
K43N
D36E
A83E
K75N
D113E
N56S
S89L
Y31H
K101E
C
Log Receptor Fluorescence Intensity
Log Virus Fluorescence Intensity
D42N
K75N
S89L
H96K
D
% Bound
WT
Y31H
D36E
D42N
N56S
K75N
A83E
S89L
H90P
H96K
K101E
D113E
E60R/
K62E
fJAM-A Mutant
E
D42K
D42A
K43N
E41Q
S97A
H96E
F
% Bound
WT
D42K
D42A
K43N
E41Q
S97A
H96E
fJAM-A Mutant

predicted to be involved in fJAM-A dimer formation. Mutations to the charged residues involved in salt bridge formations have been shown to prevent hJAM-A dimerization (Guglielmi et al., 2007, Kostrewa et al., 2001). Each construct was transiently transfected into CHO-S cells and FCV-5 binding was detected by flow cytometry (Figure 3.5C). The level of FCV-5 binding to cells expressing the various constructs is presented as the percentage of receptor-positive cells that bound virus (Figure 3.5D). Of the initial panel of mutant receptors we examined, only cells expressing fJAM-A D42N were bound by FCV-5 less effectively than wild type (~ 2.2 fold fewer cells bound virus) (Figure 3.5D). FCV-5 bound all of the other mutants to levels not significantly different than the wild type fJAM-A (Figures.3.5C and D). To further investigate the role of fJAM-A residue 42 in binding, we prepared two additional fJAM-A mutants where the charge on residue 42 was reversed (D42K) or removed (D42A); neither of these changes significantly decreased FCV-5 binding when compared to binding to the wild type receptor (Figures 3.5E and F). As residue 43 of JAM-A also differed between feline (lysine) and human (asparagine) sequences, we examined binding of FCV-5 to cells expressing fJAM-A K43N. We found that FCV-5 bound 3.5-fold fewer cells expressing this mutant than those expressing the wild type receptor (Figures 3.5E and F). We prepared three other mutants that had changes to charged residues that were positioned close to residues 42 and 43 in the hJAM-A structure. Two of these mutants (E41Q and H96E) bound similar levels of FCV-5 as wild type receptor. However, mutant fJAM-A S97A bound ~ 1.7-fold less virus than wild type fJAM-A (Figures 3.5E and F). D1 point mutants D42N, K43N and S97A were all bound by significantly less virus than the wild-type fJAM-A, as determined by ANOVA ($p<0.0001$). One caveat to these observations is that the cell surface expression of the D42N and K43N mutants was lower than that of the wild type fJAM-A. Thus, it is possible that some of the lower FCV cell binding could be

attributed to lower levels of expression; however, it is clear that those cells that did express lower levels of these mutants still bound far less virus than a comparable population of wild type-expressing cells. The binding of FCV isolates F9 and Deuce to selected mutants (D42N, S89L, D42K, K43N, E41Q, and E60R/K62E) was also measured, with similar binding levels noted (data not shown). Taken together these results suggest that residues D42, K43, and S97 of the fJAM-A D1 are likely involved in interactions with FCV virions.

Capacity of FCV to infect non-permissive CHO cells expressing fJAM-A or deletion and chimeric mutants of fJAM-A. We used flow cytometry to examine the capacity of low multiplicities of FCV-F9 to infect CHO-S cells transiently expressing fJAM-A and the panel of fJAM-A deletion and chimeric mutants. Controlling for levels of input capsid bound to cells (solid line), we quantified the change in geometric mean fluorescence associated with viral capsid protein levels at 24 h post-inoculation (dashed line) (Figure 3.6A). In this way, infection was assayed by increased intracellular levels of viral capsid protein resulting from viral replication. In cells expressing the full-length fJAM-A molecule, we found significantly increased expression of viral capsid protein, indicating successful virus entry and infection (Figure 3.6B). All of the mutant constructs that were unable to bind FCV (D1/ΔD2, ΔD1/D2, hJ/fJ and hC/fJ) (see Figure 3.4C) were also unable to mediate infection (Figure 3.6B). Although virus bound to cells expressing the D2 exchange mutant constructs (fJ/hJ, fJ/hC) and the GPI-anchored construct (GPI-fJAM), we were unable to detect infection in cells expressing these constructs (Figure 3.6B). We also prepared a mutant construct of fJAM-A that lacked three conserved C-terminal residues of the cytosolic tail (Phe, Leu, Val) known to be required for binding of PDZ domain-containing proteins (Bazzoni et al., 2000). Both viral binding and infection of CHO-S cells expressing this construct were comparable to that mediated by the wild-type

Figure 3.6. FCV infection of cells expressing chimeric, deletion or select D1 point mutant constructs. (A) F9 was bound to two sets of cells expressing chimeric or deletion constructs for 30 minutes on ice. One set of F9-inoculated cells was resuspended in growth medium and placed at 37ºC for 24 hours; the other set of cells was washed and immediately immunostained for the virus and receptor to determine background binding of virus. After 24 hours, the infected cells were washed and immunostained for virus and receptor as above. Bound (solid line) and 24 h incubated samples (dashed line) were then analyzed by flow cytometry. (B) Infectivity was measured by determining the change in mean log virus fluorescence intensity between bound and incubated samples. The average of the change in geometric mean ($n \geq 4$) ± standard error is shown. (C) Cells expressing select D1 point mutant constructs were prepared and analyzed in the same fashion. (D) The change in mean virus fluorescence intensity was used as a measure for infection, and the average of the change in geometric mean ($n \geq 4$) ± standard error is shown.

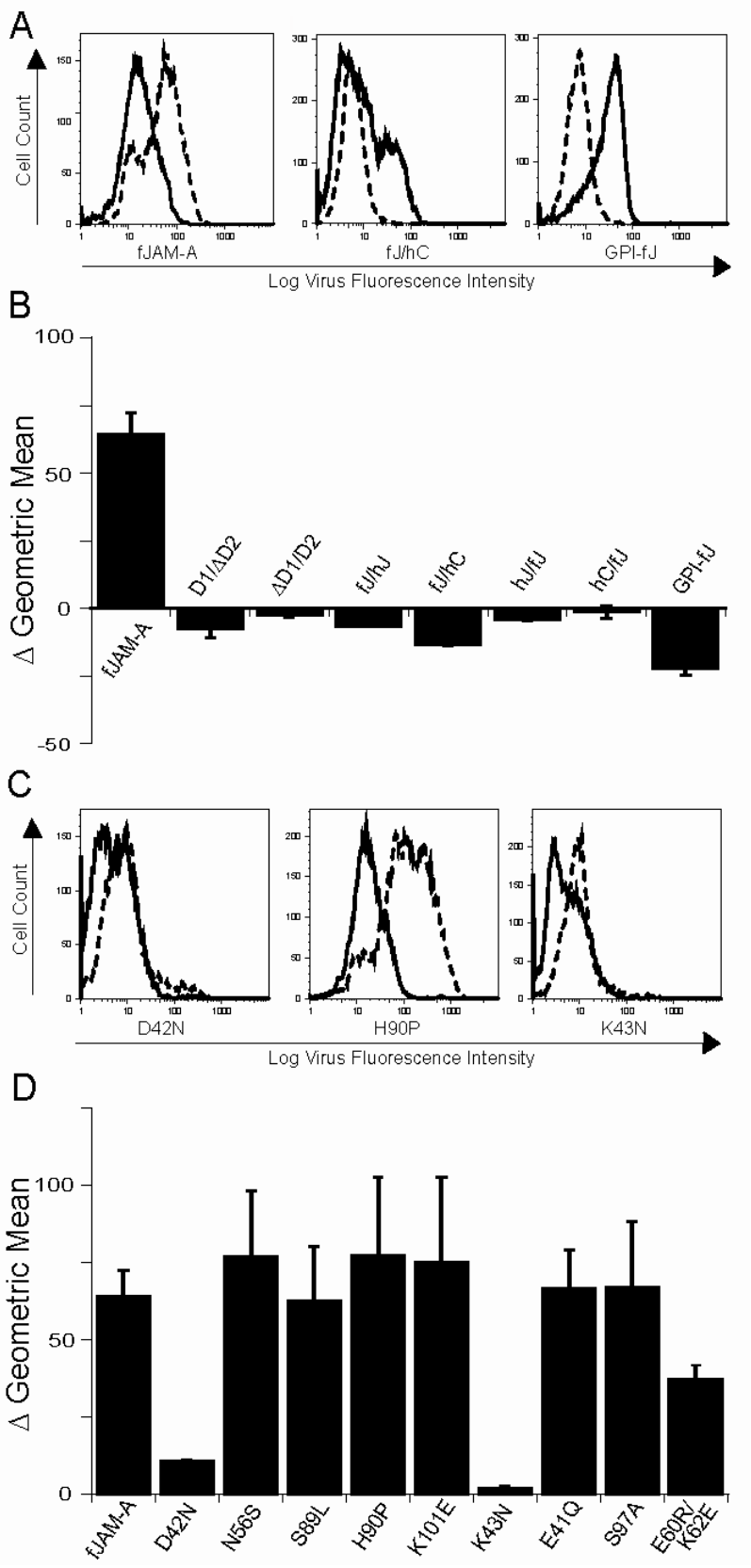
A
Cell Count
fJAM-A
fJ/hC
GPI-fJ
Log Virus Fluorescence Intensity
B
Δ Geometric Mean
100
50
0
-50
fJAM-A
D1/ΔD2
ΔD1/D2
fJ/hJ
fJ/hC
hJ/fJ
hC/fJ
GPI-fJ
C
Cell Count
D42N
H90P
K43N
Log Virus Fluorescence Intensity
D
Δ Geometric Mean
100
50
0
fJAM-A
D42N
N56S
S89L
H90P
K101E
K43N
E41Q
S97A
E60R/K62E

receptor construct (data not shown). From these results, we conclude that all domains (D1, D2, transmembrane and cytoplasmic) of the fJAM-A receptor are necessary for infection, but that interactions with proteins that contain a PDZ domain are not required.

FCV infection of fJAM-A D1 point mutants. We similarly analyzed the fJAM-A D1 point mutants for their capacity to confer susceptibility to FCV infection in CHO-S cells. We found that the two fJAM-A mutants with decreased capacity to bind virus (D42N, K43N) (see Figures 3.5D and F) also showed a decreased capacity to confer susceptibility to infection in CHO-S cells relative to the wild type receptor (Figures 3.6C and D). The other point mutations investigated (N56S, S89L, H90P, K101E, E41Q) conferred susceptibility to infection at levels similar to the wild-type receptor. The mutant S97A, which demonstrated a significant decrease in virus binding (see Figure 3.5F), was also able to confer similar levels of susceptibility to infection as the wild-type receptor. Lastly, the dimerization mutant (E60R/K62E) also conferred susceptibility to CHO-S cell infection by F9.

Isolate variation in the capacity to infect fJAM-A expressing cells. In the above experiments we used the F9 vaccine strain to assay for infection. However, we found that not all of the FCV isolates we examined were able to infect CHO-S cells expressing the wild type fJAM-A receptor (data not shown). We selected 6 FCV isolates (including the vaccine strain, F9) to investigate the capacity of different isolates to infect transiently transfected adherent CHO-K1 cells (Figure 3.7A). We found that four isolates (FCV-5, Deuce, 127 and F9) were able to productively infect CHO-K1 cells transiently expressing fJAM-A, with yields ranging from 0.5 to 1.2 logs greater than the input titer. The viral yields, however, were considerably lower than the yields observed in CRFK cells incubated for 24 h (2.8 – 4.8 logs). Two isolates, Kaos and 131, were unable to productively infect the transfected CHO-K1 cells.

Incubation of these isolates with the fJAM expressing CHO-K1 cells resulted in a net loss of titer similar to that observed following incubation with CHO-K1 controls. The process of transfection using cationic liposomes has been shown to induce a robust type I interferon response (Park et al., 2003), and FCV infection is sensitive to the presence of type I interferon (Baldwin et al., 2004, Fulton & Burge, 1985, Mochizuki et al., 1994). To eliminate the potential effects of a transfection-induced anti-viral state, we created a CHO-K1 cell line stably expressing fJAM-A, and then repeated the infection assay in the fJAM-A stable cells. The four isolates able to productively infect the transiently transfected cells demonstrated enhanced infectivity in the stable cell lines, with yields of 1.1 to 2.3 logs higher than the input titer following 48 h incubation. However, infection of FCV isolates 131 and Kaos was still greatly restricted in the stably transfected cell line. Neither isolate displayed a net increase in viral yield after 24 hours; after 48 hours, the titer of FCV 131 had increased 0.35 logs, while Kaos showed no change in titer over the bound virus sample.

To further investigate the ability of FCV isolates to infect cells expressing fJAM-A, we transfected 4 additional cell lines with the receptor and incubated the cells for 24 or 48 hours with the selected FCV isolates (Fig. 7B). Results varied by both cell line and FCV isolate. Transfected Vero cells were the only cell line identified that supported a productive infection of all FCV isolates tested. In contrast, transfected HeLa cells were unable to support a productive infection by any of the FCV isolates investigated. Transfected CHL cells supported infection by Deuce, Kaos, FCV-127, FCV-131 and F9 (following 48 h incubation), but not FCV-5; Flp-In T-REx 293 cells supported infection by Deuce, Kaos, and FCV-127, but not isolates FCV-5, FCV-131 and F9. FCV isolates Deuce and 127 were able to productively infect all of the transfected cell lines we tested, other than HeLa cells; isolates FCV-5, Kaos,

Figure.3.7. FCV isolate infectivity in non-permissive cell lines expressing fJAM-A. (A) FCV isolates (MOI = 0.5) were incubated with monolayers of CHO-K1 cells expressing fJAM-A (transiently or stably) for 24 or 48 hours. Virus was also incubated for 24 hours with empty CHO-K1 cells, CHO-K1 cells transfected with the empty vector (CHO-Mock), and CRFK cells. Infectivity of the samples was determined by plaque assay, and the change in titer from virus-bound only samples calculated. The mean $\log_{10}$ change in titer of three replicates ± SD of a representative experiment is shown. (B) Monolayers of 4 additional non-permissive cell lines (CHL, Flp-In T-REx 293, Vero, and HeLa) were transiently transfected with fJAM-A and incubated with virus (MOI = 0.5) for 24 (CHL, Vero, HeLa) or 48 (Flp-In T-REx 293) hours. Infectivity of the samples was determined by plaque assay, and the change in titer from virus-bound only samples calculated. The mean $\log_{10}$ titer of three replicates ± SD is shown.

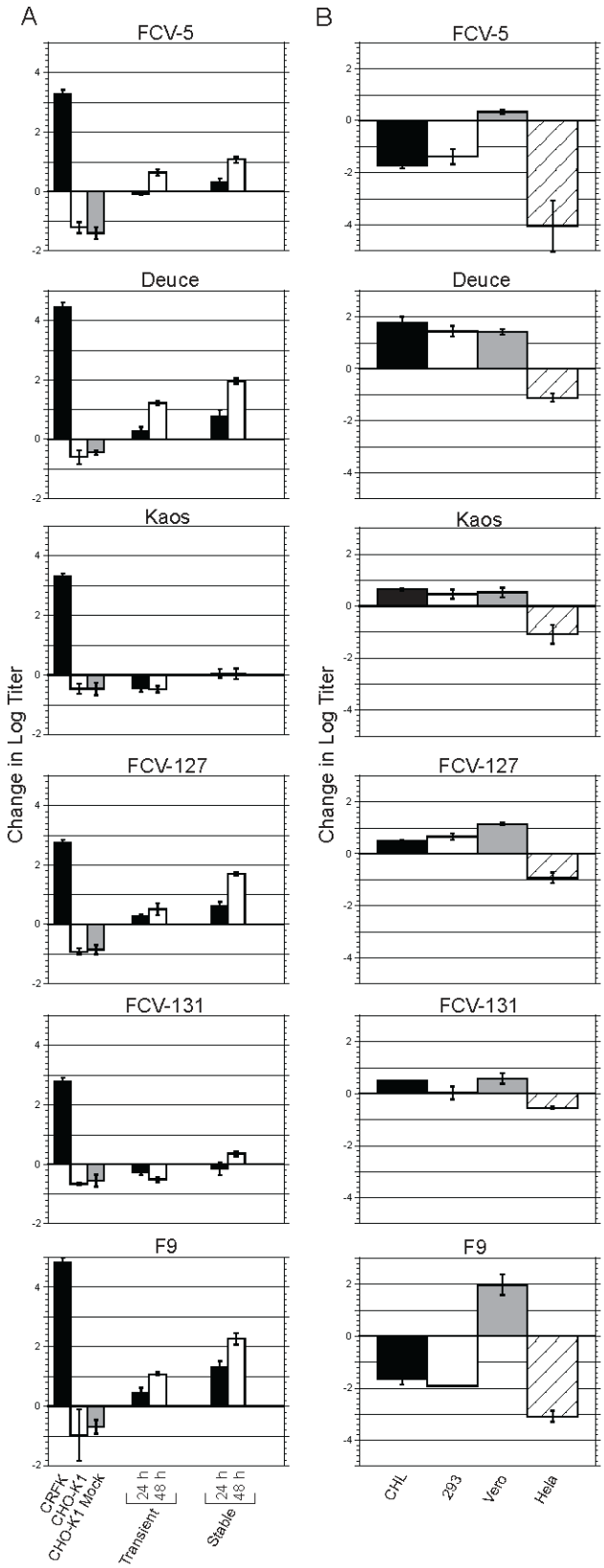
A
B
FCV-5
Deuce
Kaos
FCV-127
FCV-131
F9
Change in Log Titer
CRFK
CHO-K1
CHO-K1 Mock
Transient
24 h
48 h
Stable
24 h
48 h
CHL
293
Vero
Hela

FCV-131, and F9 were more restricted and showed differential capacities to infect the other transfected cell lines. All isolates were capable of productive infection in at least one fJAM-A expressing non-permissive cell line.

3.5 Discussion

Makino et al. showed that fJAM-A is a receptor for FCV (Makino et al., 2006). Here we have confirmed and extended those results. We have shown that binding of FCV to fJAM-A requires the membrane-distal D1 domain; furthermore, mutations to three residues within D1 (D42, K43, and S97) decreased viral binding. The D1 domain of fJAM-A is predicted to contain two antiparallel β-sheets (strands ABED and GFCC'C''). Structural and biochemical analyses of human and murine JAM-A molecules revealed dimer formation though extensive interactions between the GFCC' faces of two D1 domains (dimerization interface); at the center of the dimer interface are several charged residues critical in mediating JAM-A/JAM-A dimer formation by forming four salt bridges (dimerization motif) (Guglielmi et al., 2007, Prota et al., 2003). Residues D42 and K43 are predicted to reside in a short turn between β-strands A and B on the β-sheet opposite the dimerization face of hJAM-A, in close proximity to the short linker region between D1 and D2. Interestingly, these residues are also contained within a peptide that blocks binding of mAb (F11) to human JAM-A (F11R) on the surface of platelets. This mAb induces platelet secretion and aggregation and these stimulatory activities are inhibited by a peptide that contains residues 28-50 of human JAM-A (Babinska et al., 2002a).

We hypothesize that the decreased binding observed in mutations of fJAM-A residues D42 and K43 is due to the importance of these residues in the FCV/fJAM-A interaction. However, the possibility exists that the mutations D42N and K43N introduce N-linked glycosylation sites in the fJAM-A receptor. Although the mutated

fJAM-A constructs do not contain a classical Asn-X-Ser/Thr glycosylation motif at the position of the mutation, we cannot rule out atypical glycosylation. The presence of a glycan, and not the actual residue could then be responsible for the decreased binding. Another possibility that we cannot completely exclude is that the lower levels of surface expressed fJAM-A mutants D42N and K43N relative to the wild-type fJAM-A (see Figs. 5C and 5E) were responsible for the decreased virus binding. However, a distinct population of CHO-S cells expressed these mutants at levels comparable to cells expressing the wild type receptor, yet these cells bound significantly less virus (see Figs. 5C and 5E). Furthermore, mutating residue 97, which resides on a loop between β-strands E and F in very close proximity to residues 42 and 43, to an alanine resulted in significantly reduced viral binding with expression levels similar to those of the wild-type fJAM-A. Thus, taken together our data support the hypothesis that FCV binds to the D1 domain of fJAM-A in the vicinity of these residues.

Makino et al. reported that the FCV isolates they examined (which included the vaccine strain F9) could bind human 293T and monkey Vero cell lines, and that anti-hJAM-A antibodies decreased that binding (Makino et al., 2006). Confounding this observation, Stuart and Brown (2007) showed negligible binding of radio-labeled F9 virions to Vero and 293T cells (Stuart & Brown, 2007). In agreement with the findings of Stuart and Brown, we were unable to detect an interaction between FCV and hJAM-A expressed on the surface of CHO cells. Furthermore, we did not detect an interaction between FCV and soluble recombinant hJAM-A ectodomain by ELISA or surface plasmon resonance studies (data not shown). Therefore, the binding detected by Makino et al. seems unlikely to have been mediated by hJAM-A.

The mammalian reovirus σ1 protein interacts with human JAM-A via residues E61 and K63 present at the dimer interface of D1 and it is the charge on these residues that is important for binding (Guglielmi et al., 2007). Mutations to just one of the

residues of the dimerization motif prevented the formation of hJAM-A/hJAM-A dimers (Guglielmi et al., 2007). In contrast, FCV binding to cells expressing the E60R/K62E dimerization mutant of fJAM-A was similar to that of the wild-type fJAM-A (79% and 75%, respectively). The E60R/K62E mutations reverses the charge of two residues involved in forming the four predicted salt bridges important in dimerization (R58-E60; E60-R58; K62-E120; E120-K62) (Prota et al., 2003). Thus, we conclude that the charge of fJAM-A residues E60 and K62 (corresponding to hJAM-A E61 and K63) are not important in FCV binding. In addition, we predict the E60R/K62E mutant is unable to form fJAM-A/fJAM-A dimers. Therefore, the observed binding of FCV to the dimerization mutant suggests that FCV can interact with both monomeric and dimeric forms of fJAM-A.

The FCV-fJAM-A receptor interaction is also different from the adenovirus-CAR receptor interaction. The adenovirus attachment fiber protein is similar to the reovirus σ1 protein. The fiber protein is a trimer with a globular C-terminal knob that engages the coxsackie and adenovirus receptor (CAR), at its amino terminal D1 domain (Freimuth et al., 1999). Like the σ1 head domain, the fiber knob attaches at the dimer interface to residues important in CAR-CAR interactions at the dimer interface (Bewley et al., 1999, Seiradake et al., 2006, Stehle & Dermody, 2004).

Similar to caliciviruses, coxsackieviruses (Picornaviridae) are small, nonenveloped, positive-strand RNA viruses. Group B coxsackieviruses (CVB) utilize CAR as a host cell receptor (Bergelson et al., 1997, He et al., 2001, Martino et al., 2000). CVB also engages the amino terminal Ig-like domain D1 of CAR. However, unlike adenoviruses, the CVB interaction with CAR does not involve critical residues in the dimerization motif, although the binding site is on the distal end and the lateral side (A-G face) of CAR D1 and lies close to the dimer interface (He et al., 2001). Residues D42, K43, and S97, which we found were important for FCV binding, are

predicted to also be part of the orthologous lateral A-G face of fJAM-A; however, these residues lie much closer to the D1-D2 linker than the dimerization interface.

The ectodomain of fJAM-A was sufficient to mediate FCV binding, but when expressed on the cell surface with a GPI-anchor, it could not mediate infection. In contrast, a GPI-CAR receptor mediated CVB and adenovirus binding and infection (Wang & Bergelson, 1999). This finding suggests that the transmembrane and/or the cytosolic domains of fJAM-A are required for productive FCV infection of non-permissive cells. We first hypothesized that signaling via the consensus C-terminal type II PDZ domain-binding motif at the carboxyl terminus of the cytoplasmic tail of fJAM-A might be required for infection; however, a construct that lacked the predicted PDZ binding motif (last three amino acids of fJAM-A, Phe-Leu-Val) was as efficient as the wild type receptor in mediating FCV infection of CHO cells. Taken together, our data suggest a model where FCV binding to the fJAM-A ectodomain transduces signals through its transmembrane and cytosolic domains that are required for infection. Evidence suggesting such a model for CVB was reported by Coyne and Bergelson (2006), where interaction of CVB with the cellular receptor decay-accelerated factor activates kinases that trigger actin rearrangements and phosphorylation events necessary for mediating viral infection (Coyne & Bergelson, 2006).

Makino et al. (2006) reported that fJAM-A expression on nonpermissive hamster lung cells conferred susceptibility to FCV infection. Here we show that expression of fJAM-A on the surface of five different cell lines was not necessarily sufficient to support productive infection for all FCV isolates. Not all of the cell lines that we investigated supported productive infection by all of the isolates; furthermore the ability of FCV isolates to productively infect each cell line tested varied. Only Vero cells were able to support productive infection by all the FCV isolates we

examined. While native non-transfected Vero cells have been reported to support infection by some FCV isolates (Makino et al., 2006), none of the isolates we tested were capable of infecting Vero cells in the absence of fJAM-A.

The capacity of different FCV isolates to infect CHO-K1 cells that expressed fJAM-A varied. Indeed, we found that some isolates (FCV-131 and Kaos) were unable to productively infect these cells. Stuart and Brown (2007) reported that cell binding and infection by FCV is partially mediated by an N-linked glycoprotein containing α-2,6-linked, but not α-2,3-linked sialic acids (Stuart & Brown, 2007). CHO cells lack the sialyltransferase necessary for generating α-2,6-sialic acid linkages and express predominantly α-2,3-linked sialic acid glycans (Lee et al., 1989). Therefore, our results infer that at least a subset of FCV isolates are capable of binding and infecting fJAM-A expressing cells independently of α-2,6-sialic acid linkages. fJAM-A contains a single putative N-linked glycosylation site at residue N184 in D2. The glycosylation status of this site, as well as the role of glycosylation in FCV binding and infection, warrant further investigation. It is also possible that there is an additional surface receptor for FCV. The findings that not all FCV isolates were capable of infecting non-permissive cell lines expressing fJAM-A lends support to the idea that fJAM-A alone is not sufficient for FCV infection by all isolates and that additional co-receptors may be required.

In the last 10 years there have been sporadic reports of highly virulent outbreaks of FCV disease in cats (Coyne et al., 2006, Hurley et al., 2004, Pedersen et al., 2000, Schorr-Evans et al., 2003). The virus isolates responsible for these outbreaks have been termed virulent systemic (VS-) FCV (Hurley et al., 2004). The pathology associated with VS-FCV outbreaks indicates breakdown of epithelial and endothelial barrier function (Pedersen et al., 2000, Pesavento et al., 2004). These observations may reflect the capacity of FCV to target fJAM-A, as it is known that JAM-A is

required for maintenance of epithelial and endothelial tight junctions. It is possible that FCV can disrupt the homophilic interactions that occur between JAM-A molecules on apposing cells and thus disrupt tight junctions and barrier integrity, an effect proposed for secreted adenovirus fiber protein (Walters et al., 2002).

JAM-A is also expressed on platelets, including feline platelets (Stokol and Parker, unpublished data). In some cases of VS-FCV, thrombocytopenia has been noted together with disseminated intravascular coagulation (Foley et al., 2006, Hurley et al., 2004, Pedersen et al., 2000, Schorr-Evans et al., 2003). It is possible that large amounts of FCV in the blood might disrupt normal platelet function. A monoclonal antibody (F11) that binds human JAM-A induces platelet secretion and aggregation. Binding of F11 to the surface of platelets is blocked by a peptide that incorporates the first 23 residues of the hJAM-A D1 (residues 28 to 50) (Babinska et al., 2002a). As we have shown, FCV likely interacts with residues D42 and K43 on fJAM-A. Therefore, it is possible that FCV binding to fJAM-A might induce secretion and aggregation of feline platelets, and that this in turn might be responsible for some of the pathogenic sequelae seen with VS-FCV disease. We are currently examining these and other possibilities.

3.6 Acknowledgments

We thank Kristen Guglielmi, Meg Crapster-Pregont, Stephen Campbell, and Dr. Patricia Pesavento for excellent technical assistance. We thank Karin Hoelzer for advice on statistical analysis. We thank Dr. Terry Dermody and Dr. Doug Lublin for the generous gift of reagents. This work was supported by grants from The Cornell Feline Health Center, and the Winn foundation. R. J. O. is the recipient of a scholarship from Cornell University. We dedicate this paper to the memory of Dr. James Richards, a tireless advocate for feline research.

REFERENCES

Babinska, A., Kedees, M. H., Athar, H., Ahmed, T., Batuman, O., Ehrlich, Y. H., Hussain, M. M. & Kornecki, E. (2002a). F11-receptor (F11R/JAM) mediates platelet adhesion to endothelial cells: role in inflammatory thrombosis. *Thromb Haemost* **88**, 843-50.

Babinska, A., Kedees, M. H., Athar, H., Sobocki, T., Sobocka, M. B., Ahmed, T., Ehrlich, Y. H., Hussain, M. M. & Kornecki, E. (2002b). Two regions of the human platelet F11-receptor (F11R) are critical for platelet aggregation, potentiation and adhesion. *Thromb Haemost* **87**, 712-21.

Baldwin, S. L., Powell, T. D., Sellins, K. S., Radecki, S. V., John Cohen, J. & Milhausen, M. J. (2004). The biological effects of five feline IFN-alpha subtypes. *Vet Immunol Immunopathol* **99**, 153-67.

Barton, E. S., Forrest, J. C., Connolly, J. L., Chappell, J. D., Liu, Y., Schnell, F. J., Nusrat, A., Parkos, C. A. & Dermody, T. S. (2001). Junction adhesion molecule is a receptor for reovirus. *Cell* **104**, 441-51.

Bazzoni, G., Martinez-Estrada, O. M., Orsenigo, F., Cordenonsi, M., Citi, S. & Dejana, E. (2000). Interaction of junctional adhesion molecule with the tight junction components ZO-1, cingulin, and occludin. *J Biol Chem* **275**, 20520-6.

Bergelson, J. M., Cunningham, J. A., Droguett, G., Kurt-Jones, E. A., Krithivas, A., Hong, J. S., Horwitz, M. S., Crowell, R. L. & Finberg, R. W. (1997). Isolation of a common receptor for Coxsackie B viruses and adenoviruses 2 and 5. *Science* **275**, 1320-3.

Bewley, M. C., Springer, K., Zhang, Y. B., Freimuth, P. & Flanagan, J. M. (1999). Structural analysis of the mechanism of adenovirus binding to its human cellular receptor, CAR. *Science* **286**, 1579-83.

Campbell, J. A., Schelling, P., Wetzel, J. D., Johnson, E. M., Forrest, J. C., Wilson, G. A., Aurrand-Lions, M., Imhof, B. A., Stehle, T. & Dermody, T. S. (2005). Junctional adhesion molecule a serves as a receptor for prototype and field-isolate strains of mammalian reovirus. *J Virol* **79**, 7967-78.

Cohen, C. J., Shieh, J. T., Pickles, R. J., Okegawa, T., Hsieh, J. T. & Bergelson, J. M. (2001). The coxsackievirus and adenovirus receptor is a transmembrane component of the tight junction. *Proc Natl Acad Sci U S A* **98**, 15191-6.

Coyne, C. B. & Bergelson, J. M. (2006). Virus-induced Abl and Fyn kinase signals permit coxsackievirus entry through epithelial tight junctions. *Cell* **124**, 119-31.

Coyne, K. P., Jones, B. R., Kipar, A., Chantrey, J., Porter, C. J., Barber, P. J., Dawson, S., Gaskell, R. M. & Radford, A. D. (2006). Lethal outbreak of disease associated with feline calicivirus infection in cats. *Vet Rec* **158**, 544-50.

Delano, W. L. (2002). The PyMOL Molecular Graphics System. Pala Alto, CA, USA: DeLano Scientific.

Ebnet, K., Schulz, C. U., Meyer Zu Brickwedde, M. K., Pendl, G. G. & Vestweber, D. (2000). Junctional adhesion molecule interacts with the PDZ domain-containing proteins AF-6 and ZO-1. *J Biol Chem* **275**, 27979-88.

Foley, J., Hurley, K., Pesavento, P. A., Poland, A. & Pedersen, N. C. (2006). Virulent systemic feline calicivirus infection: local cytokine modulation and contribution of viral mutants. *J Feline Med Surg* **8**, 55-61.

Forrest, J. C., Campbell, J. A., Schelling, P., Stehle, T. & Dermody, T. S. (2003). Structure-function analysis of reovirus binding to junctional adhesion molecule 1. Implications for the mechanism of reovirus attachment. *J Biol Chem* **278**, 48434-44.

Freimuth, P., Springer, K., Berard, C., Hainfeld, J., Bewley, M. & Flanagan, J. (1999). Coxsackievirus and adenovirus receptor amino-terminal immunoglobulin V-related domain binds adenovirus type 2 and fiber knob from adenovirus type 12. *J Virol* **73**, 1392-8.

Fulton, R. W. & Burge, L. J. (1985). Susceptibility of feline herpesvirus 1 and a feline calicivirus to feline interferon and recombinant human leukocyte interferons. *Antimicrob Agents Chemother* **28**, 698-9.

Goodfellow, I. G., Evans, D. J., Blom, A. M., Kerrigan, D., Miners, J. S., Morgan, B. P. & Spiller, O. B. (2005). Inhibition of coxsackie B virus infection by soluble forms of its receptors: binding affinities, altered particle formation, and competition with cellular receptors. *J Virol* **79**, 12016-24.

Guglielmi, K. M., Kirchner, E., Holm, G. H., Stehle, T. & Dermody, T. S. (2007). Reovirus binding determinants in junctional adhesion molecule-a. *J Biol Chem* **282**, 17930-40.

He, Y., Chipman, P. R., Howitt, J., Bator, C. M., Whitt, M. A., Baker, T. S., Kuhn, R. J., Anderson, C. W., Freimuth, P. & Rossmann, M. G. (2001). Interaction of coxsackievirus B3 with the full length coxsackievirus-adenovirus receptor. *Nat Struct Biol* **8**, 874-8.

Hurley, K. E., Pesavento, P. A., Pedersen, N. C., Poland, A. M., Wilson, E. & Foley, J. E. (2004). An outbreak of virulent systemic feline calicivirus disease. *J Am Vet Med Assoc* **224**, 241-9.

Kaplan, G., Freistadt, M. S. & Racaniello, V. R. (1990). Neutralization of poliovirus by cell receptors expressed in insect cells. *J Virol* **64**, 4697-702.

Khandoga, A., Kessler, J. S., Meissner, H., Hanschen, M., Corada, M., Motoike, T., Enders, G., Dejana, E. & Krombach, F. (2005). Junctional adhesion molecule-A deficiency increases hepatic ischemia-reperfusion injury despite reduction of neutrophil transendothelial migration. *Blood* **106**, 725-33.

Kostrewa, D., Brockhaus, M., D'Arcy, A., Dale, G. E., Nelboeck, P., Schmid, G., Mueller, F., Bazzoni, G., Dejana, E., Bartfai, T., Winkler, F. K. & Hennig, M. (2001). X-ray structure of junctional adhesion molecule: structural basis for homophilic adhesion via a novel dimerization motif. *Embo J* **20**, 4391-8.

Law, L. K. & Davidson, B. L. (2005). What does it take to bind CAR? *Mol Ther* **12**, 599-609.

Lee, E. U., Roth, J. & Paulson, J. C. (1989). Alteration of terminal glycosylation sequences on N-linked oligosaccharides of Chinese hamster ovary cells by expression of beta-galactoside alpha 2,6-sialyltransferase. *J Biol Chem* **264**, 13848-55.

Liu, Y., Nusrat, A., Schnell, F. J., Reaves, T. A., Walsh, S., Pochet, M. & Parkos, C. A. (2000). Human junction adhesion molecule regulates tight junction resealing in epithelia. *J Cell Sci* **113 (Pt 13)**, 2363-74.

Makino, A., Shimojima, M., Miyazawa, T., Kato, K., Tohya, Y. & Akashi, H. (2006). Junctional adhesion molecule 1 is a functional receptor for feline calicivirus. *J Virol* **80**, 4482-90.

Malergue, F., Galland, F., Martin, F., Mansuelle, P., Aurrand-Lions, M. & Naquet, P. (1998). A novel immunoglobulin superfamily junctional molecule expressed by antigen presenting cells, endothelial cells and platelets. *Mol Immunol* **35**, 1111-9.

Mandell, K. J., McCall, I. C. & Parkos, C. A. (2004). Involvement of the junctional adhesion molecule-1 (JAM1) homodimer interface in regulation of epithelial barrier function. *J Biol Chem* **279**, 16254-62.

Mandell, K. J. & Parkos, C. A. (2005). The JAM family of proteins. *Adv Drug Deliv Rev* **57**, 857-67.

Marsh, M. & Helenius, A. (2006). Virus entry: open sesame. *Cell* **124**, 729-40.

Martin-Padura, I., Lostaglio, S., Schneemann, M., Williams, L., Romano, M., Fruscella, P., Panzeri, C., Stoppacciaro, A., Ruco, L., Villa, A., Simmons, D. & Dejana, E. (1998). Junctional adhesion molecule, a novel member of the immunoglobulin superfamily that distributes at intercellular junctions and modulates monocyte transmigration. *J Cell Biol* **142**, 117-27.

Martin, S., Casasnovas, J. M., Staunton, D. E. & Springer, T. A. (1993). Efficient neutralization and disruption of rhinovirus by chimeric ICAM-1/immunoglobulin molecules. *J Virol* **67**, 3561-8.

Martino, T. A., Petric, M., Weingartl, H., Bergelson, J. M., Opavsky, M. A., Richardson, C. D., Modlin, J. F., Finberg, R. W., Kain, K. C., Willis, N., Gauntt, C. J. & Liu, P. P. (2000). The coxsackie-adenovirus receptor (CAR) is used by reference strains and clinical isolates representing all six serotypes of coxsackievirus group B and by swine vesicular disease virus. *Virology* **271**, 99-108.

Mochizuki, M., Nakatani, H. & Yoshida, M. (1994). Inhibitory effects of recombinant feline interferon on the replication of feline enteropathogenic viruses in vitro. *Vet Microbiol* **39**, 145-52.

Ossiboff, R. J., Sheh, A., Shotton, J., Pesavento, P. A. & Parker, J. S. (2007). Feline caliciviruses (FCVs) isolated from cats with virulent systemic disease possess in vitro phenotypes distinct from those of other FCV isolates. *J Gen Virol* **88**, 506-27.

Ostermann, G., Weber, K. S., Zernecke, A., Schroder, A. & Weber, C. (2002). JAM-1 is a ligand of the beta(2) integrin LFA-1 involved in transendothelial migration of leukocytes. *Nat Immunol* **3**, 151-8.

Ozaki, H., Ishii, K., Horiuchi, H., Arai, H., Kawamoto, T., Okawa, K., Iwamatsu, A. & Kita, T. (1999). Cutting edge: combined treatment of TNF-alpha and IFN-gamma causes redistribution of junctional adhesion molecule in human endothelial cells. *J Immunol* **163**, 553-7.

Park, M. S., Shaw, M. L., Munoz-Jordan, J., Cros, J. F., Nakaya, T., Bouvier, N., Palese, P., Garcia-Sastre, A. & Basler, C. F. (2003). Newcastle disease virus (NDV)-based assay demonstrates interferon-antagonist activity for the NDV V protein and the Nipah virus V, W, and C proteins. *J Virol* **77**, 1501-11.

Pedersen, N. C., Elliott, J. B., Glasgow, A., Poland, A. & Keel, K. (2000). An isolated epizootic of hemorrhagic-like fever in cats caused by a novel and highly virulent strain of feline calicivirus. *Vet Microbiol* **73**, 281-300.

Pesavento, P. A., MacLachlan, N. J., Dillard-Telm, L., Grant, C. K. & Hurley, K. F. (2004). Pathologic, immunohistochemical, and electron microscopic findings in naturally occurring virulent systemic feline calicivirus infection in cats. *Vet Pathol* **41**, 257-63.

Prota, A. E., Campbell, J. A., Schelling, P., Forrest, J. C., Watson, M. J., Peters, T. R., Aurrand-Lions, M., Imhof, B. A., Dermody, T. S. & Stehle, T. (2003). Crystal structure of human junctional adhesion molecule 1: implications for reovirus binding. *Proc Natl Acad Sci U S A* **100**, 5366-71.

Rossmann, M. G., He, Y. & Kuhn, R. J. (2002). Picornavirus-receptor interactions. *Trends Microbiol* **10**, 324-31.

Schorr-Evans, E. M., Poland, A., Johnson, W. E. & Pedersen, N. C. (2003). An epizootic of highly virulent feline calicivirus disease in a hospital setting in New England. *J Feline Med Surg* **5**, 217-26.

Seiradake, E., Lortat-Jacob, H., Billet, O., Kremer, E. J. & Cusack, S. (2006). Structural and mutational analysis of human Ad37 and canine adenovirus 2 fiber heads in complex with the D1 domain of coxsackie and adenovirus receptor. *J Biol Chem* **281**, 33704-16.

Stehle, T. & Dermody, T. S. (2004). Structural similarities in the cellular receptors used by adenovirus and reovirus. *Viral Immunol* **17**, 129-43.

Stuart, A. D. & Brown, T. D. (2007). Alpha2,6-linked sialic acid acts as a receptor for Feline calicivirus. *J Gen Virol* **88**, 177-86.

Walters, R. W., Freimuth, P., Moninger, T. O., Ganske, I., Zabner, J. & Welsh, M. J. (2002). Adenovirus fiber disrupts CAR-mediated intercellular adhesion allowing virus escape. *Cell* **110**, 789-99.

Wang, X. & Bergelson, J. M. (1999). Coxsackievirus and adenovirus receptor cytoplasmic and transmembrane domains are not essential for coxsackievirus and adenovirus infection. *J Virol* **73**, 2559-62.

Williams, L. A., Martin-Padura, I., Dejana, E., Hogg, N. & Simmons, D. L. (1999). Identification and characterisation of human Junctional Adhesion Molecule (JAM). *Mol Immunol* **36**, 1175-88.

CHAPTER 4

Genetic and biophysical evidence for large-scale conformational changes in the capsid of a calicivirus upon interaction with its functional receptor

[Manuscript in preparation. This manuscript will include the following additional authors: Yi Zhou, Patrick Lightfoot, B. V. Venkataram Prasad and John S. L. Parker. Drs. Yi Zhou and B. V. Venkataram Prasad were responsible for generating the structural data for FCV-5 using virus purified by myself and Patrick Lightfoot. Figures 4.2 and 4.3A-C were generated by Dr. Yi Zhou]

4.1 Abstract

The capsid of nonenveloped feline calicivirus (FCV) mediates viral attachment, entry and the cytosolic delivery of the viral genome. Nonenveloped viral capsids are metastable structures that undergo conformational changes during virus entry that allow them to interact with the cell membrane. For members of the Caliciviridae, neither the nature of these structural changes in the capsid nor the factor responsible for inducing these changes is known. Feline junctional adhesion molecule A (fJAM-A) is sufficient to mediate attachment and infectious viral entry of FCV. Here we show that the infectivity of some FCV isolates is neutralized upon incubation with the soluble receptor at 37°C. We used this property to select for mutants that were resistant to preincubation with the soluble receptor. We isolated and sequenced 24 of these soluble receptor resistant mutants and have further characterized the growth properties and receptor-binding properties of 8 mutants. To identify the location of the mutations within the capsid protein within the structure of FCV, we obtained a 3.6 Angstrom structure of FCV. The location of mutations within the capsid structure indicate that many of the soluble-receptor resistant (*srr*) mutants have mutations in their capsid protein that map to the surface of the P2 domain, are buried at the protruding domain dimer interface, or are present in inaccessible regions of the capsid protein. Taken together with data showing that both the parental FCV and the *srr* mutants undergo increases in hydrophobicity upon incubation with the soluble receptor at 37 °C, these findings indicate that this model calicivirus undergoes significant conformational change upon interaction with its receptor. These changes are likely to be important for subsequent interaction of the capsid with cellular membranes and for membrane penetration and genome delivery.

4.2 Introduction

The interactions between viruses and receptors on the surface of host cells strongly influence viral pathogenesis and regulate morbidity and mortality in the host. This is because these interactions determine the types of cells that can be infected, the pathway of entry into the cell and the efficiency of productive infection.

Interactions between nonenveloped virus capsids and their receptor(s) trigger one or more steps required for infectious entry. These steps can include interaction with other receptors, exposure to low pH or endosomal proteases or other factors. Ultimately, one or more of these interactions lead to changes in capsid conformation; such changes may result in the exposure of hydrophobic regions or release of a lipid-seeking factor that can interact with, and disrupt the limiting cellular membrane to allow the capsid and/or the genome to be delivered to the interior of the cell [as reviewed in (Tsai, 2007)].

The *Caliciviridae* are small nonenveloped viruses containing a positive-sense RNA genome (~7-8 kb) that cause disease in humans and animals. Several important disease-causing members of the *Caliciviridae*, including human noroviruses, cannot be propagated in tissue culture systems. This has slowed progress on studies of the mechanisms of cellular entry of these viruses. In contrast, feline caliciviruses propagate readily in tissue culture and two cell surface receptor molecules, feline Junctional Adhesion Molecule-A (fJAM-A) and α2,6 sialic acid are known (Makino et al., 2006, Stuart & Brown, 2007).

JAM-A is a type I transmembrane glycoprotein (MW 36-41 kDa) member of the immunoglobulin superfamily (IgSF); it consists of an N-terminal signal peptide, an extracellular domain (composed of two Ig-like domains - a membrane-distal D1 and a membrane-proximal D2), a transmembrane domain, and a short cytoplasmic domain that contains a type II PDZ domain-binding motif (Ebnet et al., 2000, Mandell &

Parkos, 2005). We have previously shown that the D1 domain of the fJAM-A ectodomain is necessary and sufficient for FCV binding, and that preincubation of FCV with soluble fJAM-A results in virus neutralization (Ossiboff & Parker, 2007). Additional roles that fJAM-A and α2,6 sialic acid might play in FCV entry, however, have not been investigated.

The virions of caliciviruses are composed of 180 copies of a single capsid protein. Crystallographic structures have been determined for two members of the *Caliciviridae*, recombinant virus like particles of Norwalk virus (genus *Norovirus*) and native San Miguel sea lion virus (SMSV) virions (genus *Vesivirus*) (Chen et al., 2006, Prasad et al., 1999). The viral capsid consists of 90 dimers of the capsid protein arranged in T = 3 icosahedral symmetry. Each capsid protein contains three structural domains, an N-terminal arm (NTA), shell (S), and protruding domain (P), which is further subdivided into two sub-domains (P1 and P2) (Chen et al., 2006, Prasad et al., 1999). The most exterior sub-domain, P2, is structurally conserved between Norwalk virus and SMSV, but there is little sequence conservation. Two hypervariable regions that were identified in the primary sequence of FCV contain neutralizing epitopes (Guiver et al., 1992, Neill et al., 2000, Tohya et al., 1997). On the SMSV capsid structure these hypervariable regions map to loops that are predominantly surface-exposed. The surface residues at the dimeric interface between two capsid monomers are conserved within individual calicivirus genera and it has been suggested that this interface might be important in receptor binding (Chen et al., 2006). A cryo-electron microscopy reconstruction of the FCV vaccine strain F9 complexed with the ectodomain of fJAM-A (modeled on the crystal structures of SMSV and human JAM-A, respectively) shows that FCV engages its receptor by way of the outer face of the P2 domain (Bhella et al., 2008). The reconstructions by Bhella *et al.* (2008) also

showed that compared to cryo-EM reconstructions of the virus alone, binding of fJAM-A caused a rotation in the P dimer.

The selection of mutant viruses resistant to neutralization with soluble receptors has been used to identify virus residues important in either directly binding to or modulate the binding of virus to receptor (Colston & Racaniello, 1994, Kaplan et al., 1990, Saeki et al., 1997). Soluble receptor-resistant (*srr*) mutants of poliovirus contained mutations to both surface exposed and internal residues that were shown to regulate both receptor attachment and conformational changes in the capsid (Colston & Racaniello, 1994, Racaniello, 1996). Here we report 24 *srr* mutants and the location of their capsid mutations on a 3.6 Å structure of the virus. In addition, we describe the growth kinetics and receptor binding properties of a subpanel of 8 *srr* mutants. Using spectrofluorimetry, we show increased hydrophobicity of the capsid upon interaction with soluble fJAM-A suggesting that FCV undergoes a conformational change following incubation with soluble receptor. In the 24 *srr* mutants, we identified 20 unique mutations that were present on surface-exposed and buried regions of the capsid protein. FCV-5, three *srr* mutants, and two field isolates of FCV demonstrated increases in hydrophobicity upon incubation with the soluble receptor at 37 °C. Taken together, these findings indicate that this model calicivirus undergoes significant conformational changes upon interaction with its receptor.

4.3 Methods

Cells and viruses. Crandell-Reese feline kidney (CRFK; ATCC #CCL-94) cells were grown in Eagle's minimal essential medium (EMEM; CellGro) supplemented with 5% fetal bovine serum (HyClone), 100 U ml^{-1} of penicillin, 100 μg ml^{-1} streptomycin, 0.25 μg ml^{-1} amphotericin B, 1 mM sodium pyruvate, and non-

essential amino acids (CellGro). Suspension Chinese hamster ovary (CHO-S) cells (Invitrogen) were grown in CHO-Serum Free Medium (-SFM; Gibco).

The F9 vaccine strain (VR-782) of FCV was obtained from the ATCC. The viral isolates FCV-5, Deuce, Kaos, FCV-127, FCV-131, and FCV-796 were previously characterized (Ossiboff et al., 2007). FCV-Urbana viral stock was generated from a full-length infectious clone as previously described (Sosnovtsev & Green, 1995, Sosnovtsev et al., 1997). Briefly, CRFK cells were infected with vaccinia virus expressing T7 RNA polymerase (MVA/T7); 1 h following infection the FCV-Urbana infectious clone (pQ14) was transfected into the cells using FuGENE 6 (Roche). Samples were lysed at 18 h p.i. by successive freeze-thaw cycles and viral plaques were selected. The viral capsid gene was sequenced to verify that FCV-Urbana was present. Third passage viral stocks were prepared from twice plaque-purified viruses amplified in CRFK cells. Plaque assays were performed as previously described (Ossiboff et al., 2007).

Antibodies and reagents. A rabbit antiserum against the purified fJAM-A ectodomain was previously described (Ossiboff & Parker, 2007). Virus was detected with either an anti-FCV mouse MAb (S1-9; Custom Monoclonals International) or rabbit anti-FCV-5 antiserum. The fJAM-A extracellular domain (amino acid residues 26-232) was purified as previously described (Ossiboff & Parker, 2007). Recombinant protein was purified by glutathione affinity chromatography. When GST-free fJAM-A was desired, N-terminal GST and His tags were cleaved from the recombinant protein using HRV 3C protease (Novagen).

Neutralization of FCV-5 by fJAM-A. To investigate the effect of temperature on the neutralization of FCV-5 by fJAM-A, ~1×10^5 plaque forming units (p.f.u.) of FCV-5 in Dulbecco's modified Eagle's medium (DMEM; CellGro) + 0.1% BSA (Calbiochem) were incubated either in the presence or absence of soluble fJAM-A (4.3

μM) at 4°C for 3 h. Samples were then incubated for an additional 30 min at 4, 16, 24, or 37°C, and infectious titer of the samples was determined by plaque assay. To construct neutralization curves of FCV-5 by fJAM-A, ~1×10^5 plaque forming units (p.f.u.) of FCV-5 in DMEM + 0.1% BSA was incubated with different concentrations of soluble GST-fJAM-A or fJAM-A lacking the GST tag at 37°C for 30 min. The samples were then placed on ice or frozen at -80°C and the remaining viral titer assayed.

Selection of *soluble receptor resistant* (*srr*) mutants of FCV-5. Aliquots of FCV-5 (1×10^5 p.f.u.) were incubated with GST-fJAM-A (55 μM) at 37°C for 30 min, plaque titrated on CRFK cells in 6 well plates and overlaid with EMEM containing 5% fetal bovine serum and 1% Bacto Agar. Following incubation at 37°C in humidified 5% CO_2 for 48 h, individual plaques were selected and amplified without selection on CRFK cells in 12-well plates (Corning). Once wells showed 100% cytopathic effect (CPE), a small aliquot from each well was again incubated with 55 μM GST-fJAM-A at 37°C for 30 min and then used to infect CRFK cells in 12-well plates. In wells that developed CPE, a sample of the lysate was subjected to an additional round of GST-fJAM-A neutralization, and samples were amplified on CRFK cells in a 96-well plate (Corning). Twenty-four wells showing CPE were chosen at random and twice plaque-purified.

Sequencing the major capsid protein (VP1) of the *srr* mutants. The recovery of viral RNA, RT-PCR and sequencing of the capsid protein of the *srr* mutants was performed as previously described (Ossiboff et al., 2007). Briefly, total RNA was extracted from infected-cell lysates (RNeasy Mini; Qiagen), and first strand cDNA synthesis of the capsid region of the genome was performed using a degenerate primer and Accuscript High-Fidelity reverse transcriptase (Stratagene). The capsid open reading frame was then amplified from the first strand cDNA template (primers

available upon request). The resulting ~2.1 kb PCR products, encompassing the entirety of the capsid ORF, were purified and sequenced directly.

Purification of FCV. Confluent roller bottles (Corning) of CRFK cells were infected with FCV (multiplicity of infection [MOI] = 5) and maintained in a roller incubator for 8 h at 37°C. At 8 h p.i., cells were removed from the plastic surface by physical agitation and the cells were collected by centrifugation of the medium at 500 × *g*. The cell pellet was resuspended in 250 mM NaCl, 85 mM Tris Base, pH 7.5 and frozen at -80°C. The pellet was thawed, briefly sonicated to lyse the cells and trichlorotrifluoroethane was used to extract the virus from the cell lysate. To clarify the phases, the trichlorotrifluoroethane/lysate mixture was centrifuged for 10 min at 5850 × *g*. The aqueous phase was removed and the trichlorotrifluoroethane extraction step repeated. Following the second centrifugation, the aqueous phase was placed on a CsCl gradient (1.30 – 1.45 g/ml) in an ultracentrifuge tube (Beckman) and centrifuged at 97,000 × *g* for 16 h. Visible virus bands were collected and dialyzed exhaustively against virion buffer (150 mM NaCl, 10 mM Tris Base, 15 mM $MgCl_2$, pH 7.2) for 48-72 h at 4°C. Purified virus was stored at 4°C.

Crystallization. Crystallization trials of FCV-5 were carried out using the hanging-drop vapor diffusion method at room temperature. Crystal screens 1 and 2 from Hampton Research were used to explore various conditions. Typically, for each condition, 2 µl of the virus solution, at a concentration of 3 mg/ml, was mixed with 2 µl of the well solution and equilibrated with 0.5 ml of the well solution. Initial screening produced crystals under a few conditions including the Crystal Screen 1 condition 3 (0.4 M Ammonium phosphate) and condition 13 (30% PEG 400, 0.1 M Tris HCL pH 8.5, 0.2 M Sodium Citrate). After crystallization condition optimization and synchrotron on-site screening, crystals of the best diffraction quality were obtained using a well solution containing 0.45 M Ammonium phosphate with Additive

Screen Reagent C10 (1.0 M Glycine). Cryo-protection of crystals was obtained by soaking the crystals in the mother liquor with increasing concentration of PEG 400 through six steps: 5%, 10%, 15%, 20%, 22.5% and 25%. The equilibration time at each solution was at least 10 minutes. The crystals were then flash frozen in liquid nitrogen and shipped to synchrotron sites for data collection.

Data collection and analysis. The diffraction data from single crystals were collected under cryo-conditions at APS 19ID station with monochromatic X-rays (wavelength=0.9795A) and a detector to crystal distance of 480 mm on an ADSC 3×3 CCD detector using an oscillation angle of 0.3° and an exposure time of 3 seconds. Indexing, integration, scaling, post-refinement, and reduction of the data were carried out using the HKL2000 and D*TREK packages. Analysis of the diffraction data clearly indicated that the FCV-5 crystal belonged to the orthorhombic space group I222. The data between 30 and 3.6Å from 300 frames were scaled with an R_{merge} factor of about 22%. The overall completeness of the data to 3.6Å resolution is about 90.1%. To determine the precise orientation of the virus particle in the unit cell, self-rotation functions were calculated using the program GLRF. These calculations showed all the peaks corresponding to 5-fold (κ=72°), 3-fold (κ=120°), and 2-fold (κ=180°) axes, which are expected from a particle with icosahedral symmetry. In the I222 space group, consistent with the unit cell dimensions and the particle radius, which is estimated to be 200Å, the particle position is uniquely defined by the intersection of the crystallographic 2-fold axes. In such a setting, an icosahedral particle can assume one of the two possible orientations. This ambiguity in orientation was clearly resolved by the self-rotation function calculations using the X-ray diffraction data. Each crystallographic asymmetric unit is composed of 1/4th of the virion with a non-crystallographic 15-fold symmetry. Similar packing of icosahedral particle has been observed in Norwalk virus.

Crystal structure determination and refinement. A properly positioned and oriented SMSV-4 capsid was placed in a FCV-5 unit cell. One initial model at a resolution of 10 Å was calculated from the 15 copies of SMSV-4 related first by icosahedral 5-fold symmetry then by icosahedral 3-fold symmetry. Phase refinement and extension were carried out by iterative cycles of real space electron density averaging, solvent flattening and back transformation with the RAVE and CCP4 program packages. The phases were extended to the final 3.6 Å resolution with each step less than one reciprocal space point. An initial mask was constructed from the cryo-EM reconstruction with the program MAMA, and the mask was edited each step to avoid truncation of the density. The averaged 3.6 Å density map is of good quality and readily interpretable. After initial model building and the final refinement, the structure has an Rfree of 0.39, calculated using 10% of the data that were not included in the refinement, and a final R factor of 0.37.

Neutralization of *srr* mutants by fJAM-A. To verify that the selected *srr* mutants were resistant to neutralization by soluble receptor, a subpanel of 8 *srr* mutants (~1×10^5 p.f.u.) in DMEM + 0.1% BSA were incubated at 37°C either in the presence or absence of GST-fJAM-A (45 μM) for 30 min. Infectious titer of samples was determined by plaque assay.

Virus-binding assay by flow cytometry. FCV binding to CHO-S cells transiently expressing fJAM-A was detected as previously described (Ossiboff & Parker, 2007). Briefly, CHO-S cells (10^6 cells per sample) were transiently transfected with a DNA construct encoding fJAM-A. At 24 h post-transfection the cells were washed and incubated with FCV (MOI = 5) in phosphate-buffered saline (PBS) (137 mM NaCl, 3 mM KCl, 8 mM Na_2HPO_4 [pH 7.5]) plus 1% BSA (PBSA) on ice for 30 min. After washing to remove unbound virions, the cells were incubated with fJAM-A rabbit antiserum and anti-FCV mouse Mab in PBSA on ice for 30 min. The cells were

then washed in PBSA, fixed in 2% paraformaldehyde in PBS, and incubated with Alexa 647-conjugated goat anti-rabbit and Alexa 488-conjugated goat anti-mouse IgG for 30 min at room temperature. The cells were analyzed using a FACSCalibur (Becton Dickinson). Cells expressing fJAM-A on their surface were gated and analyzed for virus binding (10,000 cells were gated for each sample).

Plaque reduction of *srr* mutants by fJAM-A antiserum. Confluent CRFK cells in 60 mm dishes (Corning) were incubated PBSA with or without fJAM-A rabbit antiserum for 30 min at room temperature. Virus (~100 p.f.u per dish) was adsorbed for 1 h at room temperature. The monolayers were then overlaid with EMEM containing 5% fetal bovine serum and 1% BactoAgar. After incubation at 37°C for 48 h in humidified 5% CO_2, the overlay was removed and the cells were fixed with 10% buffered formalin, and stained with 1% (wt/vol) crystal violet solution. The plaques were counted, and percent reduction from controls was calculated.

Single- and multiple-cycle growth kinetics of *srr* mutants. CRFK cell monolayers were infected with *srr* mutants at multiplicities of 5 and 0.01 for single- and multiple-cycle growth curves, respectively. Virus was adsorbed to cells for 1 h at room temperature in DMEM plus 0.1% BSA; EMEM plus 5% FBS supplemented as above was then added and the cells were incubated for at 37 °C in 5% CO_2. At various times post-infection (p.i.), samples were collected and stored at -80 °C for later titration. Prior to plaque assay, all samples were frozen and thawed three times. Virus growth at each time point was calculated by subtracting the log10(p.f.u. ml^{-1}) at T = 0 from the log10(p.f.u. ml^{-1}) measured at the time point. Results are expressed as the change in plaque titer over time.

ELISA binding of FCV to fJAM-A. Purified fJAM-A ectodomain (1 μg ml^{-1}) in carbonate/bicarbonate buffer (Sigma) was bound to 96-well ELISA plates (100 ng per well) at 4°C overnight. The wells were blocked with PBS containing 0.05%

Tween 20 (PBS-T) plus 0.5% BSA for 1 h at room temperature and washed three times with PBS-T. Two-fold dilutions of purified virus (starting concentration 200 μg ml^{-1}) were prepared in PBS-T + BSA; 100 μl of each dilution of the virus was bound to plates for 3 h on ice. After the plates were washed, bound virus was detected with rabbit anti-FCV-5, followed by HRP-conjugated goat anti-rabbit IgG. Antibodies diluted in PBS-T + BSA were incubated with the plates for 90 min on ice. Following washing, substrate, 2,2'-azino-bis(3-ethylbenzthiazoline-6-sulfonic acid) (Sigma) in a citric acid-sodium phosphate buffer was added to each well and incubated for 60 min at room temperature. Absorbance was measured at 595 nm on a Microplate Biokinetics Reader (BioTek Instruments). The mean ± SE of 3 plates (2 replicates per plate) is shown.

ELISA competitive binding of FCV in the presence of soluble fJAM-A. Purified fJAM-A ectodomain (1 μg ml^{-1}) in carbonate/bicarbonate buffer was bound to 96-well ELISA plates (100 ng per well) at 4°C overnight. The wells were blocked with PBS-T + BSA for 1 h at room temperature and washed three times with PBS-T. Two-fold dilutions of fJAM-A ectodomain were prepared in PBS-T+ BSA with 750 ng purified virus (starting fJAM-A concentration 5.3 μM); 100 μl of each dilution of the fJAM-A/virus mixture was bound to plates for 3 h on ice. Plates were washed, and virus binding detected as described for assay to determine virus binding to fJAM in absence of soluble receptor. Absorbance readings for each virus were normalized, and the mean ± SE of 3 plates (2 replicates per plate) is shown.

Detection of bis-ANS binding to FCV by fluorescence spectroscopy. Purified virus (60 μg ml^{-1}, a 0.5 μM concentration of the FCV VP1 dimer) or 1.5 μM purified receptor (fJAM-A or hJAM-A ectodomain) diluted in virion buffer were incubated in a 400 μL fluorometer cell (Varian) at 37°C for 10 min to allow temperature equilibration. To detect bis-(8-anilinonaphthalene-1-sulfonate) (bis-ANS)

binding to native virus and receptor, bis-ANS was added to the sample to a final concentration of 3 μM. Bis-ANS was excited at 395 nm (slit width 5 nm) and emission collected at 495 nm (slit width 10 nm) at 2 second intervals for 10 min on a Cary Eclipse spectrofluorometer (Varian). To investigate the binding of bis-ANS to preincubated virus and receptor, virus and receptor were mixed and incubated for 10 min at 37°C. Bis-ANS was added (3 μM) and sample readings were performed as detailed above. All spectrofluorometer readings were taken with the photomultiplier tube set at 700 V.

fJAM-A neutralization of a panel of FCV isolates. To investigate the ability of GST-fJAM-A to neutralize a panel of FCV isolates, 1×10^5 p.f.u. of virus in DMEM + 0.1% BSA was incubated with absence or presence (final concentration 45 μM) of soluble GST-fJAM-A at 37°C for 30 min. A plaque assay was used to determine the remaining viral titer of the samples.

Statistical analyses. Analyse-it (Analyse-it Software) statistical analysis add-in for Microsoft Excel was used to perform ANOVA where necessary. Graphs were prepared using Kaleidagraph (Synergy Software) and Adobe Illustrator CS3 (Adobe). Protein images were prepared using PyMOL (DeLano Scientific) (Delano, 2002).

4.4 Results

FCV-5 is neutralized by preincubation with soluble fJAM-A ectodomain at 37°C. Preincubation of nonenveloped viruses such as rhinoviruses and polioviruses with their functional receptors neutralizes virus infectivity (Greve et al., 1991, Kaplan et al., 1990). In a previous study, we showed that preincubation on ice of FCV-5 with a purified soluble GST-fused form of the ectodomain of fJAM-A modestly reduced infectivity (Ossiboff & Parker, 2007); FCV-5 is a field isolate responsible for highly virulent, systemic disease in cats. During these experiments we noted that if the virus-

receptor preincubation was carried out at 37°C rather than 4°C, substantially more infectivity was lost. To quantify the extent to which FCV-5 was neutralized by preincubation with soluble receptor at 37°C and to assess the influence of receptor concentration and the form of soluble fJAM-A ectodomain on neutralization, we preincubated ~ 10^5 p.f.u. of FCV-5 with increasing concentrations of purified GST-fJAM-A or with a soluble form of fJAM-A in which the GST had been removed (sfJAM-A) for 30 min at 37°C. We found a clear relationship between the concentration of soluble receptor and the extent of virus neutralization with concentrations of GST-fJAM-A > 27.5 μM (Figure 4.1) and of sfJAM-A > 2.8 μM (data not shown) causing ~ 250-fold loss of viral titer. Cleavage of GST from the N-terminus of the fJAM-A ectodomain enhanced the ability of the protein to neutralize FCV-5 by 10-fold. As GST was fused to the D1 portion of the ectodomain, which we have shown is necessary for FCV binding, it seems likely that GST sterically hindered the FCV-ectodomain interaction.

As we had previously found only a modest reduction in FCV-5 infectivity when virus and GST-fJAM-A were preincubated at 4°C, we assessed the loss of infectivity following preincubation of virus with sfJAM-A at 4, 16, 20, and 37 °C. We found a temperature-dependence to the loss of infectivity with a 4-fold loss of infectivity at 4°C compared to ~ 250-fold loss of infectivity at 37°C (Table 4.1). We conclude that soluble forms of the fJAM-A ectodomain can substantially neutralize FCV infectivity when preincubated at 37°C and that neutralization is temperature- and concentration-dependent and saturable.

Selection of soluble receptor-resistant (*srr*) mutants of FCV. During the above experiments we found that some residual infectivity always remained after preincubation of FCV-5 with sfJAM-A at 37°C. We hypothesized that resistant mutant viruses were being selected. As we expected that analysis of these mutants would shed

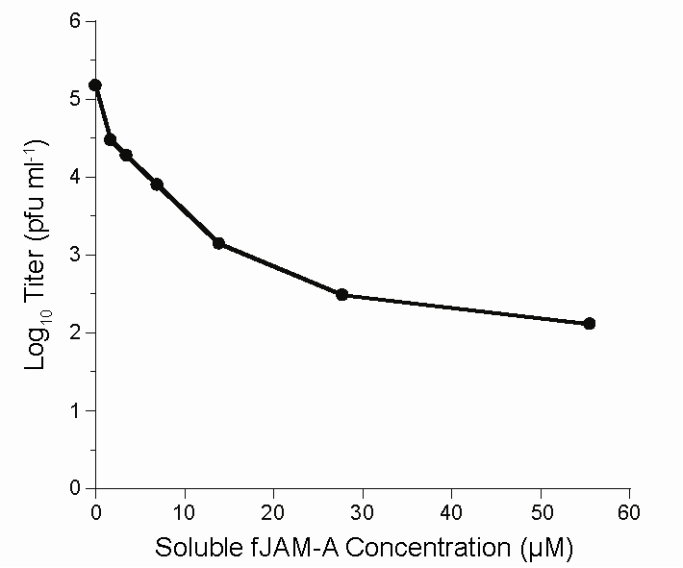

Figure 4.1. Neutralization of FCV-5 by soluble fJAM-A. FCV-5 (~ 1×10^5 p.f.u.) was incubated with varying concentrations of soluble GST-fJAM-A at 37 °C for 30 min. The virus samples were then plaque titrated on CRFK cell monolayers. The results shown indicate the mean and standard deviation of three independent experiments.

Table 4.1. Temperature dependant neutralization of FCV-5

Incubation temperature[a]	Change in log titer ± SD[b]
4°	- 0.6 ± 0.2
16°	- 1.4 ± 0.3
24°	- 2.1 ± 0.2
37°	- 2.4 ± 0.1

[a]All samples were incubated at 4°C for 3 h and then for 30 min at the temperature indicated

[b]Change in log titer (pfu/ml; as determined by plaque assay on CRFK cells) of ~1 × 10^5 p.f.u. of virus incubated with 4.4 μM sfJAM-A from samples incubated with buffer alone, ± standard deviation of at least three replicates.

light on possible capsid residues important in binding to fJAM-A or receptor-induced conformational changes in the capsid associated with neutralization, we selected 24 mutants that were resistant to preincubation with the soluble receptor. All of the mutants contained one or two point mutations within the capsid protein (Table 4.2) giving a total of 20 unique mutations. Three of these mutations were present in the leader sequence of the capsid, which is cleaved from the capsid precursor protein during capsid assembly by a virus-encoded proteinase (Carter et al., 1992, Neill et al., 1991, Sosnovtsev et al., 1998); however, all of the mutants that contained mutations in the leader sequence also had an additional mutation in another region of the capsid protein. Several residue changes were found in more than one mutant. These changes were at positions G329 (3 mutants), T438 (2 mutants), K480 (3 mutants), V516 (5 mutants), and K572 (2 mutants). These findings indicated that *srr* mutants of FCV-5 were readily obtained and propagated in vitro.

Overview of the crystal structure. In order, to map the location of *srr* mutations on the capsid we determined the crystal structure of FCV-5 at 3.6 Å resolution by molecular replacement and real space averaging (Figure 4.2). The structure was refined to a crystallographic R-factor of 0.37 (R_{free}=0.39) at 3.6 Å

Table 4.2. Identification of capsid mutations in *srr* mutants

Mutation[a]	Number of Mutants
A168S + F486L	1
T202A + T447I	1
G329D	1
G329S	1
D15N + G329S	1
E401K	1
D434N + I661T	1
T438I	1
T438A	1
N443S	2
I94T + S465N	1
K480R	1
K480Q	1
K480E + N483S	1
V516I	2
V516A	3
P116T + I535V	1
K572E	1
K572Q	1
I94T + Y575H	1

[a]Mutations are identified by the wild-type amino acid, amino acid position, and mutant amino acid.

resolution. As in other T=3 viruses, the icosahedral asymmetrical unit consisted of three independent but chemically identical subunits (Fig. 2B). These subunits are traditionally designated as A, B and C. The present model of the FCV-5 icosahedral asymmetrical unit consist of residues 129-662 of the A and C subunit, and 133-662 of the B subunit.

The polypeptide fold. The structure of each subunit comprises an NTA, an S domain and a P domain, similar to that seen in the recombinant Norwalk virus capsid (rNV) and SMSV-4. Residues 170-329 fold into a canonical eight-stranded beta-barrel structure, which has been seen in rNV, SMSV-4 and many other viral capsid proteins. These eight strands, conventionally denoted as B-I, form two four-stranded sheets,

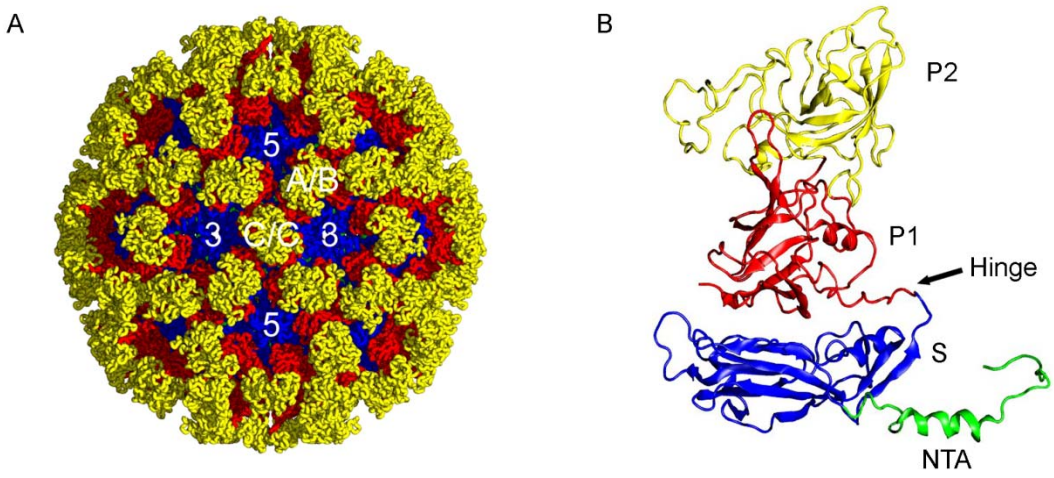

Figure 4.2. X-ray structure of Feline Calicivirus (FCV-5) capsid. (A) The X-ray structure of FCV-5 viewed along the icosahedral two fold axis. Location of a set of A/B and C/C dimers and icosahedral 5-fold and 3-fold axes are shown. (B) A ribbon representation of the B subunit structure. The N-terminal arm (NTA) (green), S domain (blue), and P1 (red) and P2 (yellow) sub-domains are indicated.

BIDG and CHEF. Two α helixes are situated between strands C and D and strands E and F, respectively. Structural comparison of the S domains of FCV-5 and SMSV-4 revealed that the most significant variations were located in the loop region connecting strands E and F.

The P domain of FCV-5 is comprised of residues 330-662 and is linked to the S domain by a flexible hinge. The P domain is further divided into two sub-domains: P1 and P2. The P1 sub-domain, consisting of two segments of polypeptide (residues 330-381 and 551-662), folds into a structure similar to that seen in that of SMSV-4. The P2 sub-domain, the outermost portion of the capsid protein, has been considered as a large insertion into the P1 sub-domain. In the P2 sub-domain, both SMSV-4 and FCV-5 form a compact barrel structure consisting of six strands, sequentially labeled as A'-F' (Figure 4.3 A&B). However, the six strands in FCV-5 vary in length and relative orientation, compared to their counterparts in SMSV-4. These six strands are connected by loops of various lengths. Structure superimposition showed that loop C'D' in FCV-5 is significantly shorter than that of SMSV-4 (Figure 4.3C). The P2 sub-domain consists of residues 382-550 and contains 7 fewer residues than that of SMSV-4. Structural comparison showed that those "inserted" residues are mainly distributed in the loop connecting strands C' and D'.

Structural comparison between different subunits. Pair-wise superposition calculations indicated that the structure of the P domain of FCV-5 adopts a very similar structure in all three subunits. The S domain, however, shows larger variations between the different subunits to facilitate the assembly of a T=3 capsid. In addition, the A and C subunits have 4 more disordered N-terminal residues than the B subunit. Superposition of the whole subunit structure revealed that the A subunit forms a more compacted structure, as evidenced by the closer association of the S and P domains. The interactions between the S and P domains are less prominent in the B subunit,

Figure 4.3. Ribbon representation of the P2 sub-domain in FCV-5 (A) and SMSV-4 (B). The β-strands are labeled from A' to F' in each case. (C) The superposition of the P domain of FCV-5 (red) and SMSV-4 (blue) shows that the six β-strands in the P2 sub-domains are similarly spatially arranged into a compact barrel, despite the low sequence similarity. (C-E) Positions of conserved residues and antigenic sites on the P2 sub-domain of the C/C dimer of FCV-5. (D) Neutralizing epitopes mapped on P2 (grey). Antigenic sites (Ags1-4; colored pink) represent B-cell linear epitopes identified by Radford *et al* (Radford et al., 1999). Monoclonal antibody escape mutations identified by Tohya *et al* are colored red (Tohya et al., 1997). (E) Degree of conservation of surface-exposed residues on the P2 sub-domain as predicted by Consurf 3.0. Solid yellow line indicates dimer interface; dotted yellow line indicates axis of conservation. (F) Locations of N-terminal and C-terminal HVRs, region C and central conserved portion of region E mapped on surface of P2 sub-domain.

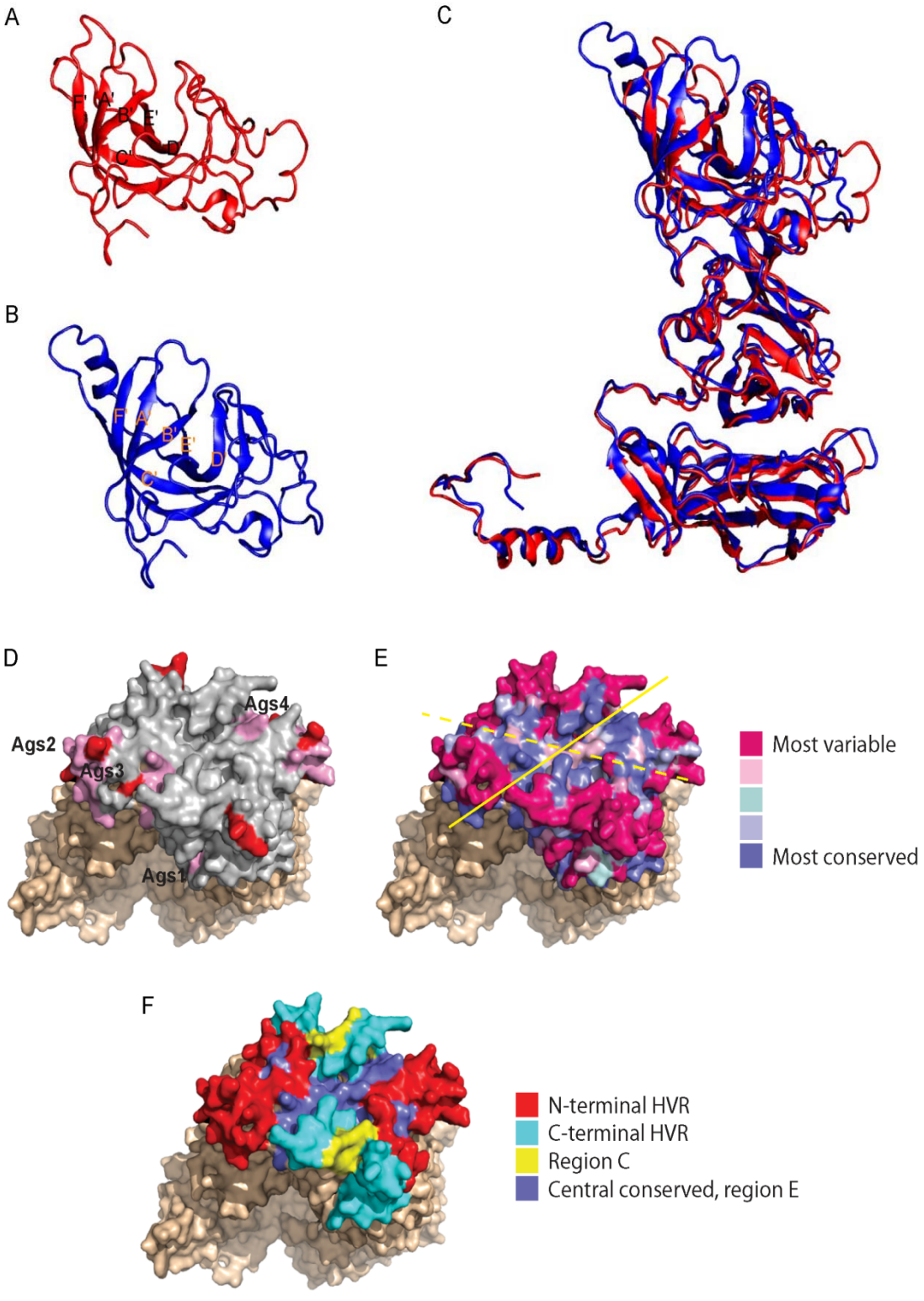
A
F'
A'
B'
E'
C'
D'
B
F'
A'
B'
E'
D'
C'
C
D
Ags4
Ags2
Ags3
Ags1
E
Most variable
Most conserved
F
N-terminal HVR
C-terminal HVR
Region C
Central conserved, region E

resulting in a more relaxed structure. The C subunit has the most open conformation, with the fewest interactions between the S and P domains. These differences contribute to the bent and flat conformations of the A/B and C/C dimers, respectively, as has been seen in the SMSV-4 and rNV structures.

Mapping of neutralizing epitopes and conserved surface regions on the P2 sub-domain of FCV-5. Hypervariable regions (C and E regions) of the FCV capsid sequence have been previously identified and neutralizing epitopes have been mapped to residues within the E region predominantly (Figure 4.3F) (Radford et al., 1999, Seal & Neill, 1995, Tohya et al., 1991, Tohya et al., 1997). Using the FCV-5 structure we mapped the location of 4 linear B-cell epitopes identified in FCV-F9 using a peptide library (Radford et al., 1999). All of these sites lie on the margins of the P2 sub-domain with one site, Ags4, at the dimer interface (Figure 4.3D). Similarly, the location of antibody escape mutations found in mutants of FCV-F4 are also located on the margins of the P2 sub-domain within hypervariable regions (Figure 4.3D) (Tohya et al., 1997). To more accurately assess the conservation of individual surface-exposed residues on the P2 sub-domain, we used CONSURF 3.0, which maps the rate of evolution as determined by an empirical Bayesian estimation among homologous proteins onto the 3-D structure (Landau et al., 2005). As input we used an alignment of 47 different FCV capsid sequences to derive an evolutionary conservation score that was used to color code individual residues on the surface of the FCV-5 capsid structure (Figure 4.3E). This analysis revealed a patchwork of conserved surface residues along the dimeric interface of the P domain that also extended laterally at a 45° angle to the dimer interface on the surface of each monomer (Figure 4.3E). This patch of conserved residues was surrounded by highly variable residues on the margins of the P2 sub-domain (Figure 4.3E).

Mapping *srr* mutations on the FCV-5 structure. Sequencing of the capsid protein of the 24 *srr* mutants revealed 17 unique amino acid changes from the parental FCV-5 mature capsid protein sequence. We mapped the location of these changed residues on the structure of FCV-5 (Figure 4.4). Three mutations were found in the NTA and S domains, and 14 mutations were present in the P domain (Figure 4.4A). Of the 24 mutants investigated, 21 (87.5%) contained mutations that mapped to the P domain of the capsid, and 18 of those mutations were to residues within the P2 sub-domain.

Of the mutations found in the NTA and S domains, one change was to a residue (A168S) within the NTA, but this mutation was accompanied by a second amino acid change in the P2 domain (F486L). Similarly, a mutant with a change in the shell domain (T202A) also had a change in the P2 domain (T447I). Three *srr* mutants contained mutations at residue G329 in the shell domain on a loop that connects the shell with the protrusion domain. Residues G329 is located at the point of the flexible hinge, and mutations at G329 (D/S) were present alone or in addition to a change in the leader sequence of the capsid (D15N) (Figure 4.4B, Table 4.2). Mutations to residue G329 were the only changes identified that occurred independently of an additional mutation within the P domain.

Three of the 21 mutated residues identified in the P domain were present within P1 sub-domain (K572E/Q, Y575H, and I661T). Residues K572 (E, Q) or Y575 (H) were buried at the dimer interface of the capsid structure (Figure 4.4B). Residue I661 was located at the base of the P1 sub-domain, in close proximity to the S domain (Figure 4.4B); the mutant containing the I661T change also had a second change within the P2 domain (D434N). The other 11 P domain mutations were in the P2 sub-domain. Eight of these mutated residues were within surface-exposed loops of P2: E401K, D434N, T438A, N443S, T447I, S465N, K480R/Q/E, V516I/A, and I535V

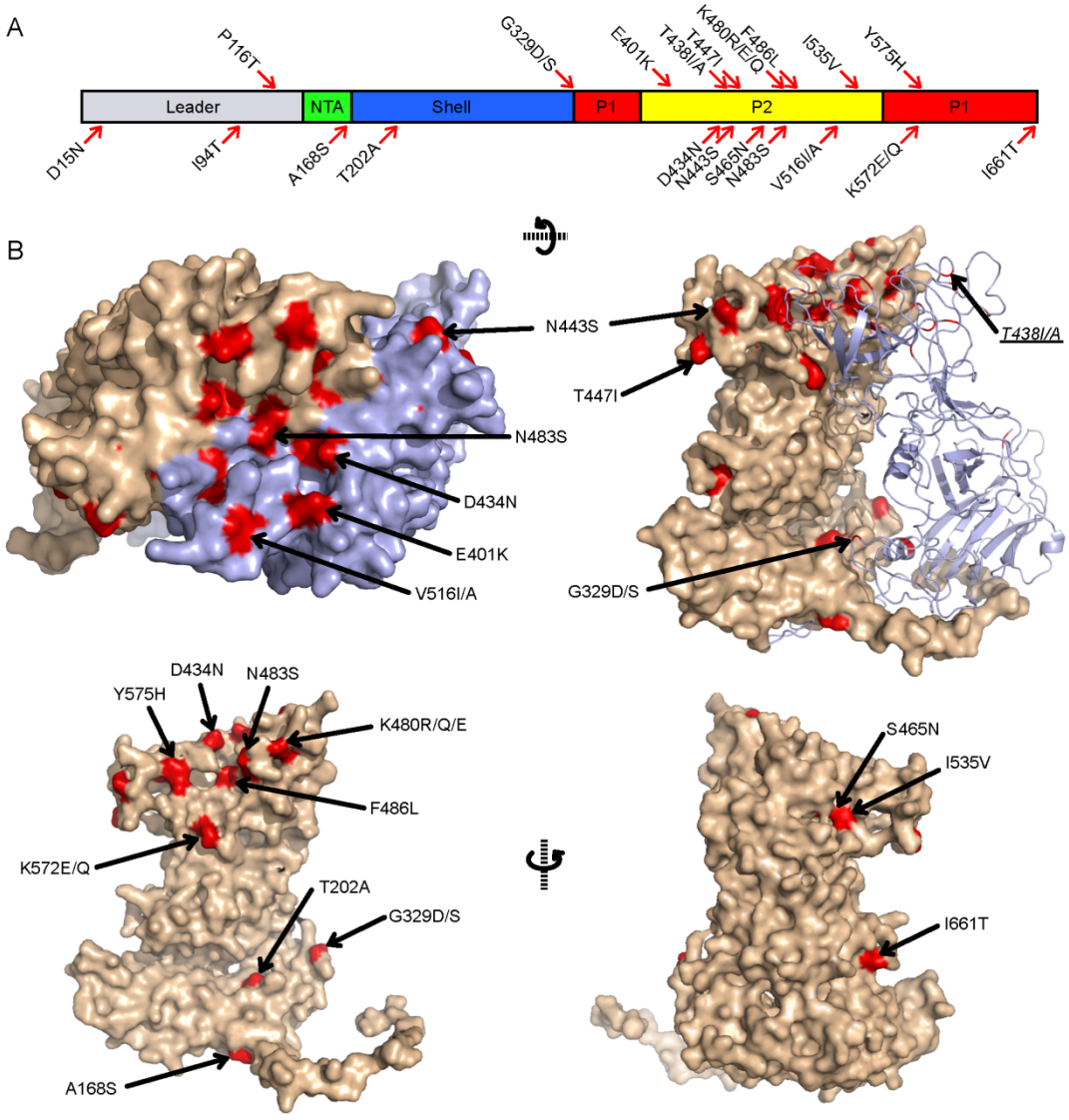

Figure.4.4. Position of mutations found in *srr* mutants in the structure of FCV-5. (A) The residues mutated in the *srr* mutants are illustrated on a schematic of the FCV capsid protein. The location of the different structural domains in the primary capsid sequence is indicated. (B) The location of the mutations in the FCV-5 atomic resolution structure.

(Figure 4.4B). Three of these surface-exposed residues were mutated in more than one *srr* mutant: N443 (2 mutants), K480 (3 mutants), and V516 (5 mutants). Two mutants had mutations to residues at the P2 dimer interface; one mutant possessed a change in the surface-exposed residue N483 (S), while another mutant contained a change to the buried residue F486 (L). Lastly, two mutants had mutations to residue T438 (I,A) that is buried in the present structure and maps to a loop near the surface of the P2 sub-domain. In summary, the location of mutations present in *srr* isolates mapped to three general regions of the structure of FCV-5: (i) Surface-exposed residues on the P2 domain; (ii) residues that are buried or not easily accessible from the surface of the capsid; and (iii) the hinge region of the capsid.

***srr* mutants are resistant to neutralization by sfJAM-A, but retain the capacity to bind fJAM-A and require cellular fJAM-A for infection.** From the original 24 *srr* mutants, we selected a representative subpanel of 8 mutant viruses to further characterize; All of these 8 mutant viruses were resistant to neutralization with sfJAM-A (Figure 4.5). To verify that the eight selected *srr* mutants still bound to fJAM-A expressed on the cell surface, we used flow cytometry to measure the capacity of each of the mutants to bind to fJAM-A expressed on the surface of CHO-S cells (Figure 4.6). We found that all of the mutants bound to CHO-S cells expressing fJAM-A. One of the mutants, K572E, however, bound to 50% fewer cells than the parental FCV-5. All of the mutants still required fJAM-A as a functional receptor, as pretreatment of CRFK cells with a rabbit antiserum against fJAM-A completely blocked infection by the mutants. We conclude from these findings that the subpanel of 8 *srr* mutants still bind and require cellular fJAM-A for cell infection.

At low multiplicity of infection, the growth of some *srr* mutants differs from parental FCV-5. To evaluate if the growth properties of the *srr* mutants differed

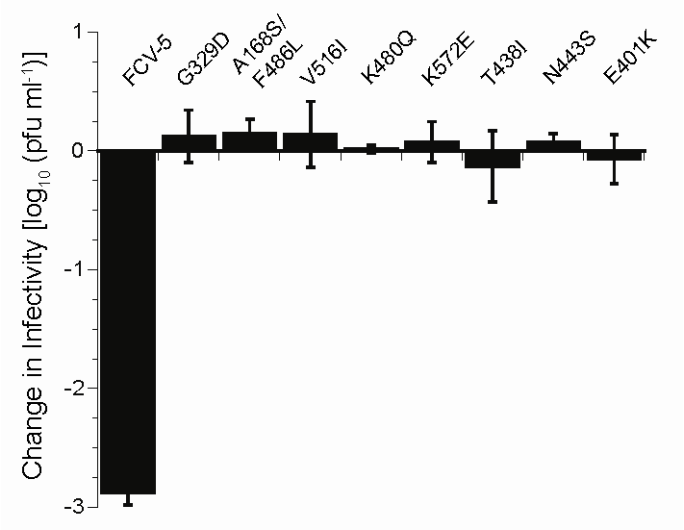

Figure 4.5. Neutralization of *srr* mutants by soluble fJAM-A. A subpanel of 8 *srr* mutants and FCV-5 (1×10^5 p.f.u.) were incubated in the presence or absence soluble GST-fJAM-A (55 μM) at 37 °C for 30 min. The infectivity of each sample was assayed by plaque-titration. The change in log titer was calculated by subtracting the titer of samples incubated with receptor from samples incubated without. The mean change in $\log_{10}$ titer ± SD of three replicates of a representative experiment is shown.

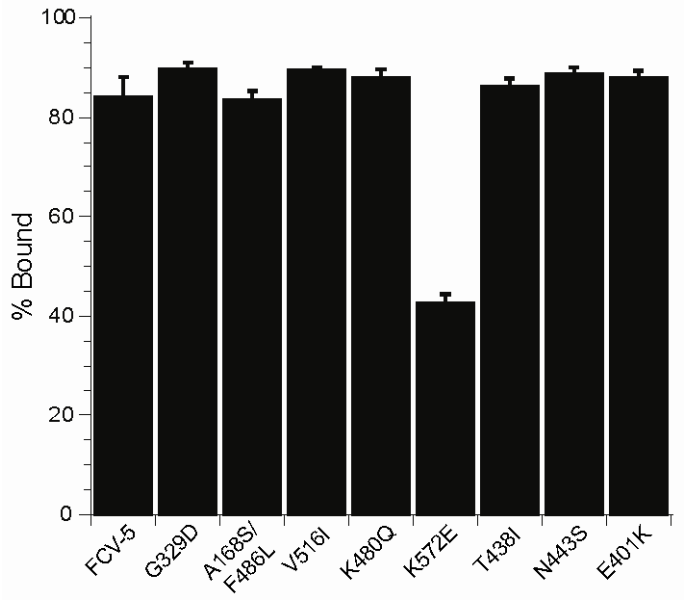

Figure 4.6. Binding of *srr* mutants to CHO cells expressing fJAM-A. Non-permissive CHO-S cells were transfected with a DNA construct encoding fJAM-A. At 24 h p.t. FCV (MOI = 5) was adsorbed to the cells on ice for 30 min. After washing with cold PBS to remove unbound virus, the cells were fixed and bound virus and cell surface fJAM-A were detected with mouse anti-FCV MAb and rabbit anti-fJAM-A antibodies, followed by Alexa 488-conjugated goat anti-mouse IgG and Alexa 647-conjugated goat anti-rabbit IgG. Virus binding and receptor expression were analyzed by flow cytometry. Virus binding was assayed by determining the percentage of fJAM-A-positive cells that bound virus. The means of 3 independent experiments (2 samples of 1×10^4 cells per experiment) ± SE are shown.

from the parental FCV-5, we generated single- and multiple-cycle growth curves for each of the eight selected *srr* mutants. The growth kinetics and final yields following a single replicative cycle (MOI = 5) for the mutant viruses were similar to the parental FCV-5 (Figure 4.7A). However, we found that during multiple replicative cycles (MOI= 0.01) there was a significant difference between the growth kinetics of the parental FCV-5 and six of the *srr* mutants at 4 h p.i. (Figure 4.7B). Two of the eight mutants (K480Q and A168S/F486L) were similar to FCV-5 producing new infectious virions by 4 h p.i. In contrast, the other 6 *srr* mutants had decreased infectivity at 4 h p.i., indicating that the production of infectious virus particles was delayed; the observed decrease for the 6 mutants was statistically different from FCV-5 as determined by ANOVA ($P < 0.005$). By 8 h p.i., all of the viruses had attained similar increases in titer, and the final virus yields were all similar. We conclude that 6 of the panel of 8 *srr* mutants analyzed have slower growth kinetics than the parental FCV-5 in cells infected at a low multiplicity.

Binding of *srr* mutants to fJAM-A. In order to assess the kinetics of binding of the *srr* mutants to fJAM-A, we purified three mutants (G329D, V516I, and K572E) and investigated their *in vitro* binding to plate-bound soluble fJAM-A in comparison to parental FCV-5 by ELISA (Figure 4.8A). All of the viruses showed saturable concentration-dependent binding to fJAM-A. The binding kinetics of FCV-5 and G329D were similar and saturation of binding to fJAM-A occurred at a similar concentration of virus. We found slight differences in the kinetics of binding of mutants V516I and K572E from those of FCV-5 and G329D with saturable binding occurring at higher concentrations of virus. We conclude that the three *srr* mutants investigated (G329D, V516I, and K572E) and FCV-5 all bind immobilized recombinant fJAM-A with relatively similar kinetics under *in vitro* conditions.

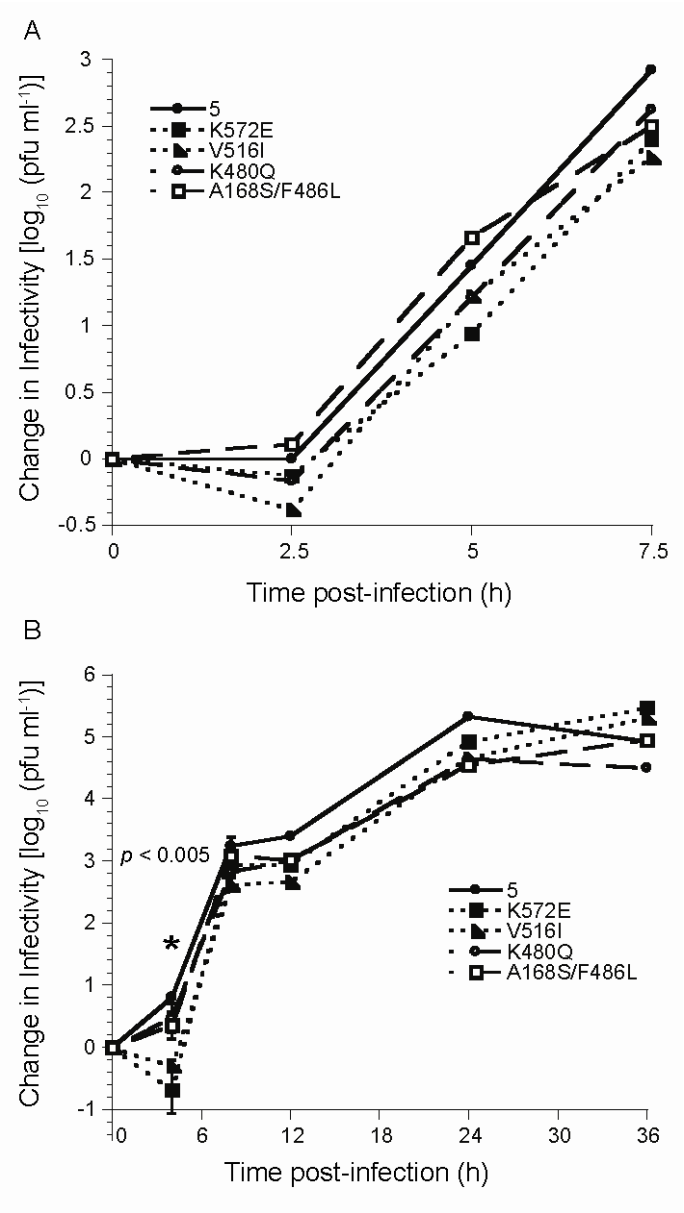

Figure 4.7. Growth of *srr* mutants. CRFK monolayers were infected with FCV-5 and the indicated *srr* mutants under (A) single- (MOI = 5) or (B) multiple- (MOI = 0.01) cycle conditions. The change in virus titer was determined by plaque assay. The mean $\log_{10}$ titer ($\log_{10}$ titer at each time point - $\log_{10}$ titer at T = 0) for each time point is shown; the error bars shown at 4 and 8 h p.i. for the multiple cycle growth represent the standard deviation of 4 replicates. The asterisks indicate significant differences between viral isolates as determined by ANOVA at these time points.

Figure 4.8. Binding of *srr* mutants to immobilized fJAM-A in (A) the absence or (B) presence of increasing concentrations of sfJAM-A. ELISA plates were coated with 100 ng of sfJAM-A ectodomain. Varying concentrations of purified FCV-5 and *srr* mutants G329D, V516I, and K572E were incubated with the immobilized protein for 3 h on ice. To investigate the effect of soluble fJAM-A on the binding of virus to immobilized receptor, 750ng of each virus and varying concentrations of soluble receptor were incubated together with plate-bound fJAM-A for 3 h on ice. Bound FCV was detected with rabbit anti-FCV serum, followed by HRP-conjugated goat anti-rabbit IgG. Colorimetric HRP substrate was added, and the amount of bound FCV-5 was quantified by absorbance at 595 nm. The means of 3 and 4 plates, respectively (2 replicates per plate) ± SE are shown. ANOVA was performed on three concentrations of soluble receptor (0.04, 0.33, and 2.7 μM) to determine statistical differences; significant differences between isolates at these concentrations are indicated by asterisks.

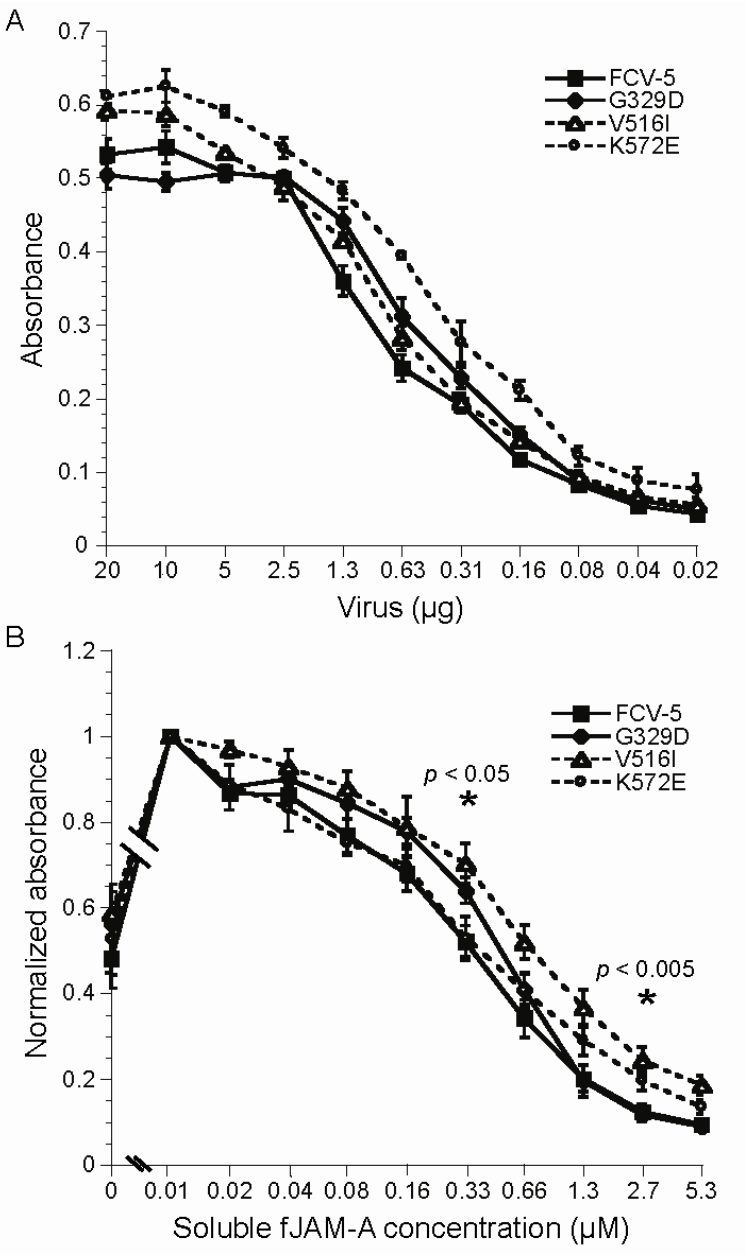
A
0.7
0.6
0.5
0.4
0.3
0.2
0.1
0
Absorbance
FCV-5
G329D
V516I
K572E
20 10 5 2.5 1.3 0.63 0.31 0.16 0.08 0.04 0.02
Virus (µg)
B
1.2
1
0.8
0.6
0.4
0.2
0
Normalized absorbance
FCV-5
G329D
V516I
K572E
p < 0.05
*
p < 0.005
*
0 0.01 0.02 0.04 0.08 0.16 0.33 0.66 1.3 2.7 5.3
Soluble fJAM-A concentration (µM)

Relative affinities of *srr* mutants for fJAM-A. To determine if the purified *srr* mutants (V516I, K572E, and G329D) differed from FCV-5 in their affinity for fJAM-A, we performed a competition ELISA experiment (Figure 4.8B). Different concentrations of soluble fJAM-A were used to complete for binding of FCV to plate-bound fJAM-A at 4°C. We found that attachment of FCV to the plate-bound receptor was strongly inhibited at the highest concentrations of soluble fJAM-A. The binding of FCV to plate bound fJAM-A correlated inversely to the concentration of soluble receptor. A 50% decrease in binding of all of the different viruses to plate-bound fJAM-A occurred at concentrations of soluble fJAM-A of between 0.33 and 0.66 μM. All of the viruses exhibited similar competition curves; however, binding of mutant V516I to plate-bound fJAM-A was 50% inhibited at a slightly higher concentration of soluble fJAM-A as can be seen by the rightward shift in the competition binding curve (Fig. 8B). Statistical analysis (ANOVA) at three concentrations of soluble receptor (0.04, 0.33, and 2.7 μM) showed significantly more viral binding of mutant V516I than FCV-5 for all but the lowest concentration of receptor ($P < 0.05$). Interestingly, we found that preincubation of virus with low concentrations of soluble fJAM-A significantly enhanced binding to plate-bound fJAM-A when compared to virus alone (see discussion). In conclusion we show that the *srr* mutants G329D, V516I, and K572E demonstrate similar affinities for fJAM-A.

Bis-ANS binding reveals a change in FCV following preincubation with soluble fJAM-A. We hypothesized that the interaction of soluble receptor with FCV caused a change in conformation of the viral capsid. We, therefore, used binding of bis-ANS as a probe to investigate changes in hydrophobicity that occurred upon interaction of FCV with fJAM-A in solution. Bis-ANS is a fluorophore that binds to exposed hydrophobic regions of protein molecules (Rosen & Weber, 1969). The sequestration of bis-ANS in hydrophobic pockets of proteins is accompanied by a

large increase in the fluorescence quantum yield of the probe. Thus, bis-ANS can be used to probe for structural changes in viral proteins that are accompanied by changes in surface hydrophobicity (de Sousa et al., 1999, Ferreira et al., 2004, Gaspar et al., 1997). We first preincubated virus or receptor alone in a cuvette in the spectrofluorometer at 37° C for 10 minutes and then added bis-ANS and collected fluorescence intensity readings over a period of 10 minutes at 37°C (Figure 4.9A&B). To quantify differences in bis-ANS fluorescence, we waited until the fluorescence emission readings had stabilized and then averaged the fluorescence intensity measurements over 1 minute. We recorded an increase in fluorescence intensity during the first 5-10 minutes after addition of bis-ANS to any of the protein samples; The fluorescence intensity stabilized by 10 min post-addition. This increase in fluorescence is likely caused by bis-ANS binding to surface-exposed hydrophobic pockets on the proteins (Figure 4.9 A,B).

To determine if the interaction of FCV with fJAM-A triggered a conformational change that would change the binding of bis-ANS to the proteins, we preincubated FCV with either hJAM-A [hJAM-A does not bind FCV (Ossiboff & Parker, 2007); Figure4. 9 A,C] or fJAM-A (Figure 4.9B,D) at 37°C for 10 minutes, then added bis-ANS and monitored changes in fluorescence intensity over 10 min. We found that the average stabilized bis-ANS fluorescence intensity of samples containing FCV-5 plus hJAM-A was equal to the sum of the intensities associated with incubation of bis-ANS with FCV-5 and hJAM-A individually (dotted line; Figure 4.9C). These findings were expected and indicate that the overall binding of bis-ANS to either protein was unchanged when they were mixed. In contrast, the average stabilized fluorescence intensity of samples containing FCV-5 plus fJAM-A was greater than the sum of the bis-ANS fluorescence intensities of the two proteins when incubated individually (Figure 4.9D). We found similar results for the three *srr*

Figure 4.9. Changes in bis-ANS binding upon interaction of FCV with sfJAM-A. At zero time, bis-ANS was added to the indicated purified virions, soluble JAM-A [(A) human or (B) feline], or virions preincubated with JAM-A. Fluorescence was recorded every 2 sec continuously for 10 min at excitation and emission wavelengths of 395 and 495nm, respectively. (C, D) Stabilized fluorescence intensities measured during the last minute for each sample were averaged. Dotted lines indicate the additive average fluorescence intensity measured for both native virus and receptor. The means ± SE (n = 3) are shown.

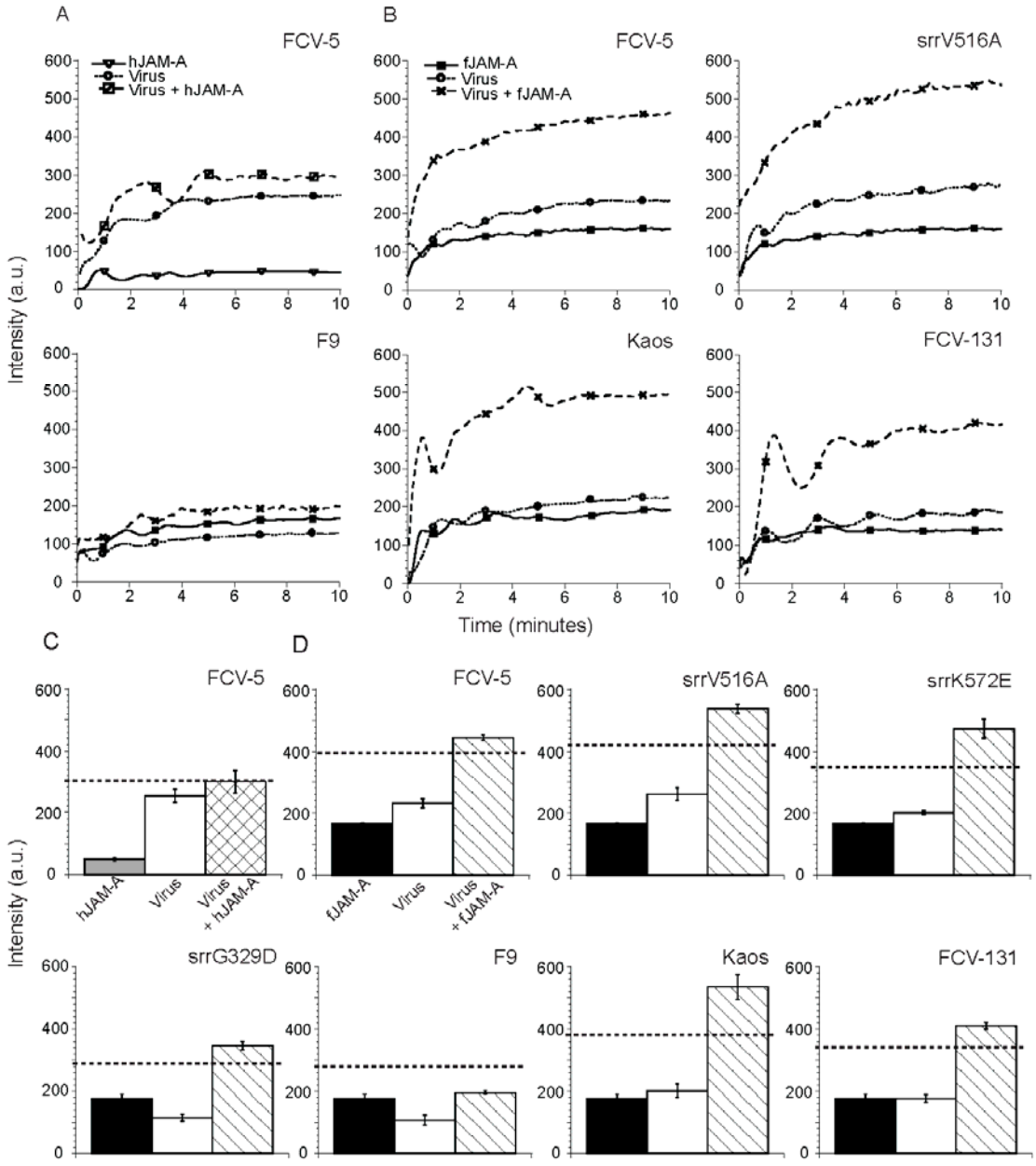
A
FCV-5
hJAM-A
Virus
Virus + hJAM-A
B
FCV-5
fJAM-A
Virus
Virus + fJAM-A
srrV516A
F9
Kaos
FCV-131
Intensity (a.u.)
Time (minutes)
C
D
FCV-5
FCV-5
srrV516A
srrK572E
hJAM-A
Virus
Virus + hJAM-A
fJAM-A
Virus
Virus + fJAM-A
srrG329D
F9
Kaos
FCV-131

mutants (V516A, K572E, and G329D) and two field isolates (Kaos and FCV-131) tested. These findings suggested that an interaction between virus and fJAM-A had changed the conformation of one or both proteins such that more bis-ANS bound. In contrast, incubation of the vaccine strain F9 with fJAM-A led to a fluorescence intensity maximum that was less than what would be expected from the sum of the intensities associated with each protein individually indicating an overall decrease in the available binding sites for bis-ANS. From these findings we conclude that interaction of fJAM-A with FCV at 37°C leads to changes in the binding of bis-ANS that are indicative of changes in hydrophobicity of virus and/or receptor.

Not all FCV isolates are neutralized by sfJAM-A. The FCV-5 isolate that we used to select for *srr* mutants was recovered from a cat suffering from severe systemic disease. As this form of FCV disease is uncommon we hypothesized that not all isolates of FCV would be neutralized by incubation with soluble fJAM-A at 37°C. To test this hypothesis, we incubated ~10^5 p.f.u. of 6 additional FCV isolates with 45 μM GST-fJAM-A at 37°C; these virus isolates included the vaccine strain F9, two additional isolates from cats suffering from virulent systemic disease, the FCV-Urbana isolate and three other field isolates recovered from cats with mild to moderate severity FCV disease. We found several additional FCV isolates that were neutralized by preincubation with sfJAM-A at 37°C; however, the vaccine strain F9, FCV-Urbana and the two isolates recovered from animals with milder disease were not neutralized under these conditions (Figure 4.10). We conclude that there are natural differences among FCV isolates in their responses to incubation with sfJAM-A at 37°C.

4.5 Discussion

Nonenveloped viruses must deliver their genetic material across the membranous barrier surrounding the host cell. Unlike enveloped viruses which

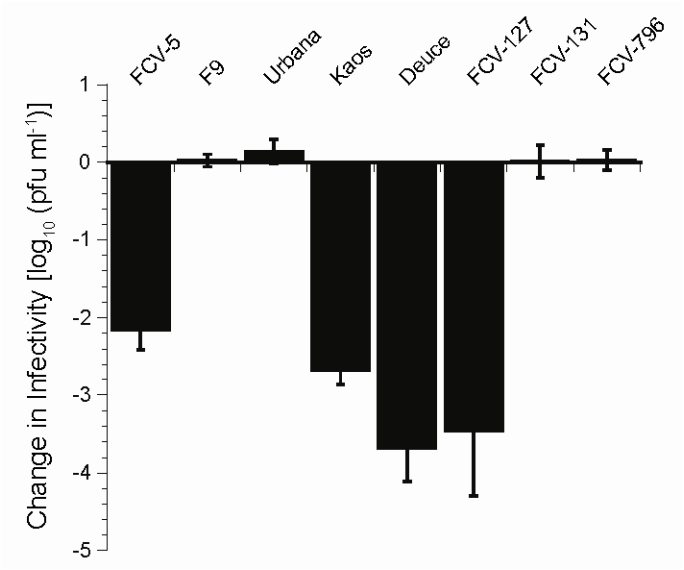

Figure 4.10. Ability of soluble fJAM-A to neutralize select FCV isolates. A panel of 6 FCV field isolates (FCV-5, Kaos, Deuce, FCV-127, FCV-131, and FCV-796) and 2 tissue culture adapted strains (F9 and Urbana) (1×10^5 p.f.u.) were incubated in the presence or absence soluble GST-fJAM-A (45 μM) at 37 °C for 30 min. The remaining infectivity in each sample was assayed by plaque titration. The change in log titer was calculated by subtracting the titer of samples incubated with receptor from samples incubated without. The mean change in $\log_{10}$ titer ± SD (n = 4) is shown.

possess a lipid membrane and enter host cells by promoting fusion of the viral and host membranes, nonenveloped viruses must disrupt cellular membranes to deliver the intact capsid or their genome into the interior. Here we present genetic and biological evidence indicating that feline calicivirus, a nonenveloped member of the *Caliciviridae*, undergoes structural rearrangements following interaction with its cellular receptor, fJAM-A that for some isolates lead to virus inactivation.

Several nonenveloped viruses including human rhinoviruses, polioviruses, and hepatitis A virus are neutralized by preincubation with their functional receptors (Kaplan et al., 1990, Marlin et al., 1990, Silberstein et al., 2001). However, the extent to which infectivity is lost at physiologic temperatures differs. For polioviruses and some human rhinoviruses, the receptor can induce irreversible conformational changes that inactivate the virus (Colston & Racaniello, 1994, Greve et al., 1991). Reductions in titer following preincubation with receptor can also be more modest and can be explained by competitive inhibition of cell surface receptor binding as occurs for rabies virus and its cellular receptor neurotrophin (Langevin & Tuffereau, 2002). These differences reflect different mechanisms of receptor-mediated neutralization. Greve et al (1991) described three mechanisms of receptor-mediated neutralization for human rhinoviruses. One mechanism involves simple competition of soluble receptor for receptor binding sites on cells. A second mechanism involved a receptor-mediated reversible conformational change that prevented infection. A third mechanism was that virus-receptor interaction led to irreversible capsid changes that were incompatible with infection (Greve et al., 1991). Differences between serotypes in the effects of soluble ICAM-1 receptor on neutralization of rhinoviruses were subsequently recognized (Hoover-Litty & Greve, 1993). Similarly, we found that some, but not all isolates of FCV were neutralized by preincubation with a soluble form of fJAM-A. The molecular events that result in FCV neutralization are unknown.

While it is possible that the mechanism of neutralization is due to steric hindrance or occupation of receptor binding sites, the prominent temperature-dependent nature of the process strongly suggests that receptor-induced conformational changes are a contributing factor. Receptor-induced conformational changes in human rhinoviruses and poliovirus are temperature-dependent (Gomez Yafal et al., 1993, Hoover-Litty & Greve, 1993). Polioviruses undergo an irreversible transition from a 160S to a 135S particle when they are incubated with soluble receptor at 37°C; this reaction has a clear temperature threshold with little to no neutralization occurring at temperatures below 33 °C (Gomez Yafal et al., 1993, Tsang et al., 2001). In contrast, although FCV-5 receptor-mediated neutralization was clearly temperature-dependent, there was no obvious temperature threshold, but rather a gradual diminishment of the neutralizing effect as the temperature decreased from 37°C to 4°C.

Analysis of soluble receptor (*srr*) mutants in poliovirus and murine coronavirus identified virus residues that either directly or indirectly facilitated receptor binding (Colston & Racaniello, 1994, Kaplan et al., 1990, Saeki et al., 1997). Of the 24 *srr* mutants FCV-5 we isolated for FCV-5, mutations to 20 unique residues were identified. Many of these mapped to surface exposed residues on top of the P2 domain of the capsid; however, several mutated residues were buried in or inaccessible from the surface of the structure. These findings are similar to those for poliovirus *srr* mutants, which contained mutations to both internal and surface exposed residues. The mutated residues for poliovirus mapped to a hydrophobic pocket in the structure. It is believed that changes to residues in this hydrophobic pocket regulate receptor attachment and conformational changes within the virus particle (Colston & Racaniello, 1994, Racaniello, 1996).

Mutations at some capsid residues were found in more than one of the panel of srr mutants we examined, suggesting that these residues are within critical regions of

the capsid that are necessary for structural flexibility or receptor interactions. Residue G329, mutated in three *srr* mutants, is located in a short loop between the S and P domains of the capsid protein; this loop is hypothesized to be a flexible hinge that allows for movement of the P domain in relation to the S domain. The flexible hinge region is common to all *Caliciviruses*. Cryo-electron microscopy reconstructions of murine norovirus in complex with neutralizing Fab fragments show that this hinge region is extended, moving the P domain up off of the surface of the shell domain (Katpally et al., 2008). In addition, a recent cryo-electron microscopy structure of FCV F9 complexed with the fJAM-A ectodomain indicated that compared to the uncomplexed capsid, the P domain of capsid bound to fJAM-A moved with respect to the S domain and suggested that hinging was required for this movement (Bhella et al., 2008). Our findings support the hypothesis that flexibility in this hinge region is important to permit conformational changes of the structural domains of the calicivirus capsid in relation to each other and indicate that this region actively moves during receptor interactions. Moreover our findings indicate that changes at residue G329 can radically alter the susceptibility of FCV to neutralization by soluble receptor.

As shown here for the structure of FCV-5, dimers are formed between the P domains of FCV capsid proteins. Intriguingly, residues at the P domain dimer interface were mutated in several *srr* mutants. It is not immediately clear how these changes would impart resistance to neutralization. One possibility, however, is that following binding to fJAM-A, the dimer interface of the P domain opens and residues that are normally buried are exposed. Mutant K572E is in the P1 domain and is relatively inaccessible from the surface of the capsid. This mutant had decreased binding to cell surface expressed fJAM-A. However, *in vitro* binding assays using purified virus and receptor indicated that the mutant possessed similar binding kinetics to both the parental FCV-5 and the two other *srr* mutants investigated. For the cell-

based assay, a monoclonal antibody was used to detect FCV binding, while a polyclonal antibody was used for the plate-based assays. It is possible, therefore, that the mutant K572E has an altered epitope that results in decreased recognition by the monoclonal antibody. An alternative possibility is that the results of the cell expressed assay, in which all receptors are oriented properly, is truly indicating a difference in the recognition and binding of mutant K572E to the receptor.

An obvious mechanism by which the srr mutants might avoid neutralization would be to have altered binding to fJAM-A and we expected to identify *srr* mutants that contained mutations which conferred altered receptor binding properties. One surface exposed residue, V516, was mutated in 5 *srr* mutants. While the binding of mutant V516I was not altered in the cell-based binding experiments, it did demonstrate higher affinity for immobilized fJAM-A in the presence of higher concentrations of soluble fJAM-A (see Fig. 8B). However, neither of the other two *srr* mutants used to investigate *in vitro* binding kinetics displayed altered kinetics from the parental strain. These results are in contrast to the findings for poliovirus, where all the reported *srr* mutants demonstrated a reduction in binding affinity (Colston & Racaniello, 1994). It is surprising that none of our *srr* mutants showed a substantive change in binding to fJAM-A as many of the mutations map to surface regions of the capsid that overlap with the receptor binding site predicted by Bhella *et al* (Bhella et al., 2008).

Another unexpected observation was that the binding of purified FCV to immobilized fJAM-A was enhanced by presence of soluble fJAM-A in low concentrations (see Fig. 8B). As fJAM-A can form dimers, and FCV binding does not seem to require or occlude the fJAM-A dimerization interface (Bhella et al., 2008, Ossiboff & Parker, 2007), this enhanced binding may be mediated by fJAM/fJAM interactions between immobilized and virus-bound soluble receptor. An alternative

explanation is that the binding of soluble fJAM-A to FCV capsids enhances the binding to the immobilized receptor allosterically.

Single-step growth curves for *srr* mutants of poliovirus demonstrated that while all of the mutants attained similar overall titers, their titers were lower than wild type P1/Mahoney poliovirus at early time points post-infection. This delayed increase in titer was attributed to an assembly defect as all of the mutants bound as efficiently as wild type poliovirus to cells at room temperature (Colston & Racaniello, 1994). In contrast, we found that parental FCV-5 and a subpanel of *srr* mutants of FCV-5 had similar kinetics of replication during single step growth curves. Most of the srr mutants, however, had significantly decreased titers in comparison to parental FCV-5 at 4 h.p.i during a multiple-step growth experiment. There are several possible explanations for our findings. One would be that the efficiency of viral entry of the mutants is decreased with a consequent lag in the onset of viral replication. However, it is also possible that capsid assembly is slowed; this explanation seems less likely as all of the mutants achieved similar titers to parental FCV-5 at later time points during multiple-step growth. Changes in the efficiency of viral entry could be attributed to changes in receptor binding, cellular trafficking, and/or uncoating. Mutant K572E demonstrated decreased binding to cell-surface expressed fJAM-A, and it was also one of isolates with delayed kinetics. Therefore, one possibility for the observed difference in growth in this mutant is decreased binding to the receptor. However, mutant G329D bound to both cell-expressed and plate-bound fJAM-A to the same extent as parental FCV-5 and mutant V516I demonstrated increased affinity for the receptor. Yet, these mutants possessed decreased capacity for growth during early time points of multiple replicative cycle growth. This suggests that the process of entry differs in these mutants. We previously showed that lower virulence field or tissue-culture adapted FCV isolates had delayed multiple cycle growth kinetics during multiple cycle growth

when compared to more virulent isolates (including FCV-5) (Ossiboff et al., 2007). Although the virulence of these *srr* mutants is currently unknown, it is possible that by selecting for mutants resistant to neutralization by soluble receptor, we may have also selected for viruses with altered virulence.

Since nonenveloped viruses must penetrate cellular membranes to deliver their genetic material, it is hypothesized that they undergo conformational alterations that are required for membrane penetration [as reviewed in (Tsai, 2007)]. With the finding that fJAM-A neutralization of FCV was temperature-dependent and the identification of *srr* mutants possessing mutations to only buried residues, we investigated the possibility that interaction with fJAM-A was inducing a conformational change in FCV using bis-ANS binding to detect changes in hydrophobicity. We found that incubation of several FCV isolates with soluble fJAM-A at physiologic temperatures resulted in an increase in hydrophobicity of the FCV/fJAM-A complex as detected by changes in bis-ANS binding. This change was specific for incubation with fJAM-A, as incubation with the human homolog, fJAM-A did not result in a net change of hydrophobicity. Several viruses expose hydrophobic regions of viral proteins secondary to structural changes (Carneiro et al., 2001, de Sousa et al., 1999, Gaspar et al., 1997). Receptor-induced conformational changes have also been demonstrated for envelope glycoproteins of Newcastle disease virus and HIV-1 by gangliosides and CD4, respectively, using changes in hydrophobicity as determined by bis-ANS binding (Ferreira et al., 2004, Jones et al., 1998). Therefore, it is likely the observed changes in bis-ANS indicate a conformational change within the virus capsid. An alternative explanation is that the increases in hydrophobicity we observed were due to changes in the receptor, not the virus. However, as there is substantial evidence for viral protein conformational changes following interaction with cellular receptors, and

such conformational changes are likely a requirement of all nonenveloped viruses, this explanation is less likely.

As described for the neutralization of human rhinoviruses by soluble ICAM-1 (Greve et al., 1991), we hypothesized that one method of FCV-5 neutralization by soluble fJAM-A was the induction of a conformational change within the virus particle that rendered it incapable of infecting cells. As such, we further hypothesized that the *srr* mutants would not exhibit a change in hydrophobicity upon incubation with soluble receptor. However, we found that the *srr* mutants demonstrated an increase in hydrophobicity similar to that observed for FCV-5. One possible explanation of this finding is that FCV neutralization by soluble receptor is not due to an induced conformational change. However, a more likely possibility is that there are several intermediates that form during the interaction of FCV with fJAM-A and the resulting steps required for entry. Two structural intermediates of picornaviruses can form following interaction with receptor or when subjected to the appropriate environmental conditions, the 135S A particle and the 80S empty particle (Crowell & Philipson, 1971, De Sena & Mandel, 1977, Fenwick & Cooper, 1962, Lonberg-Holm & Korant, 1972); furthermore, it is postulated that there are additional intermediates that are as of yet unidentified (Hogle, 2002). Therefore, our working model is that mutants resistant to neutralization undergo an initial conformational change upon interacting with fJAM-A that is either reversible or results in a stable, infectious intermediate.

Recently a cryo-electron microscopy reconstruction of the FCV F9 strain complexed with fJAM-A at 18 Å revealed that fJAM-A interacted with the top of the P2 sub-domain of the F9 capsid (Bhella et al., 2008). This interaction caused a ~ 13° anti-clockwise rotation of the P dimers about their two-fold axes of symmetry indicating substantial conformational change of the capsid upon binding of receptor.

Interestingly, we found that in contrast to the other FCV isolates we investigated the binding of bis-ANS to the F9 capsid when preincubated with sfJAM-A was lower than binding of bis-ANS to the virus alone (see Fig. 9D). Given the structural evidence for a conformational change in F9, the likely explanation is that fJAM-A binding induces a conformational change of the F9 capsid that masks hydrophobic patches rather than uncovering them. Therefore, given our observations of increased bis-ANS binding to other FCV isolates when preincubated with fJAM-A, it seems possible that the capsid conformational changes reported by Bhella *et al*. for the vaccine isolate F9 are not representative of changes that occur in the capsids of other FCV field isolates.

A further investigation of FCV isolates, including low passage field isolates and tissue culture adapted lab strains, indicated that not all FCV isolates are sensitive to fJAM-A neutralization (see Fig. 10). One naturally neutralization resistant isolate, FCV-131, also exhibited increased hydrophobicity following incubation with soluble receptor. Like the *srr* mutants, it seems likely that some field isolates undergo a conformational alteration following interaction with fJAM-A, but do not lose infectivity. Other isolates, however, may undergo more drastic, global conformational alterations that result in either a complete loss of or significant decrease in infectivity. While altered poliovirus 135S particles are still infectious, they are ~ 10^4 less infectious than native particles (Curry et al., 1996). Interestingly, we found that sensitivity of different FCV isolates to neutralization correlated with their virulence in cats. Feline calicivirus is a common pathogen of cats that typically causes no disease or mild upper respiratory disease and oral ulceration, with fatal disease being unusual. However, highly virulent isolates of FCV occur that can cause systemic signs of disease and result in mortality rates as high as 50% (Hurley et al., 2004, Pedersen et al., 2000, Pesavento et al., 2004, Schorr-Evans et al., 2003). In our panel, the most virulent isolates were susceptible to fJAM-A neutralization, while low virulence

isolates displayed resistance. It is possible that the *in vitro* assay of receptor neutralization is highlighting an important determinant of *in vivo* virulence.

4.6 Acknowledgements

We thank Christian Nelson, Meg Crapster-Pregont, Sarah Caddy, and Rachel Mays for excellent technical assistance. We thank Dr. Terry Dermody and Kristen Guglielmi for the generous gift of reagents. This work was supported by grants from The Cornell Feline Health Center, and the Winn foundation. R. J. O. is the recipient of a scholarship from Cornell University.

REFERENCES

Bhella, D., Gatherer, D., Chaudhry, Y., Pink, R. & Goodfellow, I. G. (2008). Structural insights into Calicivirus attachment and uncoating. *J Virol*.

Carneiro, F. A., Ferradosa, A. S. & Da Poian, A. T. (2001). Low pH-induced conformational changes in vesicular stomatitis virus glycoprotein involve dramatic structure reorganization. *J Biol Chem* **276**, 62-7.

Carter, M. J., Milton, I. D., Turner, P. C., Meanger, J., Bennett, M. & Gaskell, R. M. (1992). Identification and sequence determination of the capsid protein gene of feline calicivirus. *Arch Virol* **122**, 223-35.

Chen, R., Neill, J. D., Estes, M. K. & Prasad, B. V. (2006). X-ray structure of a native calicivirus: structural insights into antigenic diversity and host specificity. *Proc Natl Acad Sci U S A* **103**, 8048-53.

Colston, E. & Racaniello, V. R. (1994). Soluble receptor-resistant poliovirus mutants identify surface and internal capsid residues that control interaction with the cell receptor. *Embo J* **13**, 5855-62.

Crowell, R. L. & Philipson, L. (1971). Specific alterations of coxsackievirus B3 eluted from HeLa cells. *J Virol* **8**, 509-15.

Curry, S., Chow, M. & Hogle, J. M. (1996). The poliovirus 135S particle is infectious. *J Virol* **70**, 7125-31.

De Sena, J. & Mandel, B. (1977). Studies on the in vitro uncoating of poliovirus. II. Characteristics of the membrane-modified particle. *Virology* **78**, 554-66.

de Sousa, P. C., Jr., Tuma, R., Prevelige, P. E., Jr., Silva, J. L. & Foguel, D. (1999). Cavity defects in the procapsid of bacteriophage P22 and the mechanism of capsid maturation. *J Mol Biol* **287**, 527-38.

Delano, W. L. (2002). The PyMOL Molecular Graphics System. Pala Alto, CA, USA: DeLano Scientific.

Ebnet, K., Schulz, C. U., Meyer Zu Brickwedde, M. K., Pendl, G. G. & Vestweber, D. (2000). Junctional adhesion molecule interacts with the PDZ domain-containing proteins AF-6 and ZO-1. *J Biol Chem* **275**, 27979-88.

Fenwick, M. L. & Cooper, P. D. (1962). Early interactions between poliovirus and ERK cells: some observations on the nature and significance of the rejected particles. *Virology* **18**, 212-23.

Ferreira, L., Villar, E. & Munoz-Barroso, I. (2004). Conformational changes of Newcastle disease virus envelope glycoproteins triggered by gangliosides. *Eur J Biochem* **271**, 581-8.

Gaspar, L. P., Johnson, J. E., Silva, J. L. & Da Poian, A. T. (1997). Partially folded states of the capsid protein of cowpea severe mosaic virus in the disassembly pathway. *J Mol Biol* **273**, 456-66.

Gomez Yafal, A., Kaplan, G., Racaniello, V. R. & Hogle, J. M. (1993). Characterization of poliovirus conformational alteration mediated by soluble cell receptors. *Virology* **197**, 501-5.

Greve, J. M., Forte, C. P., Marlor, C. W., Meyer, A. M., Hoover-Litty, H., Wunderlich, D. & McClelland, A. (1991). Mechanisms of receptor-mediated rhinovirus neutralization defined by two soluble forms of ICAM-1. *J Virol* **65**, 6015-23.

Guiver, M., Littler, E., Caul, E. O. & Fox, A. J. (1992). The cloning, sequencing and expression of a major antigenic region from the feline calicivirus capsid protein. *J Gen Virol* **73 (Pt 9)**, 2429-33.

Hogle, J. M. (2002). Poliovirus cell entry: common structural themes in viral cell entry pathways. *Annu Rev Microbiol* **56**, 677-702.

Hoover-Litty, H. & Greve, J. M. (1993). Formation of rhinovirus-soluble ICAM-1 complexes and conformational changes in the virion. *J Virol* **67**, 390-7.

Hurley, K. E., Pesavento, P. A., Pedersen, N. C., Poland, A. M., Wilson, E. & Foley, J. E. (2004). An outbreak of virulent systemic feline calicivirus disease. *J Am Vet Med Assoc* **224**, 241-9.

Jones, P. L., Korte, T. & Blumenthal, R. (1998). Conformational changes in cell surface HIV-1 envelope glycoproteins are triggered by cooperation between cell surface CD4 and co-receptors. *J Biol Chem* **273**, 404-9.

Kaplan, G., Freistadt, M. S. & Racaniello, V. R. (1990). Neutralization of poliovirus by cell receptors expressed in insect cells. *J Virol* **64**, 4697-702.

Katpally, U., Wobus, C. E., Dryden, K., Virgin, H. W. t. & Smith, T. J. (2008). Structure of antibody-neutralized murine norovirus and unexpected differences from viruslike particles. *J Virol* **82**, 2079-88.

Landau, M., Mayrose, I., Rosenberg, Y., Glaser, F., Martz, E., Pupko, T. & Ben-Tal, N. (2005). ConSurf 2005: the projection of evolutionary conservation scores of residues on protein structures. *Nucleic Acids Res* **33**, W299-302.

Langevin, C. & Tuffereau, C. (2002). Mutations conferring resistance to neutralization by a soluble form of the neurotrophin receptor (p75NTR) map outside of the known antigenic sites of the rabies virus glycoprotein. *J Virol* **76**, 10756-65.

Lonberg-Holm, K. & Korant, B. D. (1972). Early interaction of rhinoviruses with host cells. *J Virol* **9**, 29-40.

Makino, A., Shimojima, M., Miyazawa, T., Kato, K., Tohya, Y. & Akashi, H. (2006). Junctional adhesion molecule 1 is a functional receptor for feline calicivirus. *J Virol* **80**, 4482-90.

Mandell, K. J. & Parkos, C. A. (2005). The JAM family of proteins. *Adv Drug Deliv Rev* **57**, 857-67.

Marlin, S. D., Staunton, D. E., Springer, T. A., Stratowa, C., Sommergruber, W. & Merluzzi, V. J. (1990). A soluble form of intercellular adhesion molecule-1 inhibits rhinovirus infection. *Nature* **344**, 70-2.

Neill, J. D., Reardon, I. M. & Heinrikson, R. L. (1991). Nucleotide sequence and expression of the capsid protein gene of feline calicivirus. *J Virol* **65**, 5440-7.

Neill, J. D., Sosnovtsev, S. V. & Green, K. Y. (2000). Recovery and altered neutralization specificities of chimeric viruses containing capsid protein domain exchanges from antigenically distinct strains of feline calicivirus. *J Virol* **74**, 1079-84.

Ossiboff, R. J. & Parker, J. S. (2007). Identification of regions and residues in feline junctional adhesion molecule required for feline calicivirus binding and infection. *J Virol* **81**, 13608-21.

Ossiboff, R. J., Sheh, A., Shotton, J., Pesavento, P. A. & Parker, J. S. (2007). Feline caliciviruses (FCVs) isolated from cats with virulent systemic disease possess in vitro phenotypes distinct from those of other FCV isolates. *J Gen Virol* **88**, 506-27.

Pedersen, N. C., Elliott, J. B., Glasgow, A., Poland, A. & Keel, K. (2000). An isolated epizootic of hemorrhagic-like fever in cats caused by a novel and highly virulent strain of feline calicivirus. *Vet Microbiol* **73**, 281-300.

Pesavento, P. A., MacLachlan, N. J., Dillard-Telm, L., Grant, C. K. & Hurley, K. F. (2004). Pathologic, immunohistochemical, and electron microscopic findings in naturally occurring virulent systemic feline calicivirus infection in cats. *Vet Pathol* **41**, 257-63.

Prasad, B. V., Hardy, M. E., Dokland, T., Bella, J., Rossmann, M. G. & Estes, M. K. (1999). X-ray crystallographic structure of the Norwalk virus capsid. *Science* **286**, 287-90.

Racaniello, V. R. (1996). Early events in poliovirus infection: virus-receptor interactions. *Proc Natl Acad Sci U S A* **93**, 11378-81.

Radford, A. D., Willoughby, K., Dawson, S., McCracken, C. & Gaskell, R. M. (1999). The capsid gene of feline calicivirus contains linear B-cell epitopes in both variable and conserved regions. *J Virol* **73**, 8496-502.

Rosen, C. G. & Weber, G. (1969). Dimer formation from 1-amino-8-naphthalenesulfonate catalyzed by bovine serum albumin. A new fluorescent molecule with exceptional binding properties. *Biochemistry* **8**, 3915-20.

Saeki, K., Ohtsuka, N. & Taguchi, F. (1997). Identification of spike protein residues of murine coronavirus responsible for receptor-binding activity by use of soluble receptor-resistant mutants. *J Virol* **71**, 9024-31.

Schorr-Evans, E. M., Poland, A., Johnson, W. E. & Pedersen, N. C. (2003). An epizootic of highly virulent feline calicivirus disease in a hospital setting in New England. *J Feline Med Surg* **5**, 217-26.

Seal, B. S. & Neill, J. D. (1995). Capsid protein gene sequence of feline calicivirus isolates 255 and LLK: further evidence for capsid protein configuration among feline caliciviruses. *Virus Genes* **9**, 183-7.

Silberstein, E., Dveksler, G. & Kaplan, G. G. (2001). Neutralization of hepatitis A virus (HAV) by an immunoadhesin containing the cysteine-rich region of HAV cellular receptor-1. *J Virol* **75**, 717-25.

Sosnovtsev, S. & Green, K. Y. (1995). RNA transcripts derived from a cloned full-length copy of the feline calicivirus genome do not require VpG for infectivity. *Virology* **210**, 383-90.

Sosnovtsev, S., Sosnovtseva, S. & Green, K. Y. (1997). Recovery of Feline Calicivirus from plasmid DNA containing a full-length copy of the genome. In *Proceedings of the First International Symposium on Caliciviruses*, pp. 125-130. Edited by D. Chasey, R. M. Gaskell & I. N. Clarke. Reading, U.K: European Society for Veterinary Virology and Central Veterinary Laboratory, Weybridge, United Kingdom.

Sosnovtsev, S. V., Sosnovtseva, S. A. & Green, K. Y. (1998). Cleavage of the feline calicivirus capsid precursor is mediated by a virus-encoded proteinase. *J Virol* **72**, 3051-9.

Stuart, A. D. & Brown, T. D. (2007). Alpha2,6-linked sialic acid acts as a receptor for Feline calicivirus. *J Gen Virol* **88**, 177-86.

Tohya, Y., Masuoka, K., Takahashi, E. & Mikami, T. (1991). Neutralizing epitopes of feline calicivirus. *Arch Virol* **117**, 173-81.

Tohya, Y., Yokoyama, N., Maeda, K., Kawaguchi, Y. & Mikami, T. (1997). Mapping of antigenic sites involved in neutralization on the capsid protein of feline calicivirus. *J Gen Virol* **78 (Pt 2)**, 303-5.

Tsai, B. (2007). Penetration of nonenveloped viruses into the cytoplasm. *Annu Rev Cell Dev Biol* **23**, 23-43.

Tsang, S. K., McDermott, B. M., Racaniello, V. R. & Hogle, J. M. (2001). Kinetic analysis of the effect of poliovirus receptor on viral uncoating: the receptor as a catalyst. *J Virol* **75**, 4984-9.

CHAPTER 5

Summary and conclusions

Feline calicivirus (FCV) is a common and emerging feline infectious disease of veterinary significance. Outbreaks of highly virulent viruses, first reported in 1998, have continued to surface sporadically causing mortality rates as high as 50%. It appears that currently available commercial vaccines afford little to no protection against these highly virulent isolates. Consequently, there is a great need in veterinary medicine for specific diagnostics and therapeutics to help identify and treat outbreaks of highly virulent FCV, in addition to improved vaccines to help prevent them. Other clinically relevant members of the *Caliciviridae* cause outbreaks of acute gastroenteritis in humans and vesicular, hemorrhagic and respiratory disease in animals. But unlike FCV, studies on many caliciviruses are limited by the lack of tissue culture systems. As such, FCV can serve as a model for the *Caliciviridae* family to better understand the basic principles of calicivirus infection and pathogenesis. The study of feline calicivirus (FCV), therefore, has important implications for both veterinary and human medicine.

In the work presented within this dissertation, I have investigated the *in vitro* properties and partial genome sequence of a panel of FCV isolates in order to identify *in vitro* correlates of *in vivo* virulence. I also investigated the molecular details of the interaction of FCV with its functional receptor, feline junctional adhesion molecule A (fJAM-A).

The results I present here show that while a panel of FCV isolates, which included seven isolates from five distinct VS-FCV outbreaks ('VS isolates'), shared many common properties, two noteworthy differences were identified. First, although all of the FCV isolates investigated had similar kinetics of growth under single-cycle conditions, VS isolates infected tissue-culture cells more efficiently under multiple-cycle growth conditions. Such efficiency suggests that differences in virus attachment or entry may determine the increased growth of VS-FCV isolates and perhaps play a

role in the increased pathogenicity of VS-FCV isolates. Second, I found that cells infected with VS isolates showed cytopathic effects earlier than cells infected with non-VS isolates. However, sequence analysis and alignments of the capsid and pro–pol regions of the genome did not reveal any conserved changes that correlated with virulence; furthermore, phylogenetic analysis suggested that, as VS-FCV isolates were no more related to each other than low virulence or tissue culture isolates, VS isolates have arisen independently several times since first being described.

To investigate the FCV-fJAM-A interaction, I expressed the fJAM-A ectodomain as a recombinant protein in bacteria. I also used this protein to generate fJAM-A specific rabbit antisera. Preincubation of soluble fJAM-A ectodomain or the D1 domain alone with FCV resulted in neutralization, suggesting that the virus interacted with the D1 domain. Virus binding assays using a cell-expressed panel of chimeric and mutant receptors confirmed that FCV binds to the membrane-distal D1 domain of fJAM-A. Using site-directed mutagenesis of select D1 residues, I identified three mutations (D42N, K43N, and S97A) that resulted in significantly decreased binding of virus to the receptor. However, while the D1 domain was sufficient to permit FCV binding, the entire fJAM-A receptor was required to confer susceptibility to infection. Finally, I showed that expression of fJAM-A alone on the surface of a non-permissive cell line did not confer susceptibility to FCV infection by all of the FCV isolates investigated.

Having shown that soluble fJAM-A ectodomain neutralized a virulent systemic FCV isolate (FCV-5) following preincubation, I proceeded to select for FCV-5 mutants that were resistant to neutralization. I obtained a panel of 24 *soluble receptor resistant* (*srr*) mutants that contained mutations to 20 unique residues within the capsid. I developed a protocol for FCV purification that I used to purify FCV-5. The purified virus was used to determine a 3.6 Å crystal structure of the virus. Using the

crystal structure, the mutations were mapped to the FCV-5 capsid. I found that *srr* isolates contained mutations to both surface-exposed and buried residues. By characterizing a subpanel of mutants, I showed that while resistant to neutralization by soluble receptor, *srr* isolates still utilized fJAM-A as a functional receptor. Although the mutants possessed similar single cycle growth kinetics, 6 of the 8 *srr* mutants demonstrated delayed kinetics of growth at early time points post-infection. As detected by an increase in hydrophobicity, I found that incubation of both parental FCV-5 and select *srr* isolates with soluble fJAM-A resulted in a conformational change. Additionally, incubation of select field isolates of varying clinical histories with soluble receptor also showed an increase in hydrophobicity. In contrast, the attenuated vaccine strain F9 demonstrated a net decrease in hydrophobicity, indicating either (i) it is not undergoing a conformational change, or (ii) the nature of the induced conformational change masks hydrophobic patches. Finally, I demonstrated that not all FCV field isolates tested were susceptible to neutralization by soluble fJAM-A. Furthermore, I noted a correlation between strain virulence and susceptibility to neutralization, with highly virulent isolates demonstrating sensitivity to neutralization, while low virulence field isolates and tissue culture adapted strains showed neutralization resistance.

In this thesis, I have enhanced the understanding of the interaction of FCV with its cellular receptor, fJAM-A, at the molecular level. I also identified *in vitro* properties of FCV isolates that correlate with their virulent nature. Furthermore, I developed a panel of reagents and protocols that will allow for further elucidation of calicivirus infection and pathogenesis.

The studies presented within this dissertation identified a few properties of FCV that correlated with the virulent nature of the isolates. Viruses isolated from cats suffering from the most severe clinical signs exhibited the capacity *in vitro* to produce

infectious virus at earlier time points than low virulence or tissue culture adapted strains when infected at a low multiplicity of infection; in contrast, all isolates demonstrated similar growth kinetics when infected at a high multiplicity of infection. There are three possible explanations for these findings. First, the highly virulent viruses may possess a stronger affinity for the receptor. As such, at lower concentrations of virus, more cells would be infected initially in multiple cycle growth. The second possibility is that they are able to enter cells more efficiently than isolates that displayed slower growth kinetics. In this explanation, viruses all bind receptor with similar affinity, but there are differences in virus entry post-receptor binding. There is also the possibility of a third explanation in which the release of progeny virus from infected cells differs between the isolates. However, at such early time points post-infection, the detected virus is most likely produced from the first round of replication and still cell-associated. Furthermore, the multiple cycle growth kinetics of all isolates are similar at later times post-infection. Given this evidence, a difference in the receptor binding or entry between the high and low virulence isolates is the most likely reason for the observed differences in growth kinetics.

FCV isolates also differed in their sensitivity to neutralization by the soluble receptor. Highly virulent isolates exhibited a significant loss of infectious titer (> 3 log plaque forming units) following preincubation with fJAM-A ectodomain at 37°C. In contrast, tissue culture adapted and low virulence field isolates were completely resistant to neutralization. Interestingly, mutants of the virulent systemic isolate FCV-5, selected for resistance to neutralization by soluble fJAM-A, showed altered growth kinetics. Instead of demonstrating the increase in log titer at early time points of multiple cycle growth characteristic of the parental strain, 6 of the 8 *srr* mutants investigated showed a decrease in infectious titer; this is a result characteristic of low virulence and tissue culture isolates. Taken together, these findings suggest that the

processes of infectious entry in tissue culture cells and neutralization by soluble receptor are linked to isolate virulence.

I propose the following model for FCV virulence (Figure 5.1). Highly virulent isolates of FCV exist in a highly metastable state. Under the conditions used to assay for virus neutralization and changes in hydrophobicity described in this dissertation, only receptor and physiologic temperatures are required to convert *native infectious* particles to *hydrophobic neutralized* particles. These structural alterations may permit interaction with cellular membranes and initiate infectious entry. Hydrophobicity data of low virulence FCV isolates and *srr* mutants indicates that incubation with soluble receptor at physiologic temperature also results in an increase in bis-ANS fluorescence intensity, suggesting a conformational change has occurred. But in contrast, the results of the neutralization experiments identify that these particles are still infectious. In this model, *native infectious* particles of low virulence isolates first convert to an intermediate *hydrophobic infectious* conformer. To undergo further conversion to particles able to initiate infectious entry (*hydrophobic neutralized*), these low virulence isolates likely require conditions or factors that have not yet been determined. The 'rapid' conversion of the highly virulent isolates would allow for faster entry than the less virulent strains, permitting the virus to produce progeny at earlier time points in the host. This advantage would then facilitate the rapid spread of the highly virulent isolates within the host, as well as potentially expanding tissue tropism by eliminating the requirement an additional cellular factor or condition. The rapid growth kinetics of FCV combined with more efficient entry of highly virulent strains may then allow the virus to stay just ahead of host defenses.

This model presenting virulent systemic isolates as highly metastable structures may also explain why outbreaks of virulent systemic FCV are isolated,

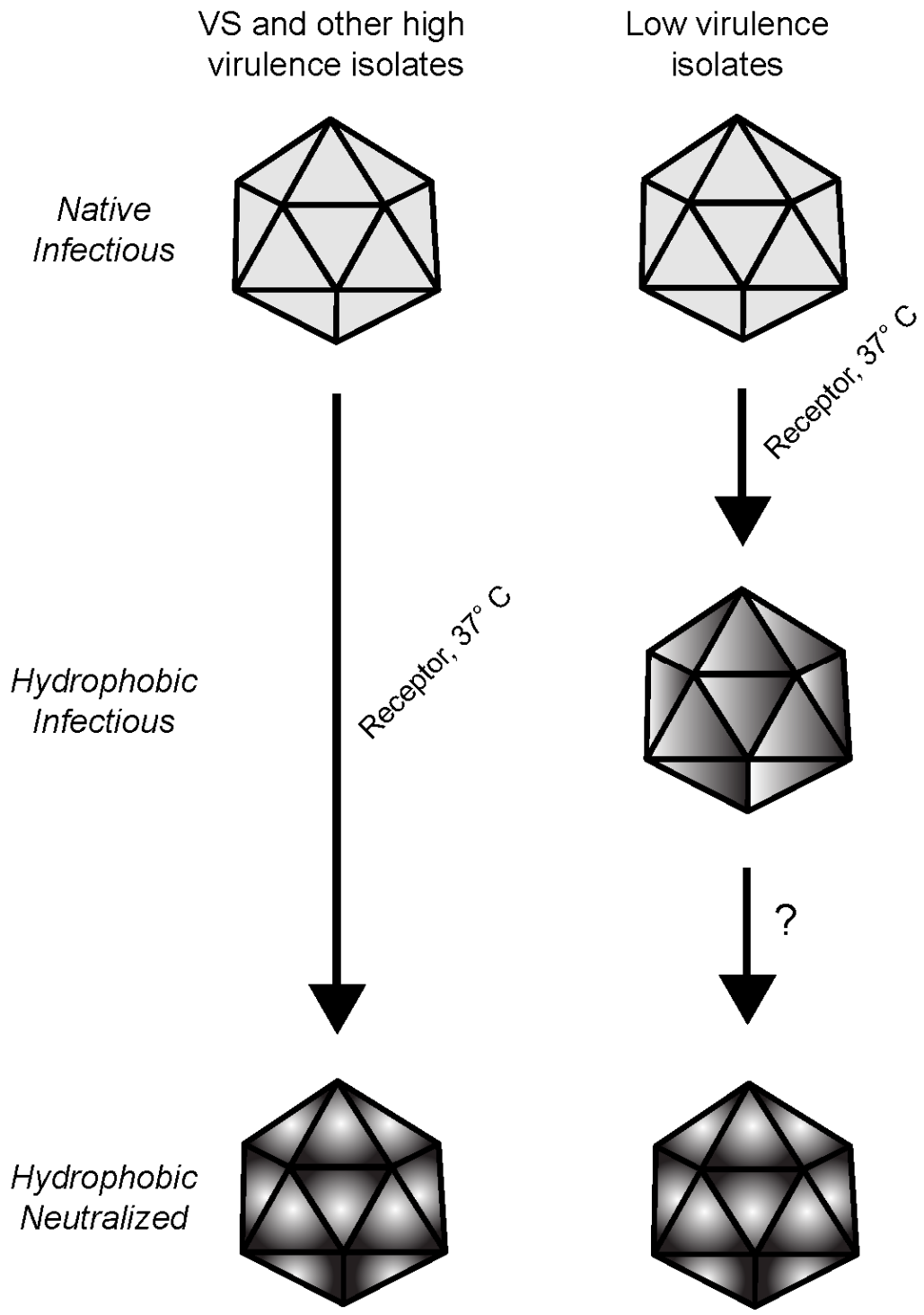

Figure 5.1. Model of FCV virulence.

infect a limited number of hosts (from a few to up to 50 cats), and then burn out without greater geographical spread (Pesavento et al., 2008). While a greater concern for veterinary medicine, these viruses may actually be less fit than their lower virulence counterparts.

As has been hypothesized for picornaviruses [as reviewed in (Hogle, 2002)], there are likely multiple viral intermediates during FCV infectious entry. The changes in hydrophobicity observed for low virulence and *srr* mutant isolates following incubation with receptor at physiological temperatures may indicate conversion to an altered particle that retains infectivity (*hydrophobic infectious* particles). The increase in hydrophobicity may also represent changes in the structure that are reversible, allowing *hydrophobic infectious* particles to revert back to *native infectious* particles. This reversion would then provide an explanation for why preincubation of some FCV isolates with soluble receptor does not affect their ability to infect cells. It would be interesting to test if *hydrophobic infectious* particles could be pushed to *hydrophobic neutralized* particles by altering conditions, such as incubating at supraphysiologic temperatures.

While the observed increase in hydrophobicity of any FCV isolate following incubation with soluble receptor is suggestive of a conformational change *in vitro*, additional studies are required to confirm this interpretation. The altered particles of picornaviruses were originally identified due to the nature of their sedimentation, with the native particle, A-particle and 80S particles all exhibiting unique sedimentation. Therefore, the sedimentation of native and receptor-incubated particles should be investigated. Another method commonly used to identify conformational changes within virus capsids is protease sensitivity. If FCV is truly demonstrating receptor-induced conformational changes, then protease cleavage sites present in the native virus may be either exposed or hidden in the altered particle. Accordingly, treating

native and receptor-incubated virus with proteases would then result in different sized peptide fragments, as determined by gel electrophoresis.

Structural studies of an FCV field isolate in complex with fJAM-A would provide an understanding of the molecular changes occurring within the capsid. A cryo-EM reconstruction has been recently published for the FCV vaccine strain F9 in complex with soluble fJAM-A ectodomain (Bhella et al., 2008). They found rotational conformational changes in the P- and S-domains following receptor binding. However, I have shown that following preincubation with receptor, F9 has decreased hydrophobicity, a unique finding for the isolates I investigated. As a vaccine strain, F9 was passaged and attenuated in tissue culture. It is possible that one of the mechanisms of virus attenuation was to alter the conditions of receptor-induced conformational changes within the capsid. To date, a collaborative effort with Dr. Prasad at Baylor College of Medicine to generate a cryo-EM reconstruction of FCV-5 in complex with fJAM-A ectodomain has had limited success. Under the conditions that have been investigated, preincubation of soluble receptor with virus has led to particle disassembly. These experiments should be continued by trying to find optimal conditions to capture the particle in an altered state. The use of small molecules such as bis-ANS, which can act as molecular wedges by binding to exposed hydrophobic pockets and locking the particle in an altered state, may also prove helpful (Lee et al., 2004).

Another important determination to make will be if altered FCV particles can directly interact with lipid membranes. If the interaction of FCV with fJAM-A induces a physiologically relevant conformational change, then the altered particles may be able to interact with or even disrupt lipid membranes, a necessary function for nonenveloped virus entry. Liposome models have been used to demonstrate such interactions for some picornaviruses (Airaksinen et al., 2001, Davis et al., 2008,

Tuthill et al., 2006). A couple of liposome-based experiments would provide important information for FCV entry. Liposomes containing fluorescent dyes, that while quenched within the liposome are dequenched when released, could be incubated with FCV preincubated with receptor. Liposome disruption by FCV would be evident by an increase in fluorescence of the total sample or a decrease in internal liposome fluorescence as determined by flow cytometry. In another set of experiments, liposomes could be decorated with fJAM-A ectodomain, and incubated with FCV. These assays could be used to demonstrate receptor-induced particle conformation in a membrane based system. This system could also be used for electron microscopy experiments to investigate the structural biology of the virus-membrane interaction.

One aspect of the receptor-virus interaction that has been overlooked for many of the assays I have described within this dissertation is the glycosylation status of the receptor and the importance of a carbohydrate co-receptor in FCV receptor binding and entry. Stuart and Brown (2007) demonstrated that FCV binds to α2,6-linked sialic acids present on a *N*-linked glycoprotein; it is not known if that glycoprotein is fJAM-A or perhaps an additional co-receptor. fJAM-A contains a single putative *N*-linked glycosylation site, present in the D2 loop of the ectodomain. The importance of this glycosylation site has not been determined. For my studies, soluble recombinant fJAM-A ectodomain was produced in bacteria, and was therefore not glycosylated. Additionally, the majority of the cell-based infection and binding assays were performed in Chinese hamster ovary (CHO) cells, which are unable to synthesize α2,6 sialic acid linkages (Lee et al., 1989). Therefore, to investigate the effect of glycosylation of fJAM-A, the glycosylation status of cell-expressed receptor should first be determined. If it is found that fJAM-A is glycosylated, then both native fJAM-A ectodomain and ectodomain glycosylation mutants should be expressed for

purification in a mammalian cell line; binding and neutralization assays should be repeated with the glycosylated form of the fJAM-A ectodomain.

Finally, while there are likely many factors involved in the ability of some isolates of FCV to cause virulent systemic disease, the studies presented here suggest that the capsid protein plays a crucial role in the process. The creation of chimeric FCVs will allow this hypothesis to be tested both *in vitro* and *in vivo*. A reverse genetics system for FCV using a full length infectious clone of the tissue-culture adapted isolate Urbana has been previously described (Sosnovtsev & Green, 1995, Sosnovtsev et al., 1997). By swapping out the ORFs responsible for the two structural proteins (VP1 and VP2) of FCV-Urbana for those of a virulent systemic FCV (such as FCV-5), we can investigate the *in vitro* properties (including multiple cycle growth, ability to cause CPE, and plaque size/morphology) of the chimeric virus in comparison to the parental viruses. The point mutations identified by the analysis of the *srr* mutants can also be introduced into the chimeric system, allowing us to compare and contrast the effects of a single mutation in the capsid protein of the viruses on *in vitro* properties of the viruses. Ultimately, experiments looking at disease pathogenesis in cats infected with FCV-5, Urbana, and the chimeric virus can be used to determine if capsid protein alone is sufficient to confer a virulent systemic phenotype to FCV.

Future investigations of the molecular and structural details of the virus-receptor interaction of FCV will hopefully serve to not only advance the ability of veterinary medicine to identify, treat, and prevent outbreaks of highly virulent isolates of FCV, but also the enhance the knowledge of the scientific community on the entry of nonenveloped viruses.

REFERENCES

Airaksinen, A., Somerharju, P. & Hovi, T. (2001). Variation in liposome binding among enteroviruses. *Virology* **279**, 539-45.

Bhella, D., Gatherer, D., Chaudhry, Y., Pink, R. & Goodfellow, I. G. (2008). Structural insights into Calicivirus attachment and uncoating. *J Virol*.

Davis, M. P., Bottley, G., Beales, L. P., Killington, R. A., Rowlands, D. J. & Tuthill, T. J. (2008). Recombinant VP4 of human rhinovirus induces permeability in model membranes. *J Virol* **82**, 4169-74.

Hogle, J. M. (2002). Poliovirus cell entry: common structural themes in viral cell entry pathways. *Annu Rev Microbiol* **56**, 677-702.

Lee, E. U., Roth, J. & Paulson, J. C. (1989). Alteration of terminal glycosylation sequences on N-linked oligosaccharides of Chinese hamster ovary cells by expression of beta-galactoside alpha 2,6-sialyltransferase. *J Biol Chem* **264**, 13848-55.

Lee, K. K., Tang, J., Taylor, D., Bothner, B. & Johnson, J. E. (2004). Small compounds targeted to subunit interfaces arrest maturation in a nonenveloped, icosahedral animal virus. *J Virol* **78**, 7208-16.

Sosnovtsev, S. & Green, K. Y. (1995). RNA transcripts derived from a cloned full-length copy of the feline calicivirus genome do not require VpG for infectivity. *Virology* **210**, 383-90.

Sosnovtsev, S., Sosnovtseva, S. & Green, K. Y. (1997). Recovery of Feline Calicivirus from plasmid DNA containing a full-length copy of the genome. In *Proceedings of the First International Symposium on Caliciviruses*, pp. 125-130. Edited by D. Chasey, R. M. Gaskell & I. N. Clarke. Reading, U.K: European Society for Veterinary Virology and Central Veterinary Laboratory, Weybridge, United Kingdom.

Stuart, A. D. & Brown, T. D. (2007). Alpha2,6-linked sialic acid acts as a receptor for Feline calicivirus. *J Gen Virol* **88**, 177-86.

Tuthill, T. J., Bubeck, D., Rowlands, D. J. & Hogle, J. M. (2006). Characterization of early steps in the poliovirus infection process: receptor-decorated liposomes induce conversion of the virus to membrane-anchored entry-intermediate particles. *J Virol* **80**, 172-80.